NTNU – Trondheim
Norwegian University of
Science and Technology

Optimal Scheduling and Loadsharing of a Hybrid Power Plant with Gensets and Battery Banks

Ying Lu

Department of Marine Technology

Norwegian University of Science and Technology

June 2019

Trondheim, Norway

Supervisor: Roger Skjetne, Professor

Co-supervisor: Laxminarayan Thorat, PhD candidate

NTNU Trondheim
Norwegian University of Science and Technology
Department of Marine Technology

MSC THESIS DESCRIPTION SHEET

Name of the candidate: Lu, Ying

Field of study: Marine control engineering

Thesis title (Norwegian): Optimal lastfordeling for eit hybrid kraftanlegg med diesel-generatorer og batteribanker

Thesis title (English): Optimal scheduling and loadsharing of a hybrid power plant with gensets and battery banks

Background

During the last 20 years, maritime electric installations have increased in size and scope, ranging from only few systems and installations to become an industry standard. Increased demands for energy-efficient and low emission multifunctional vessels with high availability and reliability have motivated electrically powered vessels with improved power and energy management systems (PEMS). In addition, a shift towards more complex electric energy production systems with hybrid power plants using energy sources such as diesel, LNG, fuel cells, and additional energy storage devices such as battery banks, super-capacitors, and flywheels.

There has also been an extensive development in the automotive industry towards more energy-efficient engines, with rapid and robust start/stop functionality, combined with battery packages to reduce emissions and fuel consumption. ESDs should supplement such a system to e.g. reduce engine transient behavior. This will next require a larger and more complicated load-sharing system and PMS functions for scheduling of gensets and ESDs.

In this project the main goal is to study optimal scheduling of gensets combined with an ESD in order to achieve a) *peak-shaving* of loads on gensets, and b) *strategic loading* of gensets using ESD power.

Work description

1) Perform a background and literature review, such as papers, articles, web-pages, reports, manuals, etc., to provide information and relevant references on:
   - Power management of hybrid electric marine power systems.
   - Gensets and ESDs.
   - Scheduling, peak-shaving, and strategic loading.

   It is of utmost importance to provide references all places where you use information from these sources. Write a list with relevant abbreviations and definitions related to the background study.

2) Provide a problem formulation for the thesis:
   a) Case study definition: Define a setup based on a ship type, hybrid power plant configuration (gensets and ESDs, with one bustie breaker between an A-side and B-side), an operation and corresponding load profile.
   b) State the control objective(s).

3) Describe relevant components in your power plant – that is, their properties, characteristics, dynamics, etc.

4) Describe relevant PMS functions for hybrid power systems, such as scheduling of power producers, loadsharing, spinning reserve, peak-shaving, strategic loading, etc.

5) Establish a simulation model for the case study – e.g. based on the Marine Systems Simulator. It is not necessary that you develop your own simulator. Instead you can configure an existing simulation model according to your plant. This must include also relevant behaviors of the ESDs, such as SoC and charging/discharging. See the works by Gurvin (MSc thesis 2017) and by Torstein I. Bø (Marine Power Plant Simulator - MSS toolbox). See also the PhD thesis of Michel Miyazaki.

6) Formulate relevant scheduling problems and the corresponding optimization problems – see the OMAE 2018 paper by Laxminarayan Thorat. New here is to include the ESDs as part of the scheduling problem. Propose a way of doing that, considering the cases:
   a) A single bus with two gensets and an ESD, and a test load time series on the bus:
      i) Perform scheduling while performing peak-shaving, that is, minimize fluctuation of gensets.
      ii) Perform scheduling while minimizing online capacity of gensets with ESD active (strategic loading), with constraints on SoC and charge/discharge.

   In each case, formulate the optimization problem on standard form, implement i Matlab, and test on your case study data. Discuss the results.

Tentatively:

7) For your optimal scheduling problems, consider the case of having two redundant buses connected through a bus-tie breaker. This is similar as above, but you must include functionality to handle if the bt-breaker is open or closed (as a given input signal).

Specifications

The scope of work may prove to be larger than initially anticipated. By the approval from the supervisor, described topics may be deleted or reduced in extent without consequences with regard to grading.

The candidate shall present personal contribution to the resolution of problems within the scope of work. Theories and conclusions should be based on mathematical derivations and logic reasoning identifying the various steps in the deduction.

The report shall be organized in a logical structure to give a clear exposition of background, results, assessments, and conclusions. The text should be brief and to the point, with a clear language. Rigorous mathematical deductions and illustrating figures are preferred over lengthy textual descriptions. The report shall have font size 11 pts., and it is not expected to be longer than 70 A4-pages, 100 B5-pages, from introduction to conclusion, unless otherwise agreed upon. It shall be written in English (preferably US) and contain the following elements: Title page, abstract, acknowledgements, thesis specification, list of symbols and acronyms, table of contents, introduction with objective, background, and scope and delimitations, main body with problem formulations, derivations/developments and results, conclusions with recommendations for further work, references, and optional appendices. All figures, tables, and equations shall be numerated. The original contribution of the candidate and material taken from other sources shall be clearly identified. Work from other sources shall be properly acknowledged using quotations and a Harvard citation style (e.g. *natbib* Latex package). The work is expected to be conducted in an honest and ethical manner, without any sort of plagiarism and misconduct. Such practice is taken very seriously by the university and will have consequences. NTNU can use the results freely in research and teaching by proper referencing, unless otherwise agreed upon.

The thesis shall be submitted with an electronic copy to the main supervisor and department according to NTNU administrative procedures. The final revised version of this thesis description shall be included after the title page. Computer code, pictures, videos, dataseries, etc., shall be included electronically with the report.

Start date: January, 2019 **Due date:** As specified by the administration.

Supervisor: Roger Skjetne
Co-advisor(s): Laxminarayan Thorat

Trondheim, 24.04.2019

Roger Skjetne
Supervisor

Preface

This master thesis was written by Ying Lu during the last semester of master's degree programme in Marine Technology at Norwegian University of Science and Technology (NTNU) Trondheim.

Ying Lu

11 June, 2019, Trondheim

Abstract

The increased power demand of shipboard electrical power system has produced considerable environmental pollution such as heavy fuel consumption and the emission of CO_2 and NO_x. In response to the degradation in the global environment, the maritime industry is experiencing a technical renovation at an ever-changing pace. The hybrid power system (HPS) which is a promising alternative to reduce fuel consumption, has aroused tremendous research interests. It takes the advantages of both a traditional electric-driven system and the energy storage devices (ESD), making it has not only higher energy efficiency but also lower noise and vibration level.

For a HPS, the demand for higher reliability and availability is higher than before. Therefore, a robust and smart power and energy management system (PMS/EMS) is required to control the power generation and distribution. PMS protects equipment from failure and reduces power loss, more importantly, maximises the performance through interaction with other control systems.

This thesis looks into the hybrid marine power system and uses the PMS to address the scheduling of gensets and Energy Storage System (ESS). Firstly, the configuration and mechanisms of the hybrid marine power system are described. The HPS model is developed in Simulink, including the genset, bus, ESS, and so forth. Secondly, the peak shaving strategy and optimal load sharing algorithms are proposed. The peak shaving strategy adopts the concept of energy band limited by ESS energy. The load sharing algorithm is based on the four working modes among the gensets and ESS. Lastly, two case studies of HPS subjecting to different level time-varying load are presented. The results show that good performances is achieved regarding load sharing with the mission of fuel consumption minimisation.

Key Words: HPS, PMS, ESS, Load sharing, Peak shaving

Acknowledgement

I would like to show my sincere gratitude to my supervisor, Professor Roger Skjetne, who offered me this thesis topic and the thesis guidelines. Also, I would like to thank my co-supervisor, Ph.D. candidate Laxminarayan Thorat, who shared his original model with me and the constructional advises on my thesis writing. A special thank to Ph.D. candidate Zhengru Ren for always supporting me.

11^{th} June, 2019, Trondheim

Ying Lu

Contents

List of Figures

List of Tables

Glossary

HPS	Hybrid Power System
PMS	Power Management System
EMS	Energy Management System
ESD	Energy Storage Device
ESS	Energy Storage System
BESS	Battery Energy Storage System
IMO	International Maritime Organisation
DP	Dynamic Positioning
MCR	Maximum Continuous Rating
FOC	Fuel Oil Consumption
SFOC	Specific Fuel Oil Consumption
AVR	Automatic Voltage Regulator
SoC	State of Charge
DoD	Depth of Discharge
AC	Alternating Current
DC	Directing Current
FPSO	Floating production, storage and offloading
KF	Kalman Filter
EKF	Extended Kalman Filter

MSS	Marine System Simulator
PPM	Process Plant Model
PID	Proportional-Integral-Derivative
MPC	Model Predictive Control
WF	Wave frequency
LF	Low frequency
DNV GL	Det Norske Veritas (Norway) and Germanischer Lloyd (Germany)
LR	Lloyds Register
DoH	Degree of Hybridisation
VSI	Voltage Source Inverter
CSI	Current Source Inverter

Chapter 1

Introduction

1.1 Background and motivation

For a long time, the issues of massive fuel consumption and atmospheric pollution caused by the maritime industry have not received universal attentions. In fact, ships which are similar to cars, are also the primary causes of environmental pollution. Figure 1.1 is a pie chart, which shows the percentages of the primary sources of CO_2 emissions in Norway. It illustrates that up to 40% of the CO_2 emissions are related to the maritime industry (oil and gas industry occupies 29% plus boats and ships 9%). In 2015, the International Maritime Organisation (IMO) estimated that the global marine industry would consume about 400 million tons of fuel every year by 2020 (Smith et al. 2015). Another analytical study by Lloyds Register (LR) concluded that the reduction in fuel consumption and emissions are the focus of global marine trends and also anticipated that the shipping emissions would double by 2030 according to the current Statistical data (Dimitris Argyros 2014). In urban densely populated ports and terminals, those air, water, and noise pollution caused by ships directly affect the human living environment, which should be taken seriously.

In response to the global call of a sustainable environment, the modern marine power system is challenged to evolve.

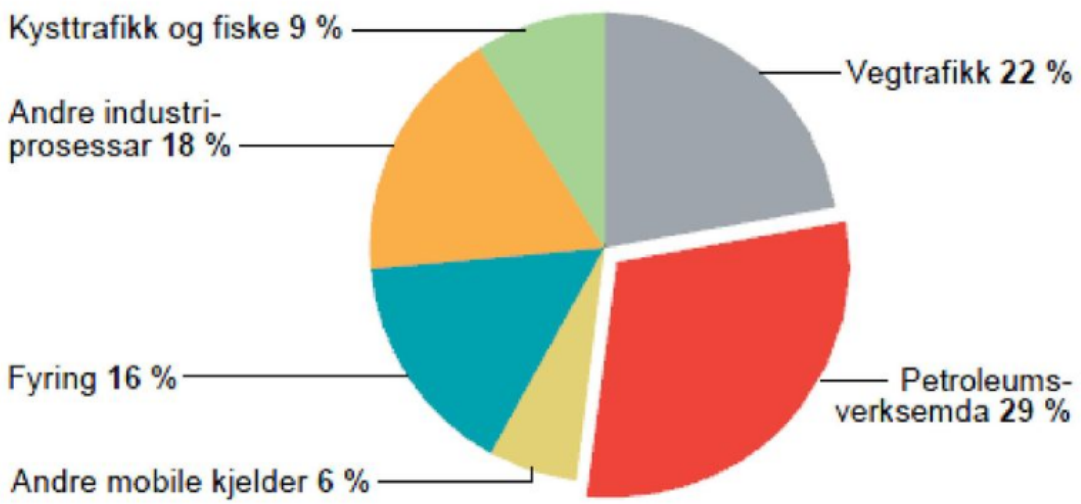

Figure 1.1: Distribution chart of primary causes of CO_2 emissions in Norway (Gudmundsson 2013).

1.1.1 New technologies

To reduce the fuel consumption and ocean pollution coming from ships, it is possible to start evolving from the diesel engine itself, such as improving the combustion mode, the working parameters, and the fuel quality. Other efficient methods that have broad applications in cars include the use of clean energy and hybrid power system (HPS).

Clean energy

One of the research direction is to utilise more clean energy, such as wind energy, solar energy, natural gas, and bio-diesel. A cruise boat named Solar sailor, sponsored by the Australia government in 2000, is the first ship which uses wind and solar panels to supply the power in the world. Though the vessel cost roughly 20% above the equivalent traditional vessel, it was expected to have the payback in 5 years (Moore 2000). This proves the possibility and economy of clean energy applied to ships.

The main roadblocks that make the clean energy less accessible so far are their characteristics of low energy density and unreliability in general ways. Typically, wind energy and solar energy are only used to supplement power in lighting or some auxiliary equipment for small-tonnage ships (Ren et al. 2019). The natural gas is another air-polite fuel that has been widely used in our daily lives. However, it necessarily requires the existed engines and generators

to have internal structure transformations, which imposes extra economic pressure to the ship owners. The bio-diesel is also a new energy resource with popularity these days though literature was not found regarding the usage in the large vessels.

Hybrid power system

A more promising alternative in the maritime industry today is to use the HPS, which can not only maintain reliability and dynamic performances but also increase overall load frequency and reduce fuel consumption (Hou 2017). The HPS refers to a system which is usually composed of two or more different types of power sources. In this thesis, we have considered a general power producer: the internal combustion diesel engine, and the Energy Storage System (ESS) such as batteries, flywheels, and super-capacitors. The applications of ESS in marine vessels has drawn more attention since it ordinarily requires less space and has a longer service life. It is believed to be able to effectively reduce the power fluctuations as a result of the variation of the environmental forces.

The world's first fully electric car and passenger ferry named Ampere, went into commercial operation here in Norway in 2005 (Explorer 2015). It was said it could save up to 60% of fuel consumption per year. Eidsvik also implemented the battery solution in an offshore vessel named Viking Queen (Eidsvik 2015). In addition, the guidebooks of using ESS as the redundant sources of power or replacements of the main power sources have been provided by many class societies such as DNV GL and LR, which contributes to attracting more researchers and manufactures into the field of HPS.

The basic working principle of HPS is that the engine and ESS drive together when the load is large, and the internal engine drags the load and charges the ESS through the generator while the load is relatively small. When the load is extremely small, the ESS is solely driven as long as there is sufficient energy stored.

The HPS stands out the conventional diesel-electric power system due to its ability to avoid transients of the diesel engine when encountering large load variations. Transients of the diesel engine could result in turbocharger lag which refers to the lack of air supply in the combustion chamber. During the time, The incomplete fuel combustion brings in larger amounts emission of NO_x and SO_x (Rakopoulos and Giakoumis 2009). Therefore, the HPS

is regarded as an effective and available approach to reduce environmental pollution, especially when being used in offshore vessels conducting long-term projects.

1.1.2 Power management system

With the increased shipboard capacity of offshore ships, more attention has been paid to the economy of electric propulsion while maintaining its safety and reliability. This is achieved by utilising the power management system (PMS) which has extensive applications in many large-scale electric propulsion systems such as Floating production, storage and offloading (FPSO), drilling vessels, and other offshore platforms.

The main purpose of PMS is to make sure that sufficient power is available for the electric demand on the ship. It is the core technology to control the electric grid because it has direct effects on all components and consumers. By monitoring and calculating the power supply of the generator units as well as the load demand from the consumers, the PMS can choose an optimised strategy from the power generation to the electricity use. It can also minimise the power loss and fuel consumption to meet the requirements of various operating modes such as navigation, dynamic positioning (DP), and maneuvering.

In the PMS, the mechanical energy produced by the prime mover is firstly converted into the electrical energy by the generator, which is later directly transmitted to the propulsion motor. The electric motor then converts the electric energy into mechanical energy for the propeller, resulting in the movement of the ship. The propeller system is the main power load, generally consuming around 70%-80% of the total power and considered to be extremely important to the safety of the ship. With PMS, it is feasible to control and optimise the power generation according to load demand by the propeller, maximise the ship performance, and, most importantly, prevent the system from failures.

A considerable number of literature has investigated the applications of PMS in the hybrid marine power system. A case study by Radan et al. 2016 showed that the optimal use of PMS integrated with ESS leads to a fuel reduction up to 30% and genset operating duration by 48% compared to a non-optimal use of power system. The authors (Bø 2016; Dahl, Thorat, and Skjetne 2018) adopted the approach of the adaptive Model Predictive Control (MPC) for the scheduling of power control in different PMS systems. Another author (Han, Charpentier,

and Tang 2014) developed a mathematical model of using both fuel cell and battery banks, and presented a PMS solution for the power control in a low power boat. Another paper by Thorat and Skjetne 2018 used linear programming for optimal online load sharing and minimisation of specific fuel oil consumption.

1.2 Objectives

The present thesis aims to develop a control model of a hybrid marine power system and utilise a functional power and energy management system for the scheduling of gensets and ESS. By conducting simulations, the main target is to study the scheduling of gensets combined with an ESS. Optimal controlling strategies of the PMS are proposed to achieve: a) peak-shaving of loads on gensets, and b) strategic load sharing of gensets using the ESS power.

1.3 Thesis outline

Chapter 2: Gives an introduction to the primary devices in the modern diesel-electric propulsion system along with their dynamic characteristics.

Chapter 3: Includes a brief review of ESDs, with emphasis on the modeling of the battery by using State of Charge (SoC).

Chapter 4: Introduces the functions of PMS, and the working principles of peak shaving and load sharing.

Chapter 5: Develops a mathematical model of the hybrid marine power system based on the dynamic characteristics which are described in Chapter 2 and Chapter 3.

Chapter 6: Proposes a scenario-based control scheme for scheduling of load sharing, and an optimal peak shaving strategy. The algorithms of PMS, switching among working modes, and calculation of fuel consumption are presented.

Chapter 7: Conducts several case studies to verify the fidelity of PMS algorithms. The peak shaving results by utilising ESS are also shown.

Chapter 8: Conducts two case studies of HPS subjecting to different levels of time-varying load. The goal is to discuss the feasibility and efficiency of the algorithms from the simula-

tion results.

Chapter 2

Hybrid marine power system

HPS is recognised as the most practical and efficient approach to decrease fuel consumption and gas emissions so far. In this thesis, except for diesel generator set being as a prime mover, a ESS is added to the power grid to produce large thruster output in a short time. The dynamic characteristics of primary components for the diesel-electric propulsion system are explained in this chapter while the ESS is introduced in the next Chapter.

2.1 Diesel generator set

The ship electric propulsion system refers to using the electric motor, generally the DC motor or AC motor to drive the ship propeller instead of directly using the prime mover to drive the propeller. Figure 2.1 is a single line diagram that shows a typical configuration of main components in a modern diesel-electric propulsion system, including the gensets, switchboard, bus-tie, converter, motor, and thruster.

A modern diesel generator unit is composed of engine, governor, excitation system, and synchronous generator. Being as an essential power generation equipment, it requires a necessary speed and voltage control by the AVR and the governor, as shown in Figure 2.2.

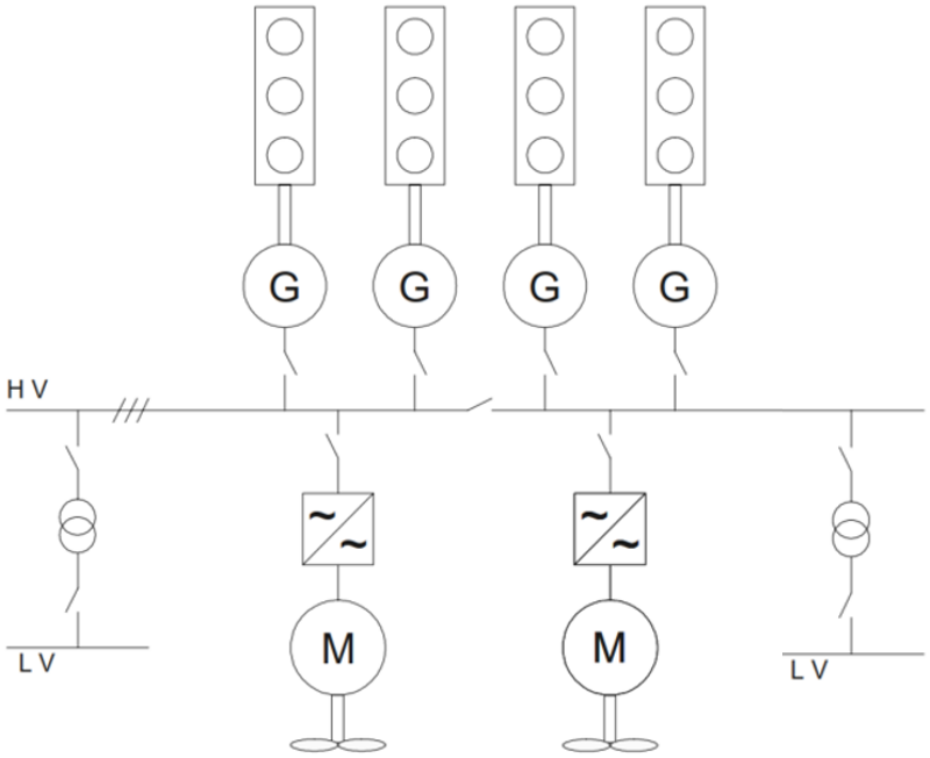

Figure 2.1: A typical single-line diagram of a diesel electric propulsion system including multiple gensets, converts, switchboard, bus-tie, motor, and thruster.

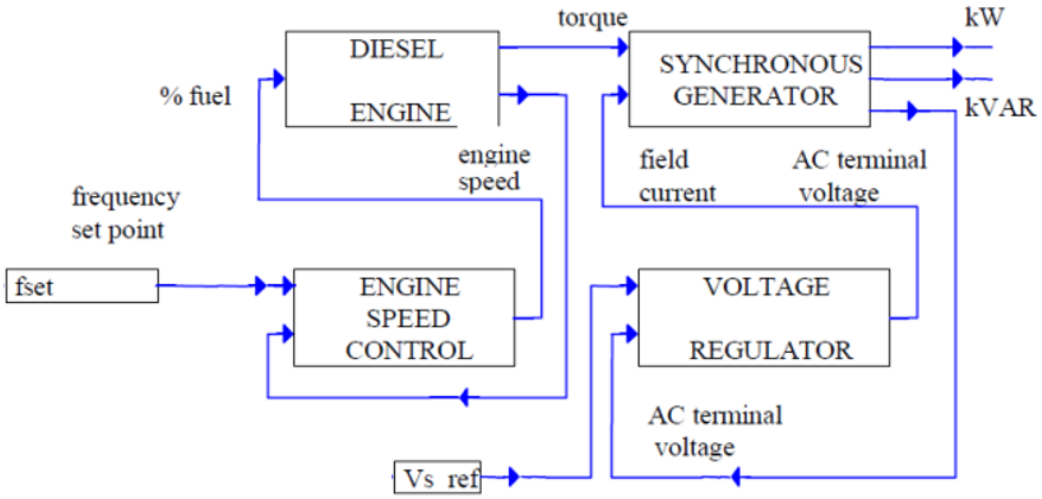

Figure 2.2: Schematic diagram of speed and voltage control in a genset (Benhamed et al. 2016).

2.1.1 Diesel engine

Nowadays most diesel engines are four-stroke engines. Four strokes refer to suction stroke where the fuel is injected, compression stroke where the air is compressed to produce high

pressure and temperature, power stroke where fuel consumption happens, and exhaust stroke where burned exhaust gas is released. The fuel combustion produces an amount of heat energy to drive the rotation of the shaft, in other words, the heat energy is transmitted to mechanical energy. In an inline-four stroke engine, there is always one piston doing work, making the four-cylinder engines usually run more smoothly. Since the fuel is consumed once every four strokes, the four-stroke engine has a higher fuel efficiency than the two-cylinder engines.

In a diesel-electric propulsion system, the diesel engines are mostly medium-speed driven because of lower weight and costs (Ådnanes 2003). Figure 2.3 is an example of the Specific Fuel Oil Consumption (SFOC) of a medium-speed diesel engine where its optimum operating range lies between 70% to 80% of the power. The X-axis refers to the ratio of average power output and maximum continuous rating (MCR). It shows that a medium-speed diesel engine has a fuel consumption of less than 200g per kWh at the lowest power rating. It is hence a vital goal to keep the diesel engine rotating at its optimal operating speed.

Another point to state is that the efficiency of the diesel engine features a significant drop when there is a massive load raise in the bus. In this process, sufficient air can not enter the turbocharger immediately. Therefore, un-full fuel combustion is mostly possible to happen, and a large amount of harmful gas is hence produced.

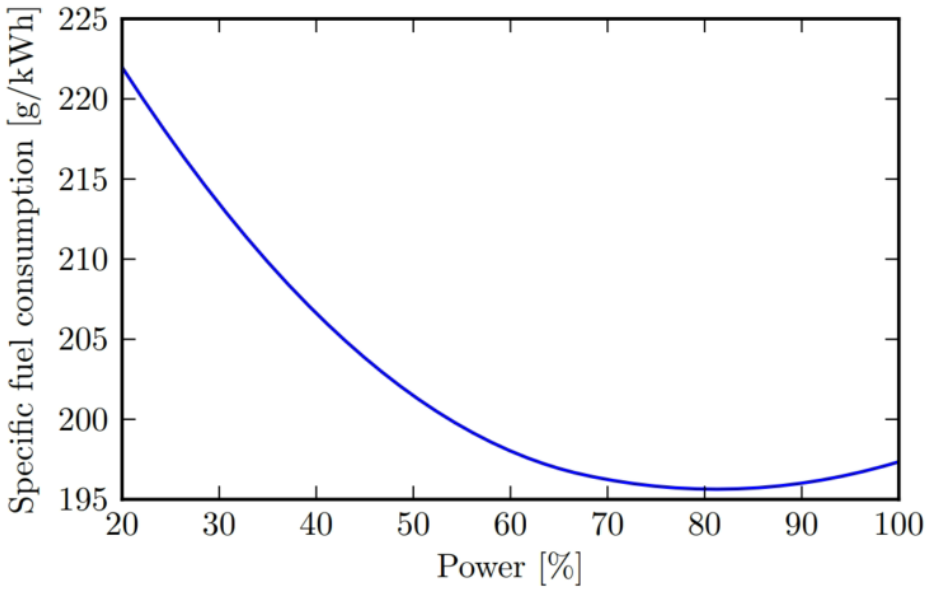

Figure 2.3: SFOC of a typical diesel engine (Bø 2016).

2.1.2 Generator

The generator is an electric device that converts the mechanical energy produced by the diesel engine into electrical energy based on the Faraday laws of electromagnetic induction. There are a variety of generators such as DC generator, AC generator, single phase generator, three-phase generator, and so forth. The primary components of generators are the non-rotating part called stator, and the rotating part called rotor. In most generators, the rotor which has the poles acts as an electric-magnet while the stator with armature windings usually carries high current level. Then the relative movement between the stator flux (magnetic field) and the rotor windings induce the field current, which results in the generation of voltage. The stronger magnetic field which gives a higher rate of flux change leads to a higher voltage.

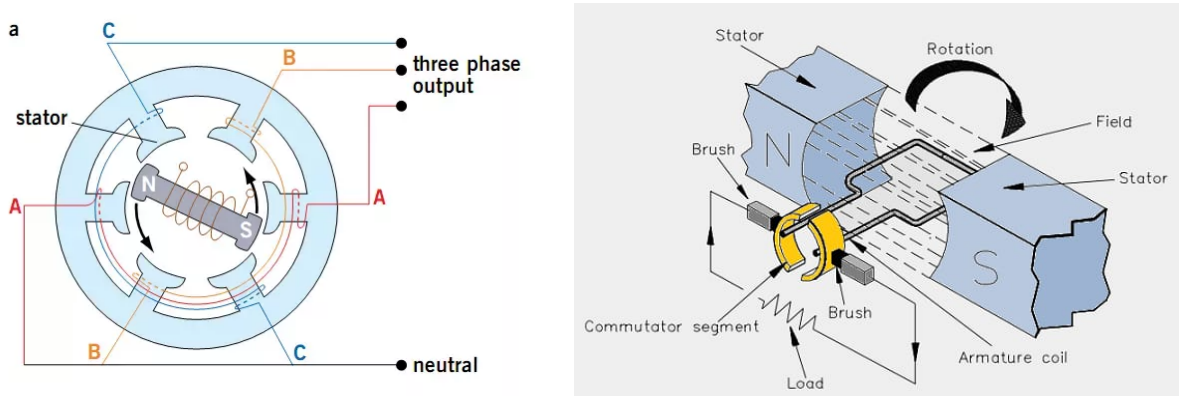

Figure 2.4: Working principle of the a three phase AC generator: the three phase structure (left), and the rotor is cutting the stator flux to produce the alternating current (right) (Butler 2003).

Synchronous generators are the most widely used three-phase AC generators applied in the heavy-load ships. The working principle is summarised as: firstly, A DC is provided to the rotor, making the rotor becomes an electric-magnet with N poles and S poles. Then the prime mover (the diesel engine) drives the rotor to rotate which creates an opposite direction of the magnetic field in the stator. The magnetic field of stator rotates following the rotation of the rotor to induce the three-phase voltage, as seen in Figure 2.4. The three-phase voltages have the same magnitude but 120 out of phase in time. The synchronous refers to the frequency of the induced voltage is in synchronism with the rotor speed.

In general, there are three types of excitation method of DC in the rotor windings (Shahl 2010):

- Slip rings: a gadget mounted on the rotor which links the rotor's field winding to an external DC source. The excitation current/voltage can be adjusted by moving the slip rings to change the magnetic field.
- DC generator exciter: a device that is directly connected to the AC generator to provide DC.
- Brushless exciter: a device that has a rotating rectifier and field circuits mounted on the rotor, and armature circuits on the stator. The armature circuits create a magnetic field that induces current in the field circuits on the rotor. The induced current then is converted to DC by the rotating rectifier, as seen in Figure 2.5. It is often applied On large generators and motors.

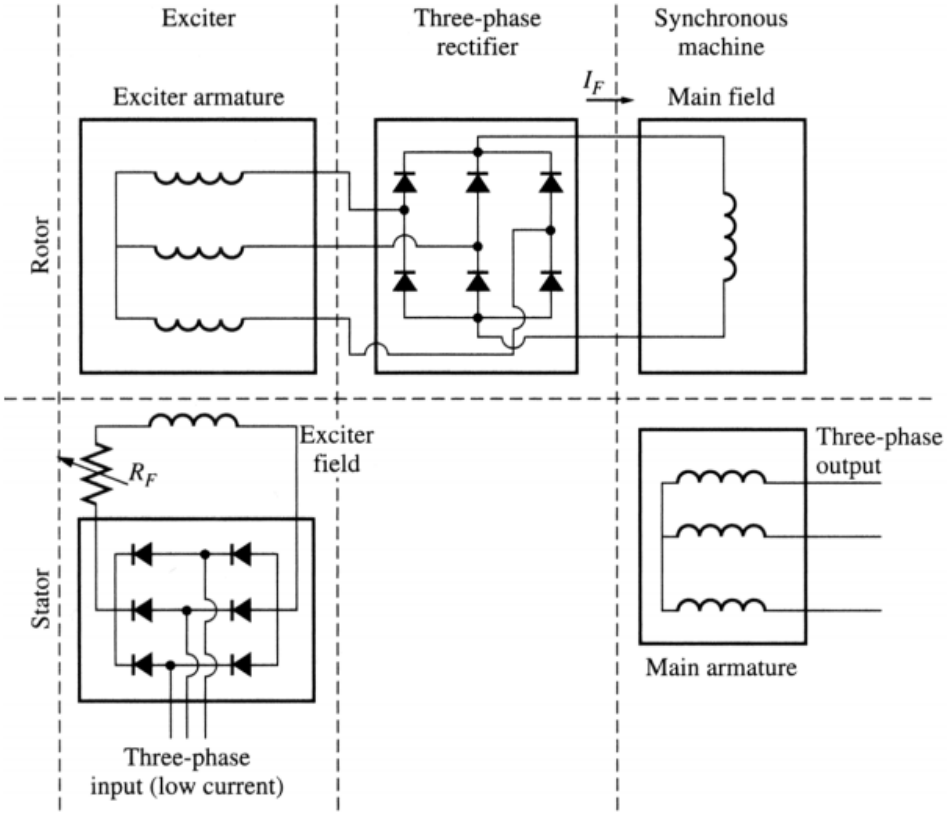

Figure 2.5: The working principle of brushless rectifier (UNLV 2013).

The frequency of induced voltage f depends on the rotational speed which is given by:

$$f = \frac{\omega}{2\pi} = \frac{P \cdot \omega_m}{2\pi} = \frac{(P \cdot 2\pi \cdot n)/60}{2\pi} = p \cdot \frac{n}{60} \tag{2.1}$$

where p is the number of pole pairs, ω_m is the mechanical speed, n is the rotational speed

of the rotor. The high-speed synchronous generator has a small p such as 1 or 2 while the low-speed generators may have a more significant number.

2.1.3 Governor

The speed governor is a device used to regulate the mean speed of the engine to a predefined level whenever the load changes. If the load on the engine increase, the engine rotational speed decreases. Then More fuel should be injected to the combustion chamber for raising the speed to its standard operating value. Speed governor can detect the actual speed and compare it to the reference value, then alter one valve in the engine to control the supply of fuel to the cylinder (Fukui et al. 1992). If the actual speed is smaller than the desired speed, the governor will increase the fuel and vise versa. In this way, the engine can avoid damage due to extremely high operating speed, and the generator can obtain a stable speed within acceptable variation limits. Section 4.2.1 gives the details of governor modeling.

2.1.4 Automatic voltage regulator

Sudden change in the load tends to cause variation in the voltage output. To avoid the variation, the excitation system should change correspondingly to make the terminal voltage generated as usual, which is controlled by Automatics Voltage Regulator (AVR). The AVR detects the terminal voltage of the generator and compare it with a stable reference, which gives the voltage error. Then it adjusts the field current to convert the fluctuated terminal voltage into the constant one. It also reduces the overvoltages which could occur due to a sudden loss of load in the system. However, it usually has a slow response to fast transient load. The working principle of AVR is shown in Figure 2.6.

2.2 Converter

2.2.1 Rectifier

A rectifier is one kind of converter that converts AC to DC by allowing one direction of current to pass. This is done with the help of several semiconductors such as diodes and thyristors

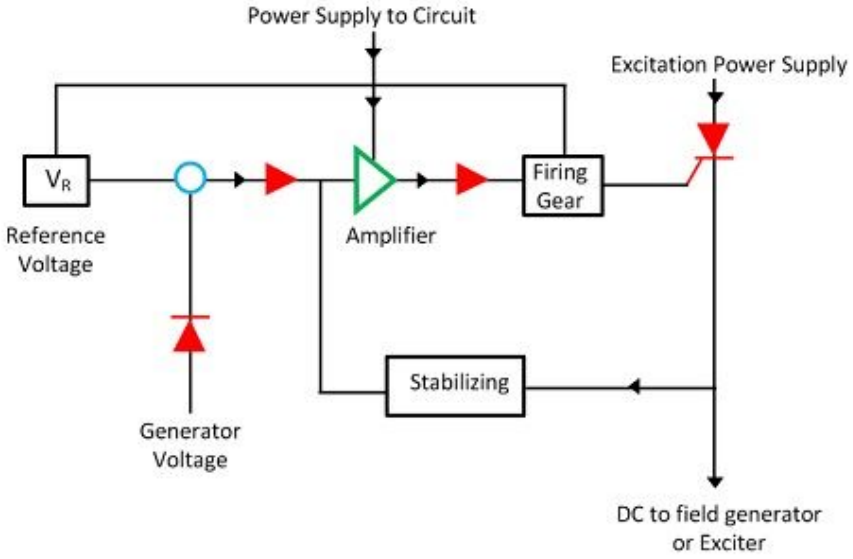

Figure 2.6: Schematic overview of AVR working principle (Global 2017).

which allow current to pass only when it is forward biased. The rectifier is important to the energy transmission system because most loads are charged with DC while the current on the main bus is AC. It is easier to manipulate the DC waveform which is nearly a straight line than the sinusoidal AC waveform. There are basically two types of three-phase rectifiers: half-wave rectifier and full-wave rectifier (Gao 2015).

The Half-wave rectifier has 3 thyristors which are star-connected. With only one thyristor on the line, only the positive current is allowed to pass through. In other words, half of the waveform is blocked by the thyristor. Figure 2.7 shows that the signal output from rectifier is in phase with the highest voltage magnitude.

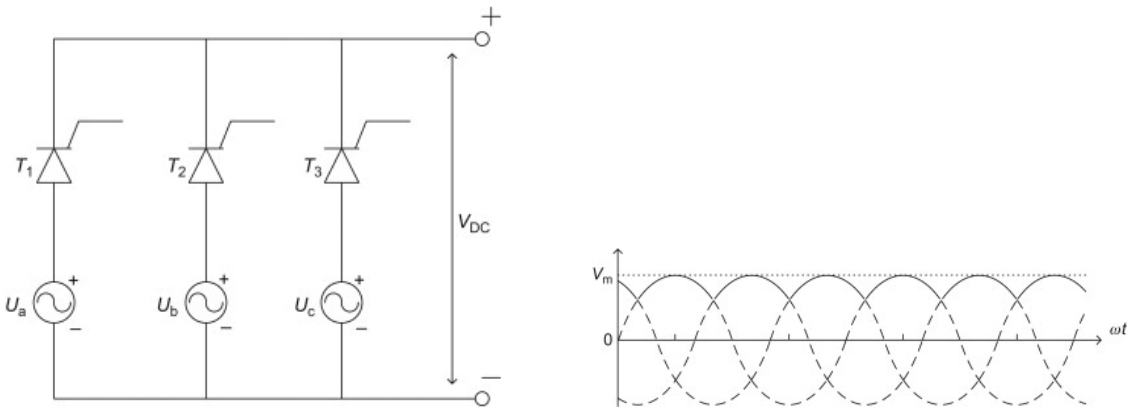

Figure 2.7: Working principle of a half-wave Rectifier: Configuration (left) and the signal output (right) (Gao 2015).

The full wave rectifier has six thyristors connected in a bridge structure. The thyristors can be turned on and off to control the current flow. Two thyristors with opposite directions on one line allow both positive current and negative current to pass through. Figure 2.8 shows the configuration and the signal output of full-wave rectifier. In fact, a more cheap way to achieve the same performance is to use 3 thyristors and 3 diodes since it is sufficient to control on or off of 3 diodes.

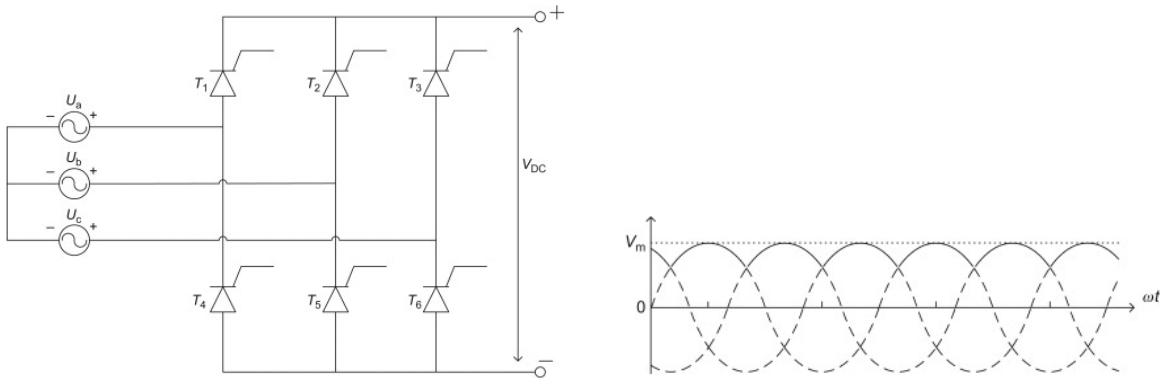

Figure 2.8: Working principle of a full-wave rectifier: Configuration (left) and the signal output (right).

2.2.2 Inverter

Inverter, conversely, is the electric device that converts DC to AC. Like rectifier, a three-phase inverter is composed of 6 transistors connected in a bridge structure. Therefore, sometimes the inverter is bi-directional and can be also used as a rectifier. There are two different types of inverter: voltage source inverter (VSI) and current source inverter (CSI) with similar structures, as seen in Figure 2.9. The major difference of two types is that the CSI usually has capacitors connected in the load branch and a conductor with the source branch with the purpose to avoid high current variation when loads change (Gao 2015).

2.3 DC link

As the name implies, the DC link is the electric device that connects the rectifier and inverter. The electric system employed in the ship requires high frequency to drive the motor. In order to meet the requirement, the input provided to the three-phase inverter should be constant

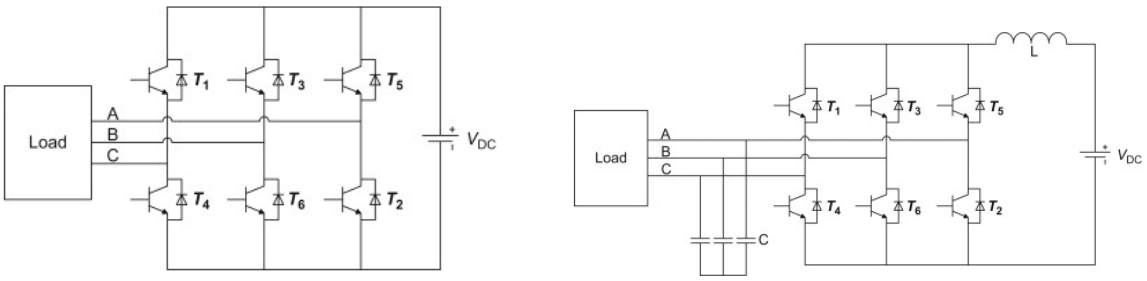

Figure 2.9: Configurations of the two different types of inverter: Voltage Source Inverter (left), and Current Source Inverter (right) (Gao 2015).

high-frequency DC voltage. However, the output of the rectifier is the pulsating DC which cannot be directly used by the rectifier. By implementing a high rating capacitor with enough DC voltage storage between the rectifier and the inverter, a large amount of DC voltage can be stored in the DC link capacitor and released constantly and smoothly to the inverter. To summarise, the dc link capacitor acts as an energy storage device in the inverter which can help prevent the transients from the load side from going back to the distributor side and also serves to smoothen the pulses in the rectified DC.

The selection of a DC link depends on the power rating of the drive. With lower voltage, the DC link usually utilises a capacitor while with higher voltage, it may have an inductor connected in series and a capacitor connected in parallel. In this thesis, only a DC link capacitor will be used.

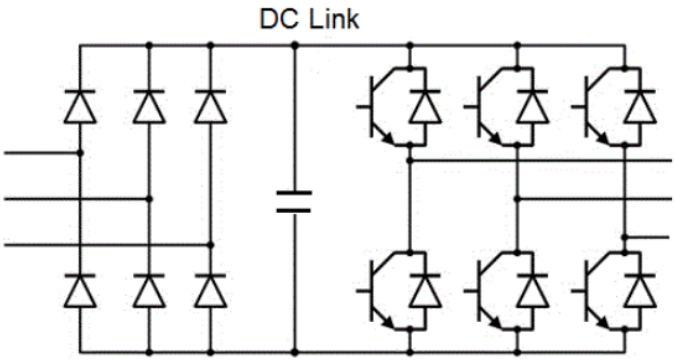

Figure 2.10: DC link capacitor

2.4 Motor

The motor is usually the destination to which energy flows. It converts the electrical energy into mechanical energy again, resulting in the movement of the thruster and the vessel. It is also the major electric consumer where up to 75% of the energy is consumed. The motor has two main categories: the AC motor (includes the induction motor and synchronous motor) and the Dc motor. Two main standards can be used to differentiate them. Firstly, the power source, as name indicated, are AC and DC respectively. Secondly, the speed of DC motor is controlled by varying the armature winding's current while the speed of an AC motor is controlled by varying the frequency (Carrow 2000).

A DC motor is the one that powered from DC such as a battery or an AC-to-Dc power converter, and it has brushes and a commutator except for the stator and rotor. An induction motor is named because the electric current in the rotor that required to produce the mechanical force is obtained by electromagnetic induction from the magnetic flux created by the current-wounded stator. Synchronous motor refers to that the frequency of the shaft rotation is in synchronised with it of the current supplied to the stator. Induction motor occupies the largest share in the marine industry due to its simple, brushless, low-cost structure (Patel 2011).

Most of the induction motors have three stator coils wound with wires which are shifted in 120, and the rotor in a squirrel-cage configuration, as seen in Figure 2.11. The current of stator coils in the P-poles configuration creates a magnetic flux that rotates at a constant speed of n_s. This is the synchronous speed, given by (Patel 2011):

$$n_s = \frac{120 \times f}{P} \tag{2.2}$$

where f is the bus frequency and P is given by

$$P = \frac{\pi \times statordiameter}{statorcoilspan} \tag{2.3}$$

The induction motor is technically a special transformer which converts the energy by the use of magnetic flux instead of the electrical connection, brush or the slip rings. Compared to other types of motor, it is rugged and has a longer life expectancy.

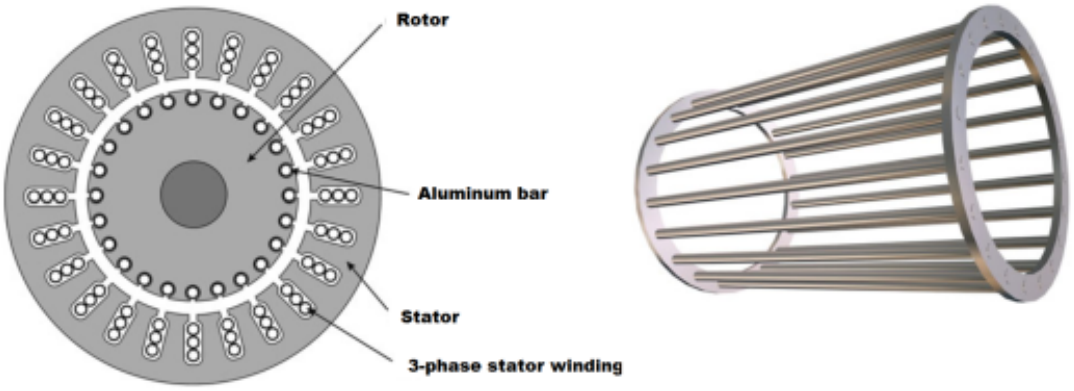

Figure 2.11: Three-phase induction motor (left) and its squirrel cage construction (right) (Borutzky 2011).

The rotor speed n_r is normally smaller than the synchronous speed n_s, which gives the identification of rotor slip s. The equation of s is given by

$$s = \frac{n_s - n_r}{n_s} \tag{2.4}$$

2.5 Transformer

The transformer is used to connect the ESS and the DC bus to ensure the voltage output of ESS coincide with the constant bus voltage. The transformer is the static device that transfers power from one circuit to another circuit with different frequency. It is widely used for increasing or decreasing the alternating voltages in the electric circuit due to its simple structure. The DC-DC transformer used in battery circuit usually requires high energy conversion efficiency.

Figure 2.12 shows that a transformer mainly has three parts: the primary winding, the secondary winding, and the magnetic core. The varying current in the primary windings causes varying flux, which passes through the laminated core, delivering power to another circuit. The voltage equations of the transformer is expressed by

$$a = \frac{T_1}{T_2} = \frac{V_2}{V_1} \tag{2.5}$$

where a is the turn ratio, T_1 and T_2 are the number of the windings on the primary and

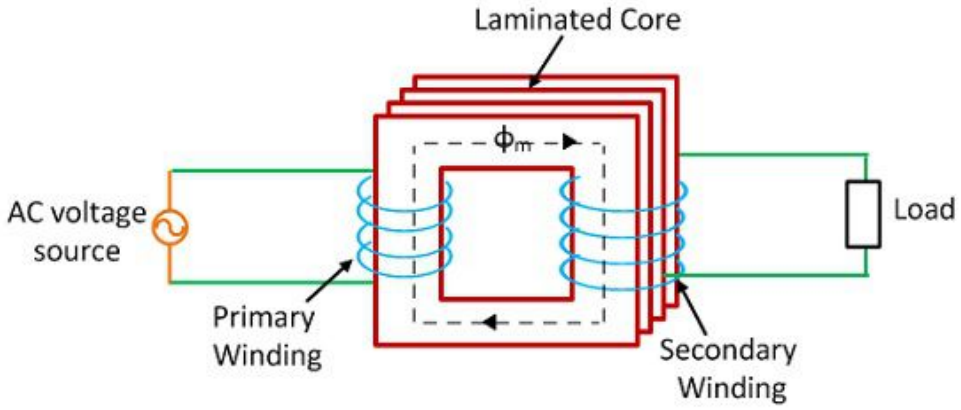

Figure 2.12: Working principle of the transformer (Global 2017).

secondary side, respectively, and V_1 and V_2 are the voltage on the two sides.

Chapter 3

Energy Storage Systems

This chapter introduces the categories of ESS, the ESS connection ways to the power plant, and the methodology of battery modeling.

The benefits of implementing ESS in the shipboard electrical system are multi-folds (Radan et al. 2016), as summarised in the following:

- Allows for fewer generators connected to the grid, which increases the load response per individual engine and the power efficiency in most cases.
- Acts as a power reserve source to prevent the power plant from failure due to its little response time to the load demand.
- Reduce unnecessary fuel consumption and shipping emissions.
- Limit the number of generator start/stops. This can avoid unnecessary delayed time and worn in generators, thus enhancing system safety and reliability.

3.1 Types of ESS

Figure 3.1 gives a overview of four types of ESS different in energy density and power density, including the capacitor, the super-capacitor, the batter, and the fuel cell.

The energy density refers to the amount of energy stored in a unit mass, and the power density refers to the amount of power stored in a unit mass. An ESS with a high energy density is capable of storing a large amount of energy in a small mass. However, it does not necessarily

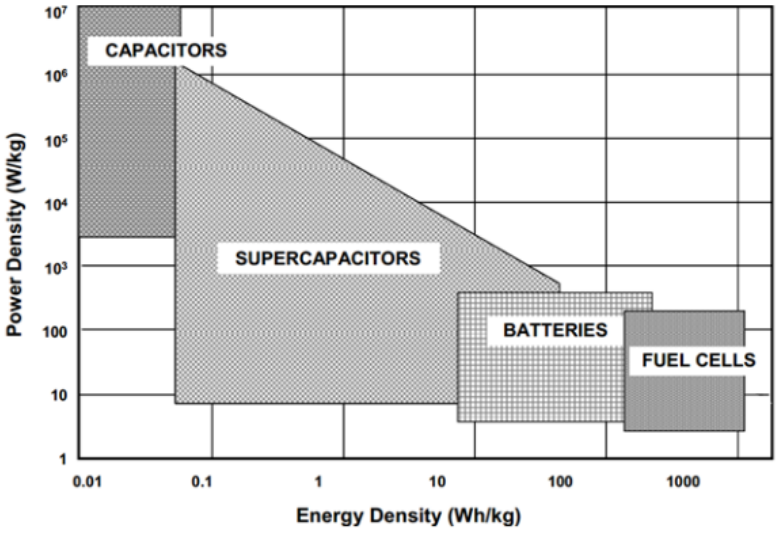

Figure 3.1: Schematic overview of THE power and energy density of four main types of ESS (Kötz and Carlen 2000).

mean the system has larger power output. An ESS with a high power density is capable of providing a large power output quickly. In Figure 3.1, the battery has a high energy density but a low power density, meaning it can provide relatively small power in a long time. The capacitor has a high power density but a low energy density, meaning it can quickly give off the power which lasts for a short time (Layton 2008).

3.1.1 Flywheel

The flywheel is usually attached at the end of the engine or attached to the crankshaft to reduce speed fluctuation during engine operation. The engine speed is discontinuous since the working process of engine's each cylinder is discontinuous. The flywheel has a large moment of inertia, so it can store a large amount of energy when the engine speed increase and release energy when the engine speed decreases.

The flywheel is suitable for providing short-term power, for example, a period of 15 mins because of its high cyclic ability and quick charge/discharge characteristic. However, the biggest disadvantage of the flywheel is the high cost and high self-discharge rate which is typically over 20% per hour (Zhou et al. 2013).

3.1.2 Super-capacitor

The Super-capacity is another energy storage device that is widely used in the HPS. Its working principle is similar to the standard capacity but has a much higher capacitance and a lower voltage limit. It is usually used in series with a battery to provide the power. It has similar advantages with flywheels where instant charge and discharge can happen. Besides, the lifespan of a super-capacitor is much longer than the rechargeable batteries as it usually has more than 100000 charge cycles. However, the low energy density and high-discharge rate make it can absorb or release a high amount of power only for short-term operation. It can lose as much as 10-20% of their charge per day. Another disadvantage is that its lifetime is greatly affected by the varying temperature and voltage.

Note that the super-capacitor is not appropriate for smoothing the power on a period longer than 1 min (Zhou et al. 2013). Unlike battery which provides almost a constant voltage regardless of the load variations, the super-capacity has the more massive voltage loss with varying load.

3.1.3 Fuel cell

The fuel cell is the chemical device that directly converts the chemical energy of a fuel into electrical energy. It is similar to a battery but with no need for being charged by the external connections, since it uses oxygen as the catalyst. It is capable of producing energy as long as there is fuel inside the device. It is recognised as one of the most promising electric technology as it has minimal gas emission and no noise pollution. However, the challenge in production, storage, and high cost in maintenance make it a less common choice for HPS used in ships.

3.1.4 Battery

The battery is the most widely used ESS in HPS, especially for cars due to its economy and high energy density. Table 3.1 compares a typical Li-ion battery and super-capacitor in many specific aspects. Though super-capacitor is overwhelming in cyclability and operating temperature, it's application is limited by the high discharge rate where battery stands out. It

is also an economic choice to choose battery instead of the super-capacitor due to obvious price advantage. Considering the scale of ship type and its long-term task, the battery has more reasons to be applied in this thesis.

Table 3.1: Comparison between the super-capacitor and Li-ion battery

Features	Li-ion Battery	Super-capacitor
Gravimetric energy (Wh/kg)	100–265	4–10
Volumetric energy (Wh/L)	220–400	4–14
voltage of a cell (V)	3.5	2.7–3
Power density (W/kg)	1500	3000–40000
Resistance (Ω)	500	40–3000
Efficiency (%)	75–90	98
Cyclability	500-1000	500 000–20 000 000
Life	5–10 years	10–15 years
Self-discharge (% per month)	2	40–50A
voltage on discharge	stable	decreasing
cost per kWh	200–1000 €	10 000 €
Charge temperature	0–45	-45–65
Discharging temperature	0–45	-45–65

To conclude, for short-term applications, the flywheel and super-capacitor are more appropriate candidates; whereas, for a long-term marine power system, the battery and fuel cell are more safe and smart choices.

3.2 Battery energy storage system

Figure 3.2 gives a brief scheme of variable application of BESS based on the requirements. BESS is a practical solution when it comes to load levelling, frequency control, and peak shaving.

Frequency control

In the real electric industry, an auxiliary generator which operates far below its rated capacity in the grid is used to supplement in case of the failure/loss of the biggest genset. The BESS can be a better alternative to increase the system frequency if unexpected generator loss happens due to its faster response time. It can release full capacity in a few milliseconds compared to that a typical generator needs 15–30 s.

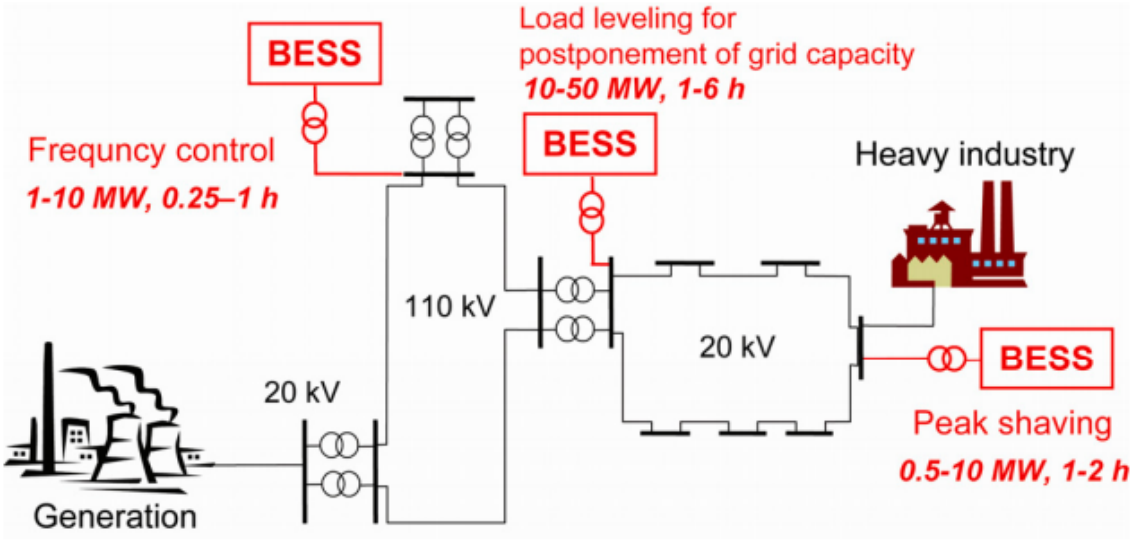

Figure 3.2: Specific application of BES in an electric power system (Oudalov et al. 2006).

Load leveling

The increased demand for onboard electricity requires the instalment of transmission and distribution facilities, which might takes years and extra cost. The BESS can help to postpone the instalments by supporting the load demand from the high-electricity consumers. When it is connected to the final use of electricity, i.e., the consumer side, it can be used to store energy during night hours and release the energy during day hours.

Peak shaving

The end-user peak shaving can be achieved by instalment of BESS. Peak hours usually last for a short time, which can be easily compensated by the stored energy in the BESS. The electricity bills hence, are reduced.

3.2.1 Types of connection

Generally, there are two types of BESS connection ways in the HPS: the series connection and the parallel connection.

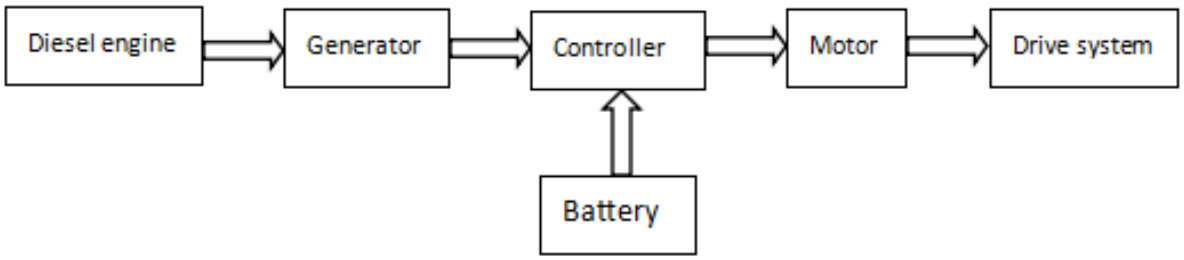

Figure 3.3: Sketch of the series connection in HPS.

Series connection

Working principle: The diesel engine drives the generator to generate electricity for the motor to drive the transmission system and to charge the battery. The battery drives the motor separately at start-up and low load or drives with the genset during motor acceleration.

Parallel connection

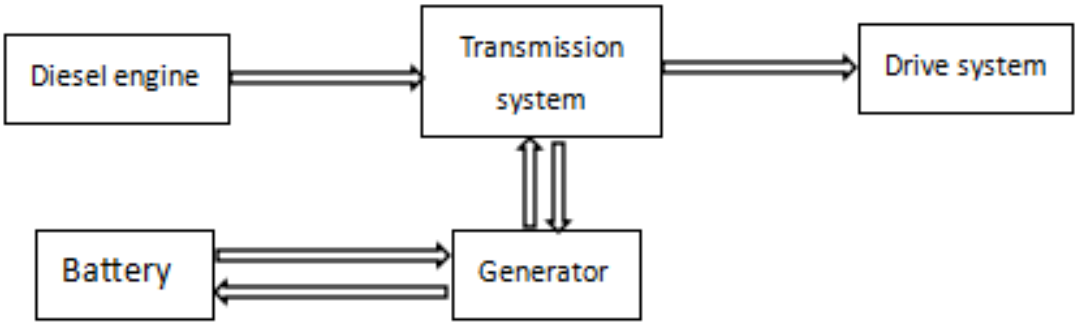

Figure 3.4: Sketch of the parallel connection in HPS.

Working principle: The engine and the battery/motor can independently supply torque to the transmission system, either separately or together. The generator is an AC synchronous generator which can also be used to charge the battery. The power transmission through the diesel engine, the transmission system, and the generator can be realized by a mechanism such as a planetary gear.

3.2.2 Types of battery

Types of the battery includes the lead-acid battery, nickel-based battery, Li-ion battery, flow battery, and so on. The Table 3.2 gives a brief comparison of fours types of commonly used battery.

Table 3.2: Comparison of four commonly batteries used in HPS ((Emmanuel 2018)).

	Lead-acid	Ni-MH	Ni-Cd	Li-ion
Degree of maturity	⋆⋆⋆	⋆⋆	⋆⋆	⋆⋆⋆⋆
Energy Density [Wh/L]	200-500	140-300	50-150	300-700
Self-discharge rate	\	1.3-2.9%/month	10%/month	\
Cycle life	1000	180-2000	2000	1500
Total efficiency%	72-78	66-92	72-78	80-90

Li-ion battery is used in the thesis. It has advantages of lighter weight and smaller volume than other types of battery. It also has the highest energy density from 50-150 Wh/L and the highest power density from 500-2000 w/kg among all batteries. Other benefits include a high efficiency, low memory effect, and a low self-discharge rate. Its drawbacks includes the short lifetime about 3000 cycles at 80% depth of discharge and the characteristic of being fragile sometimes. Besides, the battery's lifespan is greatly affected by temperature and deep discharge (Zhou et al. 2013).

3.2.3 Methodology of battery modeling

Over the years researchers around the world have built effective models of different types of battery. There are mainly three commonly used types of battery models with various applications: electrochemical mechanism model, mathematical models, and equivalent circuit-based model (Chen and Rincon-Mora 2006).

The Electrochemical model, considered to have the highest accuracy but is coupled with high complexity, mainly applied for simulation of the inner design aspect of the battery. It is of great difficulty to establish a mechanism model in practical applications from the highly nonlinear characteristic curves, as shown in Figure 3.5. It can be seen that the voltage of the battery is affected by the temperature, discharge capacity, and many other factors.

The Mathematical model requires massive experimental data to predict the battery performance. Besides, it is usually used for the analysis of specific factor of the battery such as the

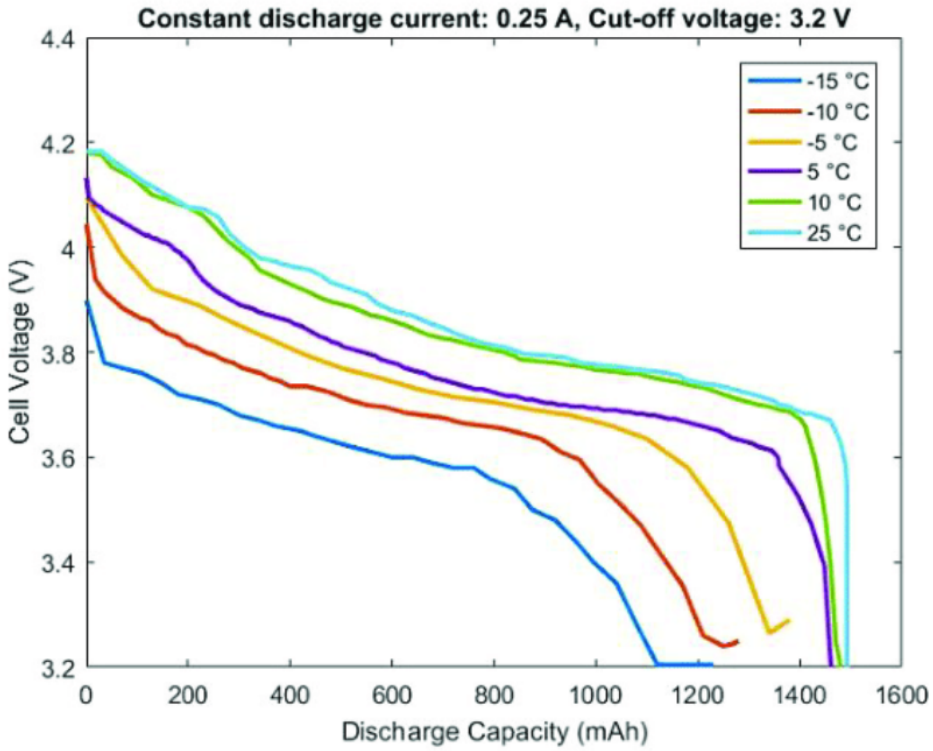

Figure 3.5: Typical Li-ion battery discharge characteristics

runtime and capacity rather than a comprehensive reflection of batter characteristics. Those two ways of modeling battery are not appropriate regarding the purpose of SoC estimation for battery (Tremblay, Dessaint, and Dekkiche 2007).

The equivalent circuit-based model uses the basic circuit components to describe the operating characteristics of the batter as well as taking into account the influence of various factors such as the voltage, current, temperature, polarisation, and so forth. The model is intuitive and easy-to-build, thus widely used. There are three types of electrical model: Thevenin-based, Impedance-based, and runtime-based, where the Thevenin-based type is commonly adopted.

State of charge is an influential factor which refers to the measure of available capacity stored in the battery. SoC is expressed as a ratio of its nominal capacity, as given by

$$SoC = SoC_0 - \frac{\int_0^t i\,dt}{Q} = 1 - DOD \tag{3.1}$$

where SoC_0 is the initial SoC, DOD is the abbreviation of depth of charge, defined as the ratio

between the amount of discharge along time and the rated capacity of battery Q [Ah].

$$DOD\% = \frac{\int_0^t i\,dt}{Q} \tag{3.2}$$

The precise battery modeling is composed of two steps: Firstly, the real-time of battery SoC is estimated. On-time method and Kalman filter (KF) method are the two commonly used methods for the SoC estimation. Secondly, the relationship between the load voltage U and State of Charge SoC, the number of cycles N, temperature T and current I is developed, which is usually expressed as the function $U = f(SoC, I, T, N)$.

The author developed an ideal model for acid battery by taking into account the internal resistance and temperature compensation (Dürr et al. 2006). However, the battery SoC used in the paper is developed based on low discharge experiments. developed A more complicated model for Ni-MH battery based on an open circuit voltage and internal resistance is developed (Kuhn et al. 2006). The application of this model is limited as all the parameters used are impedance spectroscopy. Another author proposed a method to describe the battery operating condition based on Extended Kalman Filtering (EKF) where no algebraic loop is produced (Plett 2004).

In this thesis, a generic method based on the works of Shepherd 1965 and Tremblay, Dessaint, and Dekkiche 2007 is used. Both method only uses SoC as the state variable to describe the discharge characteristic of a Li-ion battery.

Details and equations are described in Section 5.5.

Chapter 4

Power Management System

For hybrid marine power system, PMS is essential to achieve its best safety and reliability. This chapter presents the functions of PMS, the approaches for load sharing and peak load control. With the optimal control strategies and a proper equipment configuration, PMS can maximise the fuel economy by reducing fuel consumption and increasing load efficiency.

4.1 Functions of PMS

Based on Ådnanes 2003, the PMS is comprised of the following three subsystem:

- Power generation management
- Load management
- Distribution management

The power generation management provides full ship power, including motor driving and equipment electricity. Since the monitoring and controlling of prime movers are integrated together into the system, less time for a system reconfiguration in case of an equipment fault is needed. It involves two aspects of fore-thoughts: the load sharing among multiple generators and the start/stop of gensets. For example, PMS determines whether it is necessary to start another genset by analysing the available power amount When a large load is added to the grid.

The load management mainly controls the load limitation for the propellers and high-power

consumers. When there is not sufficient available power, it reacts with the load shedding which disconnects non-essential equipment to reduce the load pressure to the on-board electric grid.

The distribution management controls the connection and disconnection of bus segments. In case of a fault such as short circuit, the bus switch is promptly disconnected to isolate the fault partition. The distribution system can be reconfigured to fit the actual operation profile in an advanced PMS.

Blackout is the most severe system fault that should be strictly avoided. The prevention from blackout replies on the occurrences of generator tripping in the power network. The controlling target is described as: in case of some generator failures, the remaining generators in the grid can still guarantee the ship power supply without causing a blackout.

4.2 Load sharing

In a shipboard electric system, multiple generators are usually connected in parallel to the power grid. The total load, comprised of the active power and the reactive power, is shared by all generators. Each generator then provides the required power in accordance with its normal rating. However, the load sharing could be arbitrary if one more generator is added to the grid. For example, the generator which has a higher voltage might take most of the load while the others shed the load. Therefore, the load sharing strategy is essential to avoid overloading and stability problems of the gensets.

The active load sharing is mainly controlled by the speed governor of the diesel engine, while the reactive load sharing is controlled by the AVR. The speed governor can implement two load sharing modes: speed droop mode and isochronous mode (Bo 2012).

4.2.1 Active load sharing

Droop speed control

Droop refers to the behaviour that the generator slows down when the load is added to the generator. Figure 4.1 presents an typical example of 4% droop line for the generator. The

frequency of the generator decreases linearly from 60 Hz for no load to 57.6 Hz for a full load. This should be taken into account to the power grid because if the generator runs slower than the grid, it begins to consume power as the grid tries to make it run faster. The fluctuation in speed also causes significant severe damages to the generator.

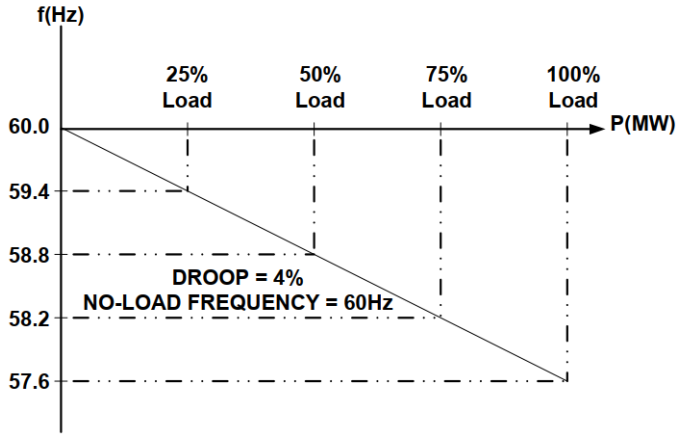

Figure 4.1: A typical droop line with 4% droop setting (Cosse et al. 2011).

The droop is calculated by

$$\%Droop = \frac{f_{NL} - f_{FL}}{f_{FL}} \times 100 \tag{4.1}$$

where f_{NL} and f_{FL} refer to the no load rated frequency and the full load rated speed, respectively.

The speed droop strategy considers the effect of droop characteristics of combined gensets to provide stable output whatever the load changes. It is done by adjusting the reference speed of system f_{ref}, as given by

$$f_{ref} = f_{NL} - \frac{P_{gen}}{P^r_{gen}} \times Droop \tag{4.2}$$

where P_{gen} is the generator power output and P^r_{gen} is the generator rated power.

Figure 4.2 demonstrates how the droop line is shifted to ensure each generator has its desired operating load percentage. The speed droop mode enables all generators to operate at the same rate of load as long as they all have the same droop setting. For example, if generator 1 takes twice the load of generator 2, it is reasonable to shift the droop rates so that the drooping rate of generator 2 is twice that of the generator 1.

The updated reference frequency is compared to the actual bus frequency, giving the fre-

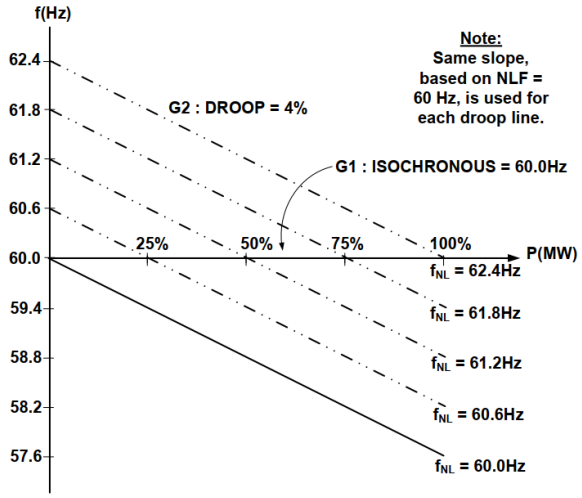

Figure 4.2: Load sharing for two generators with different desired load percentages (Patel 2011).

quency error of e_f. Then it is minimised by the PID controller, as seen in Figure 4.3.

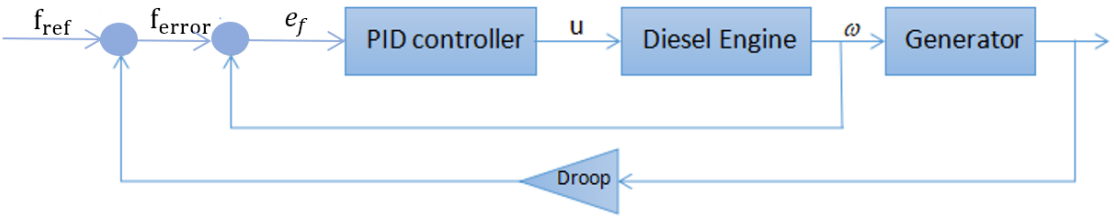

Figure 4.3: Schematic overview of generator governnor speed droop (Skjetne 2017).

The droop mode is easy to implement, as the adjustments of governor set-points directly change the bus frequency and the load sharing for on-grid generators.

Isochronous control

The isochronous load sharing does not require adjustment of the frequency set-points. Instead, it requires the addition of a load sharing line connected among the governors. The main disadvantage of the isochronous mode compared with the droop mode is that it requires much more advanced PMS and a more complicated controlling strategy. It is usually considered as an advanced method applied in the single generator application ((Cosse et al. 2011)).

4.2.2 Reactive load sharing

Similar to the droop control in the governor, the AVR can be controlled by a voltage droop characteristic, as shown in Figure 4.4. The dropping line means the voltage drops when the load increase. The difference is usually within a range of ±2.5%.

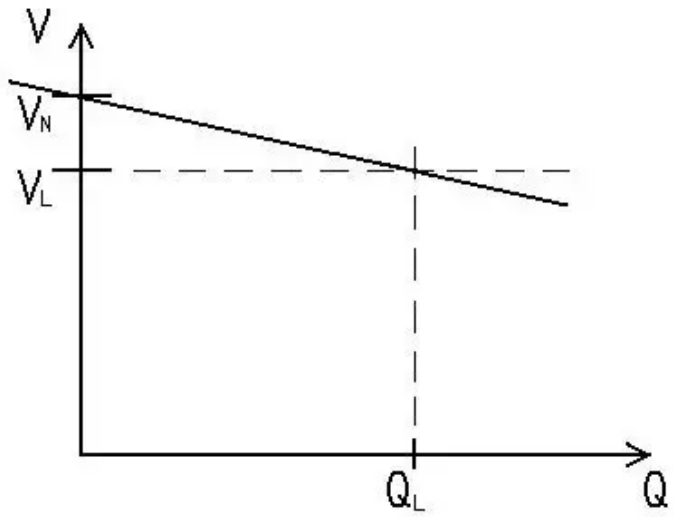

Figure 4.4: AVR setpoint V and reactive power Q.

Figure 4.5 shows the voltage drop control diagram for a genset. The updated voltage frequency is compared to the actual genset voltage, giving the voltage error of e_v. Then it is minimised by the PID controller, as seen in Figure 4.3.

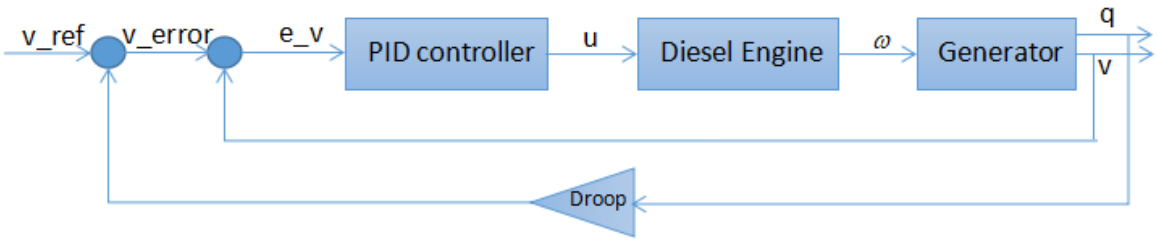

Figure 4.5: Schematic overview of generator voltage droop (Skjetne 2017).

4.3 Peak load control

Electric consumers in the grid usually have an uneven loading profile, which results in countless peak load for a long time. The peak load control is important to limit the peak electric

demand or peak hours. According to Woodward 2011, there are four possible methods to decrease the power peaks, as listed in the following:

- Load shedding: turn off some non-essential consumers to decrease the excessive load pressure to the power plant.
- Redundancy: isolate the consumers and provide sufficient power in PMS.
- Base loading: under normal conditions, the electric grid has a fairly constant load profile. This constant load, called the base load, is usually the minimum load used to design power generation. Base loading technique is applied to provide constant electrical output in the long running-time electric plant.
- Peak shaving: in contrary to base load, peak load refers to the highest load demand. The peak shaving technique is used to decline the peak load demand in a short time and can be stopped when the load decreases.

Figure 4.6 shows the difference between the concept of base loading and peak shaving.

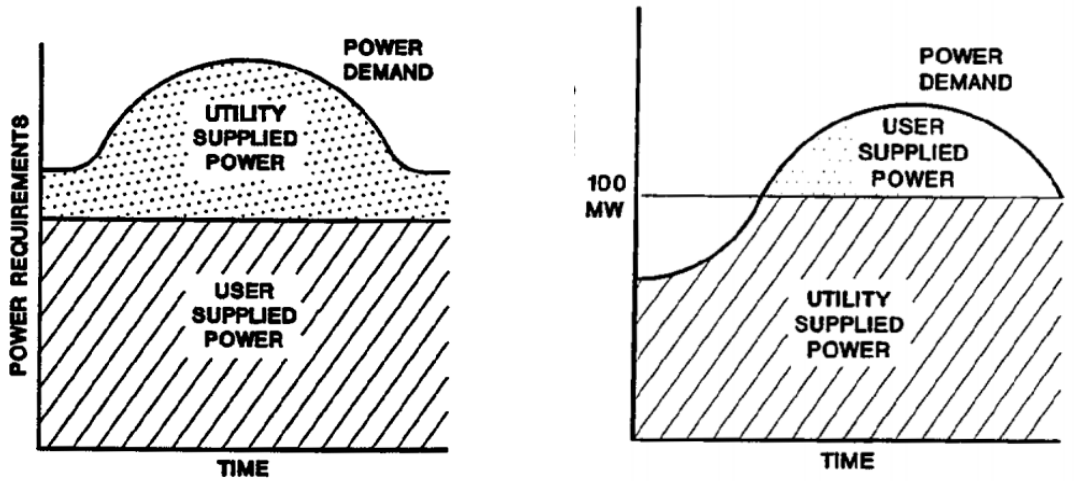

Figure 4.6: Comparison of base loading concept(left) and peak shaving concept (right) (Woodward 2011).

4.3.1 Peak shaving

Peak shaving is one of the promising applications of BSS. The storage energy stored in the BSS compensate for the increased power demand. Figure 4.7 illustrates the working principle of peak shaving: the BSS can be charged during low demand hours and discharged

during peak demand hours to reduce power peak demand as well as the electrical bills.

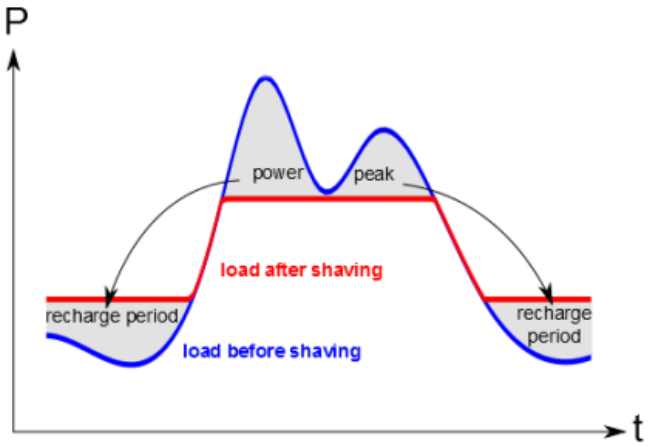

Figure 4.7: Principle of peak shaving.(Karmiris and Tengnér 2013)

There are two approaches for peak shaving strategy. The first one is to set both higher and lower boundaries for the power output of gensets. The second strategy also sets the boundaries for the generator load variation besides the boundaries set in the first strategy (Miyazaki, Sørensen, and Vartdal 2016).

The difficulties of detecting the real-time load peaks on time, selecting a proper sizing of the BSS, and taking full advantage of the BSS leave the optimisation of peak shaving a challenging problem. The optimisation algorithms are found to be complex. Most literature suggests the method of a predefined shave level depending on the maximum load (Levron and Shmilovitz 2012). However, there is a chance that the undesired peaks show up and be dismissed.

Considering there are only two gensets and one BSS connected to the bus in this thesis, an optimal but easy-to-understand shaving strategy where the errors between the varying load and available power are detected. Thus the energy of the battery can be fully exploited to supply the difference.

Details of the optimal algorithms are given in Section 6.3.

Chapter 5

Modeling of hybrid marine power system

In this chapter, a HPS is modeled in Matlab/Simulink based on the Marine System Simulator (Fossen, T. I. and T. Perez 2004; Ren et al. 2018) and an advanced simulator by Bø et al. 2015. This includes the mathematical modeling of system components, system parameters, and load profile. The simplified mathematical modeling, which can describe the main physical characteristics of the dynamic system, is the fundamental of system simulation.

5.1 System overview

In this thesis, a parallel type of configuration combining two gensets and a BSS is connected to supply the power, as shown in Figure 5.1.

5.2 Dimensioning of gensets and ESS

The first task regarding the HPS is to determine a proper sizing of BSS so that both gensets and BSS can operate in their optimal operation condition as much as possible. The Degree of hybridisation (DoH), which defined as the ratio between the battery power ($P_{battery}$) and total generated power (P_{total}), is an important deciding factor.

$$DoH = \frac{P_{battery}}{P_{battery} + P_{genset}} \tag{5.1}$$

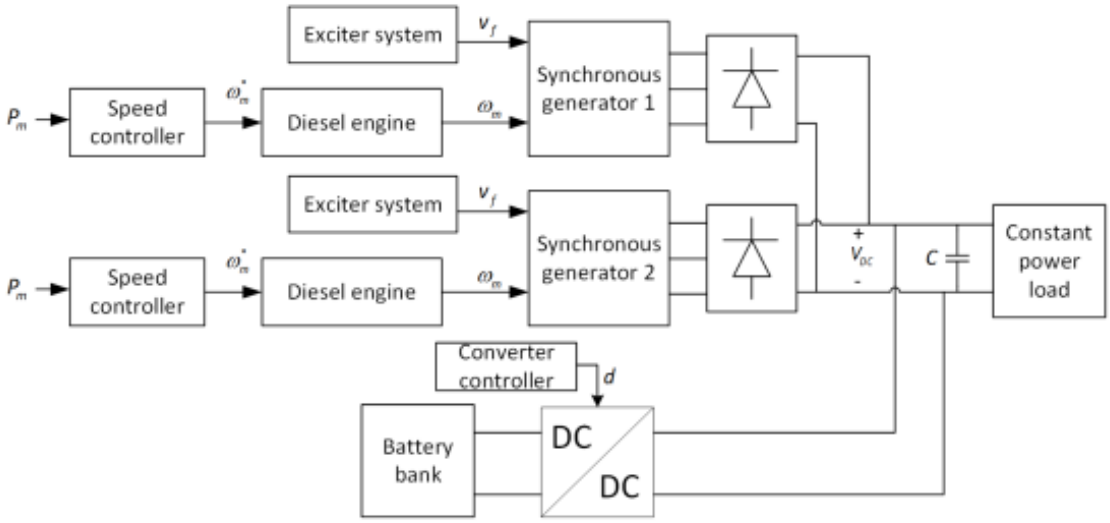

Figure 5.1: Structure overview of the gensets and BSS implemented in this work.

DoH has a great effect on the fuel economy and dynamic performances of the system. Once an optimal DoH is calculated, the sizing of ESS is obtained.

The author combines the particle optimisation based technique and simulation tool to calculate the optimal DoH (Varesi and Radan 2011). A more accurate and straightforward technique is proposed in Varesi et al. 2015. However, to simplify the work, a load-profile based methodology proposed by Cai et al. 2010 is implemented in this work.

Figure 5.2 is an actual power generation of an engine-electric power system with two generators conducting DP operation. With this load profile, DoH can be calculated by the following equation:

$$DoH = \frac{P_{ave}}{P_{max}} \tag{5.2}$$

With $P_{max} = 1.68MW$ and $P_{ave} = \frac{int_0^t P_{load}(t)}{t} = 0.25MW$, DoH is set as 0.15.

5.3 Thruster modeling

The thruster for DP vessel is mostly the fixed-pitch type or Azimuth thruster. Thruster modeling is a complex issue as many factors can affect the shaft torque and rotation speed. To simplify the problem, the thruster is modeled as a shaft propeller which is directly connected to the variable-speed motor. This gives a obvious mechanism relation since only torque transmission is consider (pitch transmission is omitted) (Sørensen and Smogeli 2009).

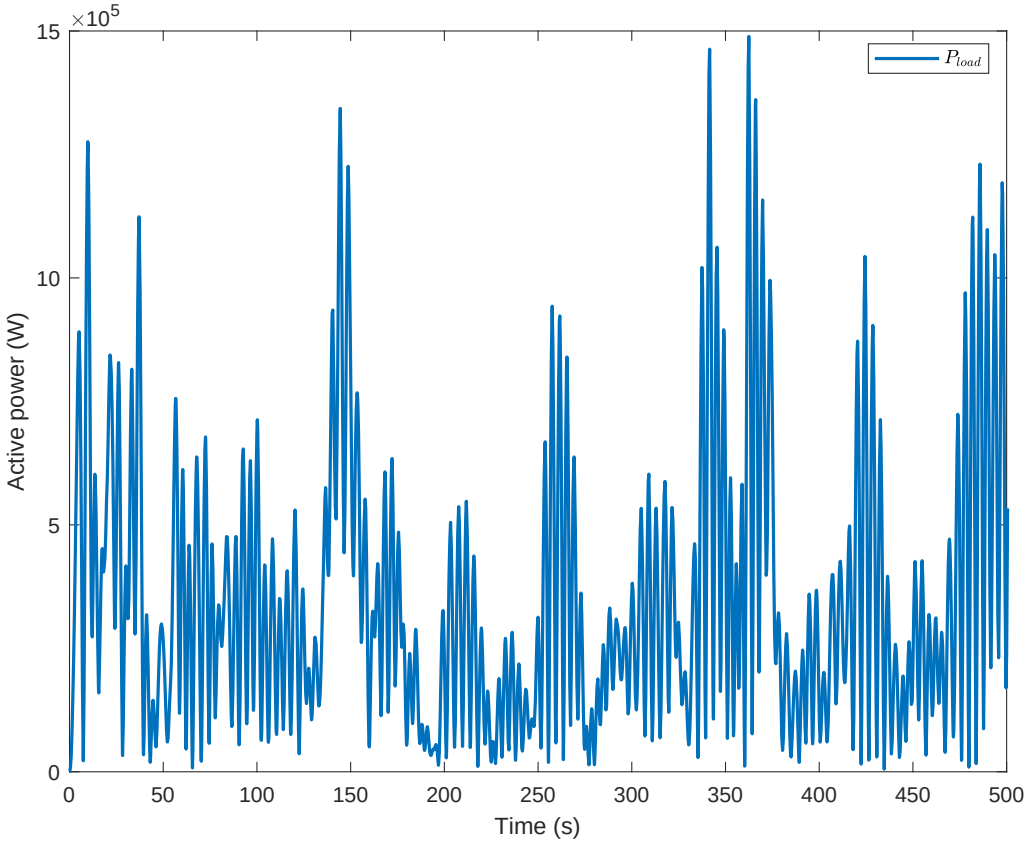

Figure 5.2: Actual load profile at dynamic positioning of a FPSO, which used to decide the sizing of battery.

Figure 5.3 illustrates the process how the desired speed n_d is obtained by the thrust allocation and the thrust characteristics curve.

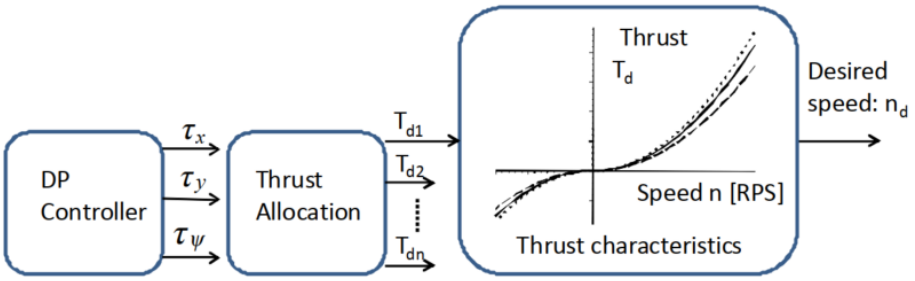

Figure 5.3: The flow chart showing the calculation of thruster speeds and thrusts Sørensen and Smogeli 2009.

The shaft thruster T and the shaft torque Q are given by

$$T = sign(n)K_T\rho D^4 n^2 \tag{5.3}$$

$$Q = sign(n)Q_T\rho D^5 n^2 \tag{5.4}$$

T and Q are the actual propeller thruster and torque, K_T and Q_T are the positive thrust and coefficients derived in the open water tests, n is the shaft speed [rpm], and D is the diameter of shaft.

Given the desired thrust T_d is obtained by thrust allocation matrix, the desired speed n_d is calculated by

$$n_d = sign(T)\sqrt{\frac{|T_d|}{K_T\rho D^4}} \tag{5.5}$$

The power consumption by the thruster then is given by

$$P_t = 2\pi n_d Q_d = sign(n_d)2\pi K_Q\rho D^5 n^3 \tag{5.6}$$

To reduce the excessive load stress and avoid frequency fluctuations of the prime mover caused by the consumers, the marine industry usually adopts a method of setting a fixed rotation rate limit on the propellers. If there is no load rate limitation, the propeller would cause a sudden increase in the grid, which leads to inevitable fluctuations. This may result in the system power loss in severe cases.

5.4 Genset modeling

5.4.1 Diesel engine

Both the diesel engine and generator are rotating mechanics. Therefore, according to the Newton's second law, the engine equation of the torque balance can be written as follows:

$$J_m\frac{d\omega_m}{dt} = \sum T_i = T_m - T_e - T_d \tag{5.7}$$

where J_m is the mechanics moment of inertia, ω_m is the angular velocity of diesel engine, T_m is the mechanical torque, and T_e and T_d are is the load and damping torque.

The relation of mechanical rotor angle θ_m, electrical rotor angle θ_e, mechanical angular velocity ω_m, and electrical frequency ω_e is given by

$$\theta_e = \frac{N}{2}\theta_m \tag{5.8}$$

$$\omega_e = \frac{d\theta_e}{dt} = \frac{N}{2}\frac{d\theta_m}{dt} = \frac{N}{2}\omega_m \tag{5.9}$$

where N is the number of poles. According to the per-unit definition, all angular velocities and torques are given by

$$\omega = \frac{\omega_e}{\omega_b} = \frac{\omega_m}{\omega_{m,b}} \tag{5.10}$$

$$\tau_j = \frac{T_j}{T_b} \tag{5.11}$$

where ω_b and $\omega_{m,b}$ refer to the rated angular velocity of diesel engine and generator respectively, and T_b is the rated rotating torque. And the inertia constant H is given by (Krause et al. 2013)

$$H = \frac{J_m \omega_m^2 b}{2T_b} \tag{5.12}$$

which yields the following motion Eq.

$$2H\frac{d\omega}{dt} = \tau_m - \tau_d - \tau_e \tag{5.13}$$

The damping torque is calculated by

$$\tau_d = D_f \omega \tag{5.14}$$

Then, the final motion equation of diesel engine is given as

$$\dot{\theta} = \omega\omega_b \tag{5.15}$$

$$\dot{\omega} = \frac{1}{2H}(-D_f\omega + k_u u - \tau_e) \tag{5.16}$$

5.4.2 Governor

The governor is modelled as PID controller based on the droop control, as described in Section 4.2.1. The controller equations are given by (Gurvin 2017)

$$\omega_{ref} = \omega_{NL} - K_{droop} p_{gen} \tag{5.17}$$

$$u = K_p(\omega_{ref} - \omega) + K_i \xi - K_d \hat{\dot{\omega}} \tag{5.18}$$

$$\dot{\xi} = \omega_{ref} - \omega + K_b(u_{saturated} - u) \tag{5.19}$$

$$\hat{\dot{\omega}} = N(\dot{\omega} - \hat{\dot{\omega}}) \tag{5.20}$$

Where K_p, K_d, and K_i are the derivative, proportional and integral gains, p_{gen} is the per unit active power generated by the generator, ω_{NL} and ω_{ref} are the No-load frequency and the reference frequency,respectively. $\hat{\dot{\omega}}$ refers to the estimated time derivative of reference.

5.4.3 Generator

The dynamic characteristics of the generator is usually adopted using the static model, which refers to that the electric angular velocity of rotor is constant. The electrical equation of generator is given by

$$\tilde{E}_a = \omega_f I_f e^{j\delta} \tag{5.21}$$

$$\tilde{V}_{as} = -\sqrt{3} Z \delta I_{as} + \delta E_a \tag{5.22}$$

where $\tilde{E}_a$ is the armature voltage, $\tilde{V}_{as}$ is the terminal voltage, δI_{as} is the stator winding current, R_f is the excitation winding resistance, I_f is the field current, Z is the Synchronous impedance. The relative angle of the synchronous generator rotor δ which is the angular displacement of the rotor relative to the synchronously rotating reference is given by:

$$\delta = \theta_e - \theta_0 \tag{5.23}$$

Where θ_e is the absolute angle and θ_0 is the synchronous electrical angle. Differential the above equation gives

$$\dot{\delta} = \omega_b(\omega - \omega_0) \tag{5.24}$$

And the per unit equation of the armature voltage is obtained from Eq. (5.21).

$$\tilde{e}_a = \omega r_f i_f e^{j\delta} \tag{5.25}$$

5.4.4 AVR

The working principle of AVR is explained in Section 2.1.4. A PI controller with droop is commonly employed to control the AVR system due to its robust performance under varying conditions and simple structure (Sahib 2015). The equation of AVR is given by (Gurvin 2017).

$$\dot{\xi}_{avr} = V_{f,ref} - |V_t| \tag{5.26}$$

$$V_{f,ref} = V_{NL}(1 - K_{droop} q_{gen}) \tag{5.27}$$

$$V_{avr} = K_p(V_{f,ref} - |V_t|) + K_i \xi_{avr} \tag{5.28}$$

$$V_{nl} = 1 + K_{droop,avr} \cdot 0.5 \tag{5.29}$$

Where$V_{avr}$and $V_{f,ref}$ are the field voltage and the reference field voltage respectively. ξ_{avr} is the error between the reference value and the actual value. V_{NL} is the no-load voltage. $Droop_{avr}$ is the droop of AVR. q_{gen} is the reactive power produced by the generator.

The droop is set to be a constant value, and a low pass filter is added to avoid the algebraic loop in the Simulink.

$$\dot{V}_f = \frac{V_f - V_{avr}}{T_{avr}} \tag{5.30}$$

where V_f is the field voltage after filtering, and T_{avr} is the low pass filter time constant.

5.5 Li-ion battery modeling

In the work, the open voltage circuit approach is used to estimate the static SoC. To be more specific, initial SoC is assigned firstly, then the variant current is integrated to estimate the SoC of the battery during usage.

The terminal voltage of battery is given by (Tremblay, Dessaint, and Dekkiche 2007)

$$V_t = E_0 - R_i \times I_b - K(\frac{Q}{Q - \int_0^t i\,dt}) + Aexp^{-B \times \int i\,dt} \tag{5.31}$$

where

V_t - Terminal voltage [V]

E_0 - Battery constant voltage [V]

Q - Battery Capacity [Ah]

R_i - Internal resistance [Ohm]

$\int_0^t i\,dt$ - Actual battery charge [Ah]

A - Exponential zone amplitude [V]

B - Exponential zone time constant inverse [Ah^{-1}]

i - Battery current [A]

K - Polarisation voltage [V]

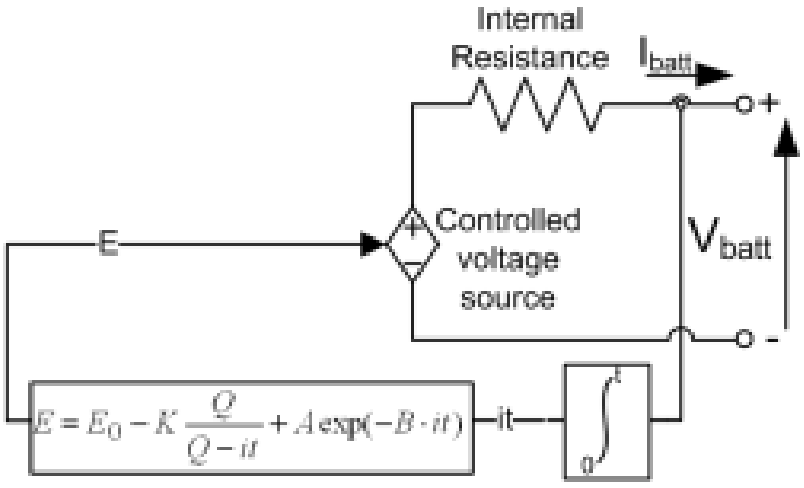

Figure 5.4: Block diagram of the battery modelling (Tremblay, Dessaint, and Dekkiche 2007).

The non-linear term $K(\frac{Q}{Q-\int_0^t i\,dt})$ represents that the non-linear battery capacity only changes with the actual charge of battery. When the battery is almost running out, no current is flowing and the voltage will be 0, which is consistent with the actual battery behaviour. In the original model, $K(\frac{Q}{Q-\int_0^t i\,dt})i$ represents both the effect of amplitude of current and actual charge of the battery, which causes an algebraic loop in the simulation computation. The modification of this model omits i to avoid the algebraic loop. The exponential term

$Aexp^{-B\times\int idt}$ represents the phenomenon that the voltage increases rapidly when the battery is almost fully charged.

The battery model is based on several assumptions, given as follows:

- The internal resistance of battery remains constant all the time.
- The battery's parameters, especially the battery capacity, remain unchanged during both the charging and discharge period.
- Temperature compensation is not considered.
- The battery has no memory effect and self-discharge effect.

The model stands out due to its simplicity since it only requires several parameters which can all be found on the manufacturer's discharge curve, as shown in Figure 5.5. It is easy to extract the three points: the fully charged voltage, the end of the exponential zone (voltage and charge), and the end of the nominal zone (voltage and charge) (Tremblay, Dessaint, and Dekkiche 2007).

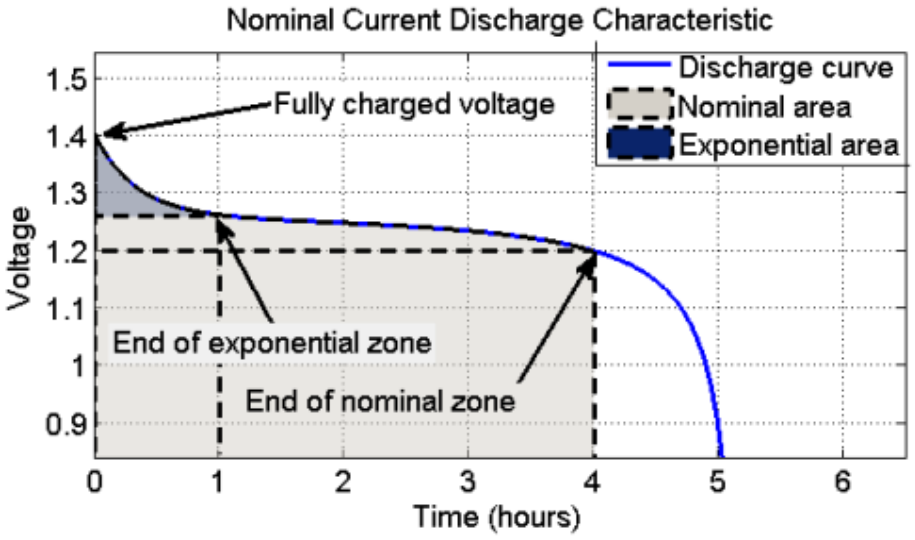

Figure 5.5: Nominal current discharge characteristic which gives three necessary points to model the battery (Tremblay, Dessaint, and Dekkiche 2007).

Figure 5.6 is the battery model developed in simulink.

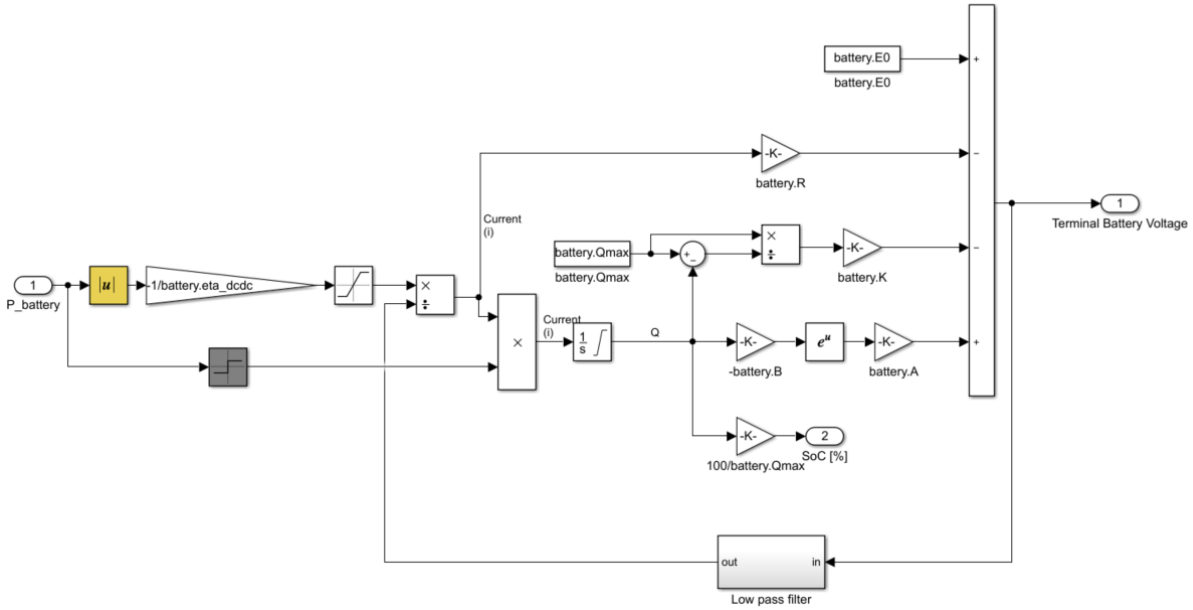

Figure 5.6: Battery model developed in Simulink.

5.6 Bus model

5.6.1 Thevenin theorem

The bus model is used to calculate the bus voltage. Since there is more than one voltage source in the configuration, it is suggested to use the Thevenin's theorem to simplify the linear circuit to an equivalent one with just one voltage source and series resistance connected to the load, as presented in Figure 5.7.

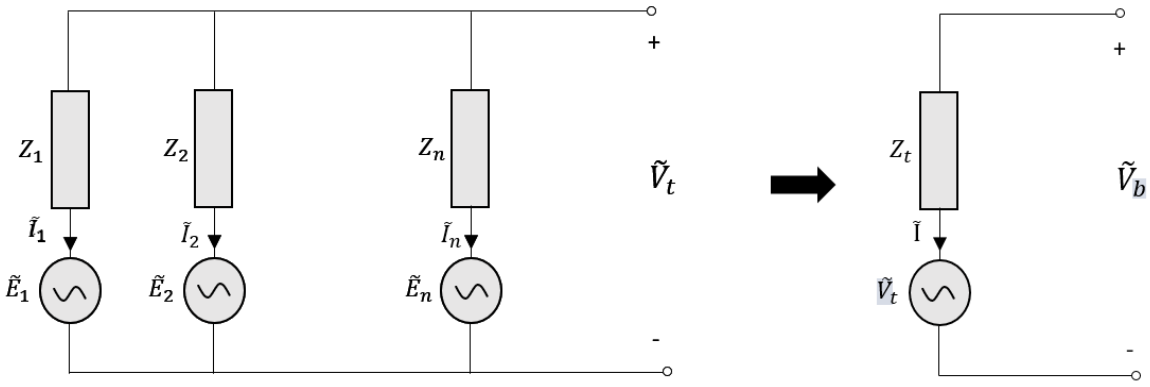

Figure 5.7: Demonstration of thenvenin equivalent circuit: n generators with various z_n are connected to the bus (left), and Z_T is the thevenin equivalent impedance (right).

5.6.2 Per unit system

The per unit system is commonly used in the electrical system calculation because it helps to scale the parameter, thus simplifying the calculations. The per unit values of any variable is defined as the ratio between the actual value and the pre-chosen base value Rao, Rao, and Vasudevan 2014. The units for the actual value and base value should be the same. Therefore, the per unit value is the dimensionless number.

Define apparent power for the bus (S_b) and the genset i (S_b, i) as base power. The base voltage is defined as V_b. The per unit values of variables are all denoted with the lowercase letters correspondingly. Then other base values are given by

$$v = \frac{V}{V_b} \tag{5.32}$$

$$i = \frac{I}{I_b} = \frac{I}{\frac{S_b}{V_b}} \tag{5.33}$$

$$Z = \frac{Z}{Z_b} = Z\frac{S_b}{V_b^2} \tag{5.34}$$

5.6.3 Bus voltage calculation

The Thevenin voltage $\tilde{V}_t$ for each generator i is calculated by

$$\tilde{E}_i - \sqrt{3}Z_i\tilde{I}_i = \tilde{V}_t \tag{5.35}$$

$$\sum \tilde{I}_i = 0 \tag{5.36}$$

where $\tilde{E}$ is the complex induced voltage, Z_i is the impedance of each generator, $\tilde{I}_i$ is the current through each generator. Eq. (5.36) refers to the sum of the currents through all the gensets should be zero since it is an open circuit diagram.

The transformations of Eq. (5.35) and Eq. 5.36 to the per unit system are given by

$$\tilde{e}_i - \sqrt{3}z_i\tilde{i}_i = \tilde{v}_t \tag{5.37}$$

$$\sum \tilde{i}\frac{S_{b,i}}{V_b} = 0 \tag{5.38}$$

which can be rewritten with the matrix as follows:

$$\begin{bmatrix} 0 & S_{b,1} & S_{b,2} & \cdots & S_{b,n} \\ 1 & \sqrt{3}z_1 & 0 & \cdots & 0 \\ \vdots & \vdots & \vdots & \ddots & \vdots \\ 1 & 0 & 0 & \cdots & \sqrt{3}z_n \end{bmatrix} \begin{bmatrix} \tilde{v}_t \\ \tilde{i}_1 \\ \vdots \\ \tilde{i}_n \end{bmatrix} = \begin{bmatrix} 0 \\ \tilde{e}_1 \\ \vdots \\ \tilde{e}_n \end{bmatrix} \tag{5.39}$$

whereS_b is the apparent power for the bus. Since it's a linear equation, the thevenin voltage $\tilde{V}_t$ can be easily calculated, as given by

$$\tilde{v}_t = \frac{\frac{S_{b,1}\tilde{e}_1}{z_1} + \frac{S_{b,2}\tilde{e}_2}{z_2} + \cdots + \frac{S_{b,n}\tilde{e}_n}{z_n}}{\frac{S_{b,1}}{z_1} + \frac{S_{b,2}}{z_2} + \cdots + \frac{S_{b,n}}{z_n}} \tag{5.40}$$

The thevenin equivalent impedance Z_t is given by

$$Z_t = \sum_{i=1}^{n} (\frac{1}{Z_i})^{-1} \tag{5.41}$$

which is written in per unit

$$z_t = S_b (\sum_i) \frac{S_i}{z_i}^{-1} \tag{5.42}$$

The active power and reactive power of load consumed is obtained by

$$P_{load} + jQ_{load} = \sqrt{3}\tilde{V}\tilde{I}^* \tag{5.43}$$

The load impedance Z_l is calculated by

$$\begin{aligned} Z_l &= \frac{\tilde{V}}{\sqrt{3}} = \frac{\tilde{V}}{\sqrt{3}} \cdot \frac{P_{load} - jQ_{load}}{\sqrt{3}\tilde{V}^*} \\ &= \frac{|\tilde{v}|^2}{P_{load-jQ_{load}}} \end{aligned} \tag{5.44}$$

which is written in per unit

$$z_l = \frac{|\tilde{v}^2|}{p_{load} - jq_{load}} \tag{5.45}$$

The current flowing throught the equivalent system is given by

$$\tilde{I} = \frac{\tilde{V}_t}{\sqrt{3}(Z_t + Z_l)} \tag{5.46}$$

Then the resulting bus voltage is calculated by

$$\tilde{V}_b = \sqrt{3} Z_l \tilde{I} = \frac{Z_l}{Z_t + Z_l} \tilde{V}_t \tag{5.47}$$

which is written in per unit

$$\tilde{v}_b = \frac{z_l}{z_t + z_l} \tilde{v}_t \tag{5.48}$$

where z_t comes from Eq. (5.42),z_l comes from Eq. (5.45), $\tilde{v}_t$ comes from solving the linear equation Eq. (5.39).

Then the complex power supplied by the generator i is calculated by

$$S_i = \sqrt{3} \tilde{V}_b \tilde{I}_i^* = \tilde{V}_b (\frac{\tilde{E}_i - \tilde{V}_b}{Z_i}) \tag{5.49}$$

$$s_i = \tilde{v}_b (\frac{\tilde{e}_i - \tilde{v}_b}{z_i}) \tag{5.50}$$

The active power and reactive power for each generator are obtained by extracting the reality and imaginary part of the apparent power, as given by

$$p_i = Re(s_i) \tag{5.51}$$

$$q_i = Im(s_i) \tag{5.52}$$

Likewise, the active power p_b and active power q_b of the bus are given by

$$S_b = \sqrt{3} \tilde{V}_b \tilde{I} * = \sqrt{3} \tilde{V}_b \frac{\tilde{E}_t^* - \tilde{V}_b}{Z_t^*} \tag{5.53}$$

$$s_b = \tilde{v}_b \frac{\tilde{e}_t^* - \tilde{v}_b}{z_t^*} \tag{5.54}$$

$$p_b = Re(s_b) \tag{5.55}$$

$$q_b = Im(s_b) \tag{5.56}$$

5.7 Load sharing

The individual active power and reactive power for each genset and battery is calculated according to the following equations (Bo 2012):

$$\sum_i p_i \frac{S_{b,i}}{S_b} = P_{bus} \tag{5.57}$$

$$\sum_i q_i \frac{S_{b,i}}{S_b} = q_{bus} \tag{5.58}$$

$$p_i = \frac{e_i v}{x_s \omega_i} sin\delta_i = \frac{v_{f,i} v}{x_s} sin\delta_i \tag{5.59}$$

$$q_i = \frac{v}{x_s}(v_{f,i} cos\delta_i - \frac{v}{\omega_i}) \tag{5.60}$$

5.8 Simulink implementation

Figure 5.8 presents how the models of primary devices in the hybrid marine power system are connected and how the power flows from the top view. Each modular is developed based on main physical characteristics and simplified mathematical equations.

The model is built in accordance with assumptions brought by Bø et al. 2015, as listed

1. The model can only be used to simulate the steady-state electric system. In other words, it is not applied to the systems with over/under frequency, failure due to short circuit and other unsteady states
2. The diesel engine modular is simplified to a mean-value model.
3. The protection relay device is not included to trip a circuit breaker when a fault is detected.

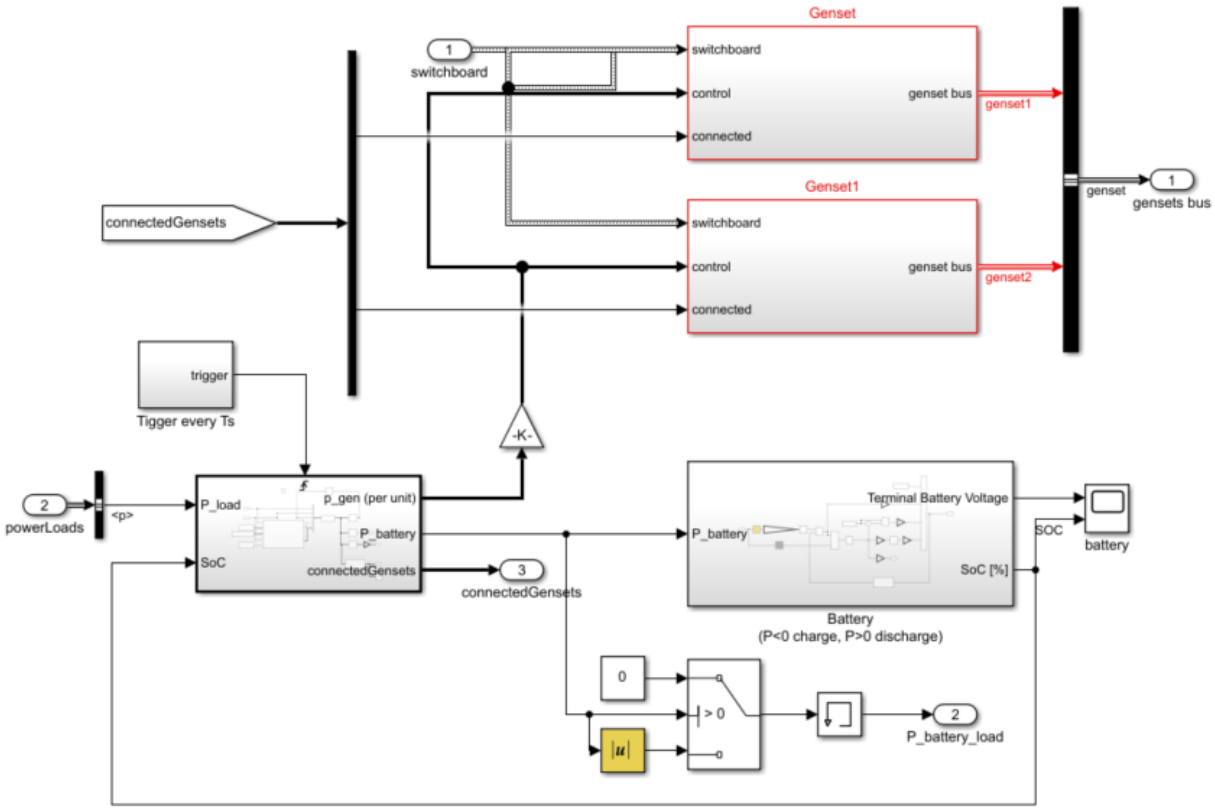

Figure 5.8: Simulink of the hybrid marine power plant at the top view, including the diesel engine, the generator, the battery, AVR, and other primary controllers.

Chapter 6

Optimal control scheme

This chapter proposes control strategies to achieve the optimal power management functions, such as peak shaving and load sharing among gensets and battery with maximum fuel economy. An innovative power management strategy is proposed. The optimised power output is calculated for the different number of involved genset. The number of gensets switches uses a moving buffer function. The peak shaving function is modelled as an non-linear programming problem, with the cost function presented.

6.1 Power flow

For the power flow, the power consumed by the loads should be equal to the total power generated by the power sources. The BESS can be both load and power source depending on the circuit flows. Assuming that the total power from generator P_{gen} is fully controllable, the power consumed by the thrusters and other on-broad devices P_{load} is independent and unpredictable, and the power flows in the battery $P_{Battery}$ is a resultant quality. The power flow relationship is given by

$$\sum_{i=1}^{2} P_{gen,i}(t) + P_{battery}(t) = P_{load}(t) \tag{6.1}$$

6.2 Minimisation of FOC

SFOC is an essential parameter with a considerable effect on the efficiency of the gensets. It is highly dependent on the percentage of MCR the engine is running with, as illustrated in Section 2.1.1. The amount of gensets FOC can be calculated by using the SFOC, which is given by

$$FOC = SFOC \cdot P_{gen} \tag{6.2}$$

Suppose that the SFOC curve is a convex continues curve, symbolised as $h(p)$ where p is the per unit power, i.e., the ratio between the actual power supplied by the genset P_{gen} and the rated power of genset P^r_{gen}, i.e.,

$$p = \frac{P_{gen}}{P^r_{gen}} \tag{6.3}$$

The optimal (lowest) value of SFOC is at 70%-80% MCR, as seen in Figure 2.3. By using the quadratic polynomial curve fitting, the function can be expressed as (Thorat and Skjetne 2018)

$$h(p) = ap^2 + bp + c \tag{6.4}$$

where [a,b,c] is the coefficient vector to define the curve.

Substituting (6.4) and (6.3) into (6.2) gives the equation of total amount of fuel consumption:

$$F_p = P^r_{gen} \cdot p \cdot h(p) \tag{6.5}$$

Given the sufficient online power supply, the goal of the PMS is to minimise the fuel consumption with both gensets switched on, i.e., $(c_1, c_2) = (1, 1)$ c_i is the symbol that shows the connection status of the gensets: disconnect($c_i = 0$) and connect ($c_i = 1$).

The cost function of fuel consumption is given by

$$\min_{p_1,p_2} \quad \sum_{i=1}^{2} c_i F_{p,i}(p_i) \tag{6.6}$$

$$\text{s.t.} \quad F_{p,i}(p_i) = P^r_{gen,i} p_i h_i(p_i) \tag{6.7}$$

$$\sum_{i=1}^{2} p^r_{gen,i} p_i = P_{load} \tag{6.8}$$

$$0 \le p_i \le 1 \tag{6.9}$$

$$P_{gen,i} = p_i \cdot P^r_{gen,i} \tag{6.10}$$

Eq. (6.8) ensures the total power supply of gensets to meet the load demand. Eq. (6.9) constrains the specific genset works no larger than its rated power. Eq. (6.10) calculates the real-time supplied power by the gensets.

6.3 Optimal peak shaving strategy

The energies, defined by integrating the power, are given by:

$$W_{battery}(t) = \int_0^t P_{battery}(t)dt \tag{6.11}$$

$$W_{gen}(t) = \int_0^t P_{gen}(t)dt \tag{6.12}$$

$$W_{load}(t) = \int_0^t P_{load}(t)dt \tag{6.13}$$

where $W_{battery}$, W_{gen}, and W_{load} are the energies of the battery stored, gensets supplied, and load consumed, respectively.

The maximum energy capacity of energy stored in the battery W_{max} is given by

$$W_{max} = \frac{1}{2} \cdot C \cdot (V^2_{max} - V^2_{min}) \tag{6.14}$$

$$0 \le W_{battery}(t) \le W_{max} \tag{6.15}$$

where C refers to the coulomb stored in the battery, and V_{max} and V_{min} are the voltage upper and lower limits for the battery to function under normal conditions. They are usually given by the manufacturer.

By substituting Eq. (6.11) into Eq. (6.15) yields

$$W_{load}(t) \leq W_{gen}(t) \leq W_{load}(t) + W_{max} \tag{6.16}$$

Figure 6.1 shows the graphical meaning of the inequalities. The energy supply of the gensets (the bold line) is limited within a tube between the load energy W_{load} and the sum of energy of load and battery $W_{load}(t) + W_{max}$. The tube is regarded as the energy band. On one hand, the gensets power should be able to meet the load supply. On the other hand, the gensets power should be limited to avoid the battery damage caused by overdischarging.

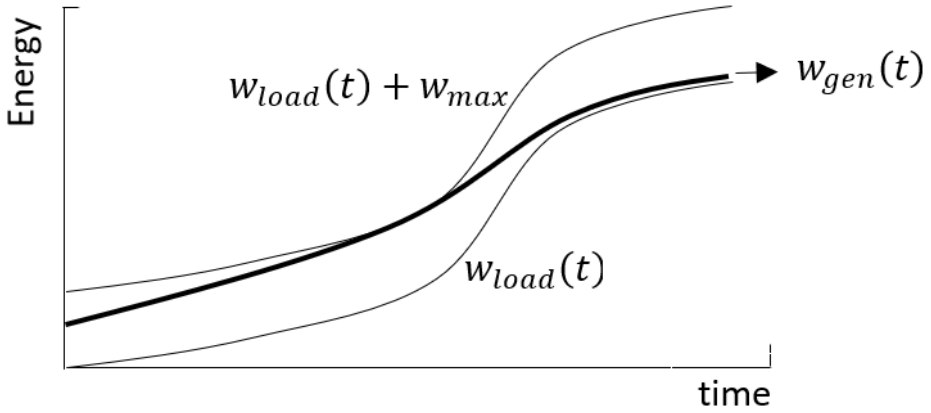

Figure 6.1: Limits for the gensets energy (the bold line).

The strategy features to find the shortest path from the initial to the end in the energy band. In this way, the power generation by gensets which is the first derivative of energy is minimised. The battery is used to the smooth the power fluctuation as much as possible, given that SoC is always within the limited working range.

The optimisation is conducted to the states at a series of time instants. Define the k^{th} time instant as $t_k := t(k)$. Additionally, $\Delta t_k = t_k - t_{k-1}$. In a discrete form, Eq. (6.11) is given by

$$W_{battery}(t_k) = \sum_{j=0}^{k} P_{battery}(t_j)\Delta t \tag{6.17}$$

$$W_{gen}(t_k) = \sum_{j=0}^{k} P_{gen}(t_j)\Delta t \tag{6.18}$$

$$W_{load}(t_k) = \sum_{j=0}^{k} P_{load}(t_j)\Delta t \tag{6.19}$$

The power peak is shaved by the battery as long as the gensets energy bounded within the band. The optimal peak shaving strategy uses the total amount of the fuel consumption $F_p(k)$ as an objective function, given by

$$\min_{p_1(k),p_2(k)} \quad \sum_{k=1}^{n}\sum_{i=1}^{2} c_i F_{p,i}(p_i(k)) \tag{6.20}$$

$$\textbf{\textit{s.t.}} \quad F_{p,i} = P^r_{gen,i} p_i h_i(p_i) \tag{6.21}$$

$$-\sum_{j=1}^{k}(p_1(j)P^r_{gen,1}\Delta t_j + p_2(j)P^r_{gen,2}\Delta t_j) \le -\sum_{j=1}^{k} P_{load}(j)\Delta t_j \quad k = 1,2,\cdots,n \tag{6.22}$$

$$\sum_{j=1}^{k}(p_1(j)P^r_{gen,1}\Delta t + p_2(j)P^r_{gen,2}\Delta t_j) \le \sum_{k=1}^{n} P_{load}(k)\Delta t_j + W_{max} \quad k = 1,2,\cdots,n \tag{6.23}$$

$$P^C_{battery} \le P_{load}(k) - \sum_{j=1}^{k} P_{gen,i}(j) \le P^D_{battery} \tag{6.24}$$

where $p_i(k)$ is short for $p_i(t_k)$. Eq. (6.24) is the constrain for the BESS charging power and discharging power, which is important to protect the BESS from the over-currents.

In the MATLAB code, Eq. (6.22) and Eq. (6.23) can be rewritten in the following linear inequality

$$Ax \le b \tag{6.25}$$

where

$$x = \begin{bmatrix} p_1(k=1) \\ p_2(k=1) \\ p_1(k=2) \\ p_2(k=2) \\ \vdots \\ p_1(k=n) \\ p_2(k=n) \end{bmatrix} \quad b = \begin{bmatrix} -P_{load}(1)\Delta t_1 \\ P_{load}(1)\Delta t_1 + W_{max} \\ \sum_{k=1}^{2} -P_{load}(k)\Delta t_k \\ \sum_{k=1}^{2} P_{load}(k)\Delta t_k + W_{max} \\ \vdots \\ \sum_{k=1}^{n} -P_{load}(k)\Delta t_k \\ \sum_{k=1}^{n} P_{load}(k)\Delta t_k + W_{max} \\ P^D_{battery} - P_{load}(1) \\ P_{load(1)-P^C_{battery}} \\ \vdots \\ P^D_{battery} - P_{load}(k) \\ P_{load}(k) - P^C_{battery} \end{bmatrix}$$

$$
A = \begin{bmatrix}
-P^r_{gen,1}\Delta t_1 & -P^r_{gen,2}\Delta t_1 & 0 & 0 & \cdots & 0 & 0 \\
P^r_{gen,1}\Delta t_1 & P^r_{gen,2}\Delta t_1 & 0 & 0 & \cdots & 0 & 0 \\
-P^r_{gen,1}\Delta t_1 & -P^r_{gen,2}\Delta t_1 & -P^r_{gen,1}\Delta t_2 & -P^r_{gen,2}\Delta t_2 & \cdots & 0 & 0 \\
P^r_{gen,1}\Delta t_1 & P^r_{gen,2}\Delta t_1 & P^r_{gen,1}\Delta t_2 & P^r_{gen,2}\Delta t_2 & \cdots & 0 & 0 \\
\vdots & \vdots & \vdots & \vdots & \vdots & \vdots & \vdots \\
-P^r_{gen,1}\Delta t_1 & -P^r_{gen,2}\Delta t_1 & -P^r_{gen,1}\Delta t_2 & -P^r_{gen,2}\Delta t_2 & \cdots & -P^r_{gen,1}\Delta t_k & -P^r_{gen,2}\Delta t_k \\
P^r_{gen,1}\Delta t_1 & P^r_{gen,2}\Delta t_1 & P^r_{gen,1}\Delta t_2 & P^r_{gen,2}\Delta t_2 & \cdots & P^r_{gen,1}\Delta t_k & P^r_{gen,2}\Delta t_k \\
-P^r_{gen,1} - P^r_{gen,2} & 0 & 0 & 0 & 0 & 0 & 0 \\
0 & -P^r_{gen,1} - P^r_{gen,2} & 0 & 0 & 0 & 0 & 0 \\
\vdots & \vdots & \vdots & \vdots & \vdots & \vdots & \vdots \\
0 & 0 & 0 & 0 & \cdots & -P^r_{gen,1} & -P_{gen,2} \\
-P^r_{gen,1} & -P^r_{gen,2} & 0 & 0 & \cdots & 0 & 0 \\
0 & 0 & -P^r_{gen,1} & -P^r_{gen,2} & \cdots & 0 & 0 \\
\vdots & \vdots & \vdots & \vdots & \vdots & \vdots & \vdots \\
0 & 0 & 0 & 0 & \cdots & P^r_{gen,1} & P^r_{gen,2}
\end{bmatrix}
$$

6.4 Scheduling of load sharing

6.4.1 Logical control strategy

Diesel gensets should operate in a predefined high-efficiency range by setting some thresholds. Meanwhile, the BESS is regarded as a 'flexible factor' of the system whenever it is needed.

In this section, three working modes are designed for the hybrid system based on the varying load on the bus: 1) the BESS is driven individually, 2) one genset and BESS cooperate, 3) two gensets and BESS are working together. The mode selection, based on the corresponding conditions, decides the power outputs from the gensets and BESS.

A brief of the working modes is presented according to the SoC of the battery and real-time power consumption by the load. In details,

1. When the load is below a certain low limit $P_{load,min}$, only the battery supplies the power.

2. When the load is higher than a certain upper limit $P_{load,max}$, the diesel engine and the battery are jointly driven
3. When the load is between $P_{load,min}$ and $P_{load,max}$, and SoC is less than a preset value, diesel engine is driven separately and charge battery at the same time
4. When the load is between $P_{load,min}$ and $P_{load,max}$, and SoC is higher than a preset value, diesel engine is driven separately and no longer charge battery.

6.4.2 Algorithms of load sharing

Based on the control scheme of load sharing presented in Sec.6.4.1, the algorithms are summarised in Algorithms 1–4.

Table 6.1: Symbols used in the algorithm

Symbol	Meaning
P^r_{gen}	Rated power of genset
P_{opt}	Optimal power generated by genset
P_{gen}	Real-time power generated by the genset
P_{load}	Power demand by the load
$\sum P^r_{gen}$	Sum amount of gensets rated power
$\overline{SoC}$	Upper limit of SOC
$\underline{SoC}$	Lower limit of SoC
SoC	Battery SoC in the present step
i	Index of the activated gensets in the present step
$\hat{i}$	Index of activated gensets in the last step
$P^C_{battery}$	Battery rated charge power
$P^D_{battery}$	Battery rated discharge power
$P_{battery}$	Battery power in the present step

Algorithm 1 Power management system

parameter: $P^r_{gen}, P^C_{battery}, P^D_{battery}, \underline{SoC}, \overline{SoC}$

input : $P_{load}, SoC, \hat{i}$

output : $P_{battery}, P_{gen}, i$

if *One genset is switched on* **then**

  if *More than one genset can supply enough power for the loads individually in the past time window* **then**

    switch to Algorithm 2, and use the smallest genset

    $[P_{battery}, P_{gen}, i] = \boldsymbol{Algorithm2}[P_{load}, SoC, \hat{i}, \underline{SoC}, \overline{SoC}]$

  else

    if *The the biggest genset is not sufficient to work individually* **then**

    Switch to Algorithm 3 and use two gensets working

    $[P_{battery}, P_{gen}, i] = \boldsymbol{Algorithm3}[P_{load}, SoC, \hat{i}, \underline{SoC}, \overline{SoC}]$

else if *Two gensets are switched on* **then**

  if *At least one genset is powerful enough to supply power in the past time window* **then**

    Switch to Algorithm 2, and use the smallest genset

    $[P_{battery}, P_{gen}, i] = \boldsymbol{Algorithm2}[P_{load}, SoC, \hat{i}, \underline{SoC}, \overline{SoC}]$

  else

    Switch to Algorithm 3, and use two gensets working mode.

    $[P_{battery}, P_{gen}, i] = \boldsymbol{Algorithm3}[P_{load}, SoC, \hat{i}, \underline{SoC}, \overline{SoC}]$

End if

Algorithm 2 One genset connected

parameter: $P^r_{gen}, P^C_{battery}, P^D_{battery}, \underline{SoC}, \overline{SoC}$
input : $\hat{i}, P_{load}, SoC$
output : $P_{gen}, P_{battery}, i$

$\boldsymbol{P_{gen}} = [0,0]^T$
if $P_{opt}(\hat{i}) \geq 1.1P_{Load}$ **then**
  $i = \hat{i}$
  if $SoC > \overline{SoC}$ **then**
    $P_{gen}(i) = 1.1P_{Load}$
    $P_{battery} = 0$
    if $P_{opt}(i) \geq 1.1(P_{load} - P^C_{battery})$ **then**
      $P_{battery} = P^C_{battery}$
      $P_{gen}(i) = 1.1(P_{load} - P_{battery})$
    else
      $P_{gen}(i) = P_{opt}(i)$
      $P_{battery} = P_{load} - P_{opt}(i)$

else if $P_{opt}(\hat{i}) + P^D_{battery} \geq 1.1P_{load}$ *and* $P_{rated}(\hat{i}) \geq P_{load}$ **then**
  $i = \hat{i}$
  if $SoC \leq \underline{SoC}$ **then**
    $P_{gen}(i) = 1.1P_{Load}$
    $P_{battery} = 0$
  else
    $P_{gen}(i) = P_{opt}(i)$
    $P_{battery} = P_{load} - P_{opt}(i)$

else if $P_{opt}(\hat{i}) + P^D_{battery} \leq 1.1P_{load}$ *and* $P^r_{gen}(\hat{i}) \geq 1.1P_{load}$ **then**
  $i = \hat{i}$
  if $SoC \leq \underline{SoC}$ **then**
    $P_{gen}(i) = 1.1P_{Load}$
    $P_{battery} = 0$
    if $SoC \geq \overline{SoC}$ **then**
      $P_{gen}(i) = P^r_{gen}(i)$
      $P_{battery} = \max(P_{load} - P_{gen}(i), 0)$
    else
      $P_{gen(i)} = P^r_{gen}(i)$
      $P_{battery} = P_{load} - P_{gen}(i)$

else if $P^r_{gen}(\hat{i}) \leq 1.1P_{load}$ *and* $P^r_{gen}(\hat{i}) + P^D_{battery} \geq 1.1P_{load}$ **then**
  $i = \hat{i}$
  if $SoC \leq \underline{SoC}$ **then**
    $P_{gen}(i) = 1.1P_{Load}$
    $P_{battery} = 0$
  else
    $P_{gen}(i) = P^r_{gen}(i)$
    $P_{battery} = P_{load} - P_{gen}(i)$

[Note: continued in the next page]

else if $P^r_{gen}(i) + P^D_{battery load}$ **then**
  $P_{gen}(i) = P^r_{gen}(i)$
  if $SoC \leq \underline{SoC}$ **then**
    $P_{battery} = 0$
  else
    $P_{battery} = P^D_{battery}$
End if

Algorithm 3 Two gensets connected

parameter: $P^r_{gen}, P^C_{battery}, P^D_{battery}, \underline{SoC}, \overline{SoC}$
input : $\hat{i}, P_{load}, SoC$
output : $P_{gen}, P_{battery}, i$

$\boldsymbol{P_{gen} = [0,0]^T}$
$\boldsymbol{i = \hat{i}}$ **if** $\sum P_{opt,i} \geq 1.1 P_{Load}$ **then**
  if $SoC \geq \overline{SoC}$ **then**
    $\sum P_{gen,i} = 1.1 P_{Load}$
    Switch to Algorithm 4
    if $\sum P_{opt,i} \geq P_{load} - P^c_{battery}$ **then**
      $P_{battery} = P^c_{battery}$
      $\sum P_{gen,i} = 1.1 P_{load} - P_{battery}$
    else
      $P_{gen}(i) = P_{opt}(i)$
      $P_{battery} = P_{load} - \sum P_{gen,i}$
else if $\sum P_{opt,i} \leq 1.1 P_{load}$, *and* $\sum P_{opt,i} + P^D_{battery} \geq 1.1 P_{load}$ **then**
  if $SoC \leq \underline{SoC}$ **then**
    Switch to Algorithm 4
    $\sum P_{gen,i} = \mathbf{min}(1.1 P_{load}, \sum P^r_{gen,i})$
    $P_{battery} = \mathbf{min}(0, P_{load} - \sum P_{gen,i})$
    if $SoC \geq \overline{SoC}$ **then**
      $P_{gen}(i) = P_{opt}(i)$
      $P_{battery} = \mathbf{max}(0, P_{load} - \sum P_{gen,i})$
    else
      $P_{gen}(i) = P_{opt}(i)$
      $P_{battery} = P_{load} - \sum P_{gen,i}$
else if $\sum P^r_{gen,i} + P^D_{battery} \leq 1.1 P_{load}$ *and* $\sum P^r_{gen,i} \geq 1.1 P_{load}$ **then**
  $\sum P_{gen,i} = 1.1 P_{load}$
  Switch to Algorithm 4
  if $SoC \leq \underline{SoC}$ **then**
    $P_{battery} = 0$
  else
    $P_{battery} = P_{load} - \sum P_{gen,i}$

[Note: continued in the next page]

else if $\sum P^r_{gen,i} + P^D_{battery} \geq 1.1P_{load}$ *and* $\sum P^r_{gen,i} \leq 1.1P_{load}$ **then**
    $P_{gen} = 1.1P_{load}$
    Switch to Algorithm 4
    if $SoC \leq SoC$ **then**
        $P_{battery} = \mathbf{min}(0, P_{load} - \sum P_{gen,i})$
        if $SoC \leq \overline{SoC}$ **then**
            $P_{battery} = \max(0, P_{load} - \sum P_{gen,i})$
        else
            $P_{battery} = P_{load} - \sum P_{gen,i}(i))$
else if *None of the above applies* **then**
    if $SoC \leq \overline{SoC}$ **then**
        $P_{battery} = 0$
        $P_{gen}(i) = P^r_{gen}$
    else
        $P_{battery} = P^D_{battery}$
        $P_{gen} = P^r_{gen}$
ENDIF

Algorithm 4 Optimal scheme of Load sharing

input : $\sum P_{gen,i}$
output : P_{gen}
parameter: P^r_{gen}, $[a,b,c]$, c_i

$$\mathbf{min}_{p_i} \quad \sum_{i=1}^{2} c_i P^r_{gen,i} h_i(p_i)$$

$$\mathbf{subject\ to} \quad \sum_{i=1}^{2} P^r_{gen,i} p_i = P_{load}$$

$$0 \leq p_1 \leq 1$$

$$P_{gen,i} = p_i \cdot P^r_{gen,i}$$

Chapter 7

Simulation results: power management system verification

This chapter aims to present the simulation results of the PMS algorithms and the optimal peak shaving strategy (described in Chapter 6) by implementing the system model (described in Chapter 5) in MATLAB. The MATLAB is adopted for the nonlinear programming.

7.1 PMS algorithms verification

This study is used to verify the fidelity of the PMS given in Algorithm 1. This is done by giving a self-defined load profile to the system and a battery SoC trend. The battery SoC serves as the input to the algorithm, which does not change with the charging or discharging processes. The PMS chooses the exclusive solution on the number of gensets connected to the grid and the charging/discharging status of BESS.

The maximum power of the two gensets and BESS are selected as 7 MW, 8 MW, and 1 MW, respectively. Figure 7.1 gives the SFOC curves for two gensets. The mathematical functions of two curves are obtained by using the method of quadratic polynomial curve fitting. Noted that the maximum power of BESS is randomly given, which is higher than the common available values to obtain obvious simulation results.

Two cases are studied. The case 1 and case 2 are simulated with a same given load profile, but different battery SoC trends. Both simulation run for 200 steps.

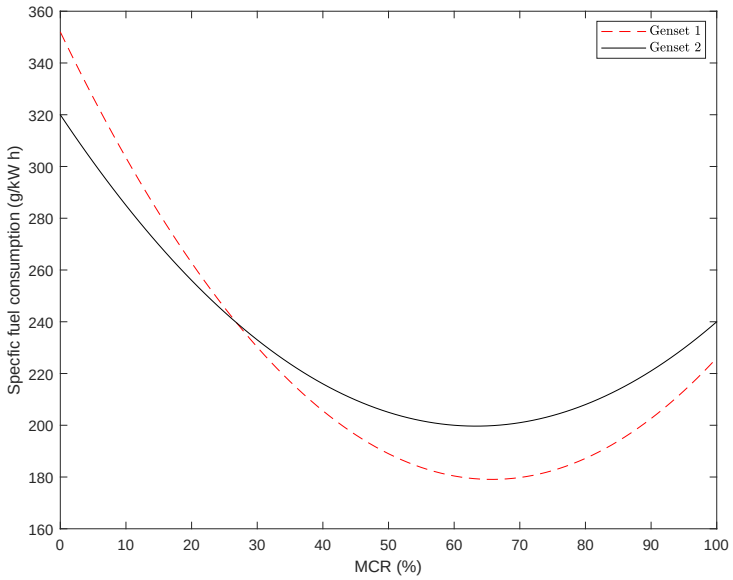

Figure 7.1: SFOC curves for two gensets used in the thesis

7.1.1 Results

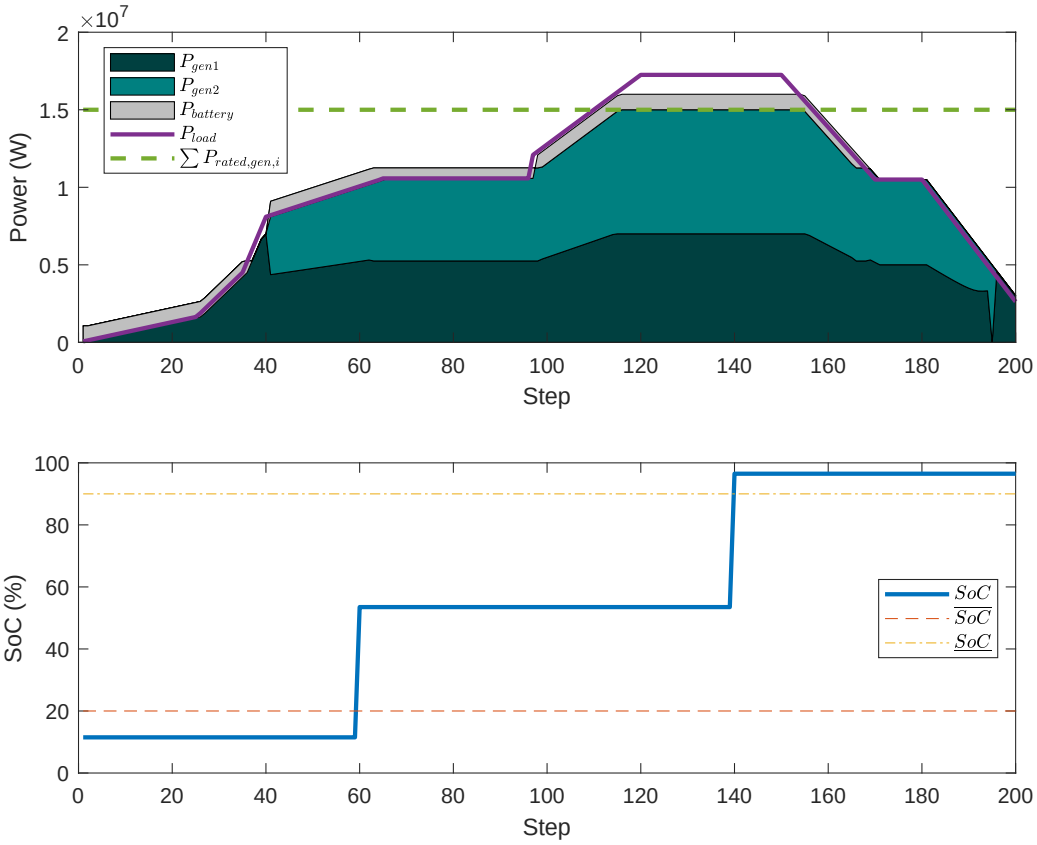

Figure 7.2: PMS algorithms verification, case 1: the power flow of gensets and BESS with respect to the specific load and SoC.

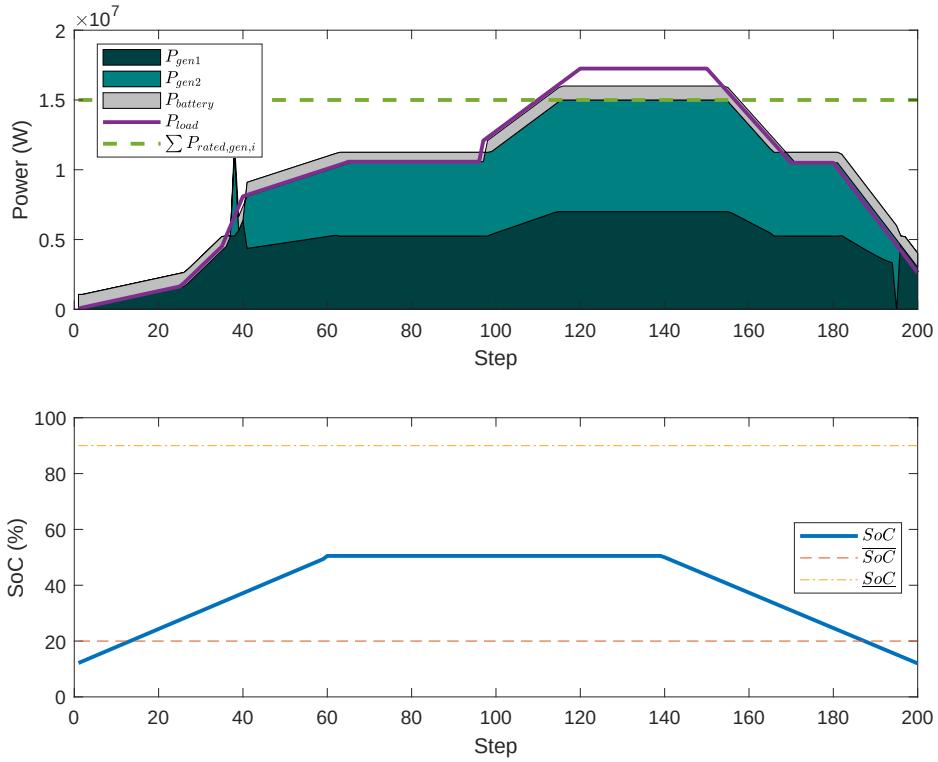

Figure 7.3: PMS algorithms verification, case 2: the power flow of gensets and BESS with respect to the specific load and SoC.

7.1.2 Discussion

In the case 1, the battery SoC is given as a constant for the first 30 s, i.e., 10%, which is below the safety SoC limit. Only one genset is required to supply the power in the PMS system. The genset No.1 is chosen to be connected to the system for power supply since genset No.1 has a better fuel performance than the genset No.2. Meanwhile, genset No.1 charges the BESS. In the figure, the charging power of battery is overlapping with the power supply by the genset No.1.

From 40 s to 60 s, the SoC is still 10 % but one connected genset could not give optimal fuel economic since the load increases. The genset No.2 joins the force to supply the power. Based on the minimum fuel consumption described in Algorithm 3, the load sharing between the two gensets is shown.

From 60 s to 100 s, the SoC is 60% and charged by the gensets which both operate at their optimal rates. From 100 s to 120 s, the load continues to increase. The increased power

demand pressure makes the two gensets operate with higher rates. This brings in more fuel consumption if the BESS does not contribute to the power generation. In the period of 120–150 s, the load exceeds the total maximum rated power provided by two gensets. Therefore, two gensets operates at their MCRs, and the BESS discharges at its rated power. From 150 s to 170 s, the simulation results are similar to those in 100–120 s. For 170–200 s, the SoC is not charged anymore as it stays at 90% which exceeds the upper limited SoC.

In case 2, the last 50 s shows a different power generation compared to Figure 7.2. The BESS is charged by the gensets since its given SoC is relatively small to it in case 1.

It is therefore concluded that the two case studies well verify the fidelity of PMS algorithms with respect to the specific load and battery SoC.

7.2 Optimal peak shaving verification

This simulation is used to verify the optimal strategy of peak shaving described in Section 6.3.

The BESS is composed of a number of equivalent batteries in series. The specifications of individual battery are given in Table 7.1.

Table 7.1: Parameters of battery model used in the process plant (PBES 2017)

Specifications	Values	Unit
R_i	0.01	Ω
E_0	96	V
K	3.5	\
A	7	\
B	0.0002	\
Capacity$C$	6.5	Kwh
Nominal Voltage	88.8	V DC
Discharging Current	225	A DC
Charging current	112	A DC
Weight	1190	kg
Charging power $P^C_{battery}$	0.01	MW
Discharging power$P^D_{battery}$	0.02	MW
SoC_{min}	0.2	\
SoC_{max}	0.9	\
Weight	89	kg

For all simulations in this section, the rated power of gensets are given as 2 MW and 4 MW with SFOC curves shown in Figure 7.1.

Four 20-second simulation results are presented.

Case 1

The BESS is composed of 10 equivalent batteries in series, giving the maximum discharging power as 0.2 MW and the maximum charging power as 0.1 MW.

Case 2

The BESS is same as that in Case 1 but with a different load profile.

Case 3

The load profile is same as it in Case 1 but with a different battery capacity. The BESS is composed of 20 equivalent batteries in series, giving the maximum discharging power as 0.4 MW and the maximum charging power as 0.2 MW.

Case 4

The load profile is same as it in Case 1 but without any constraint on battery discharging/charging power, referring to Eq. (6.24).

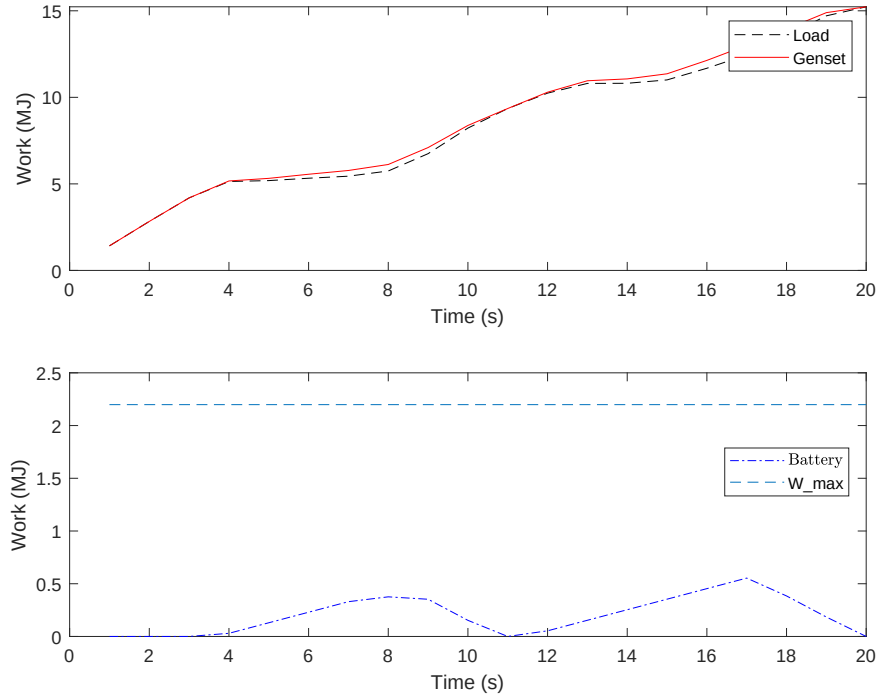

(a)

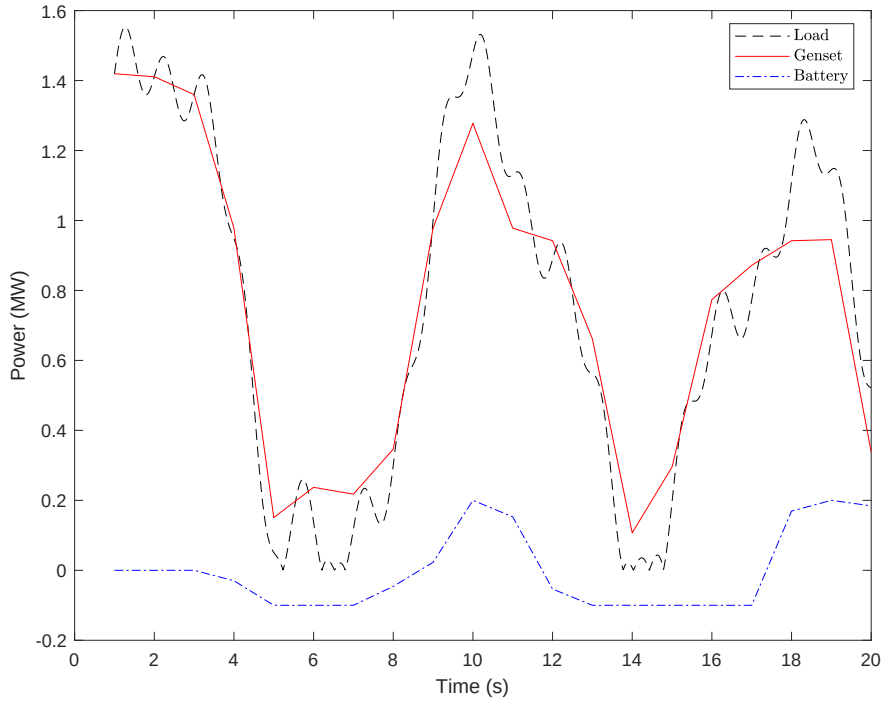

(b)

Figure 7.4: Optimal Peak shaving, Case 1: a) the energy band and battery work, and b) power generated by gensets.

7.2.1 Results

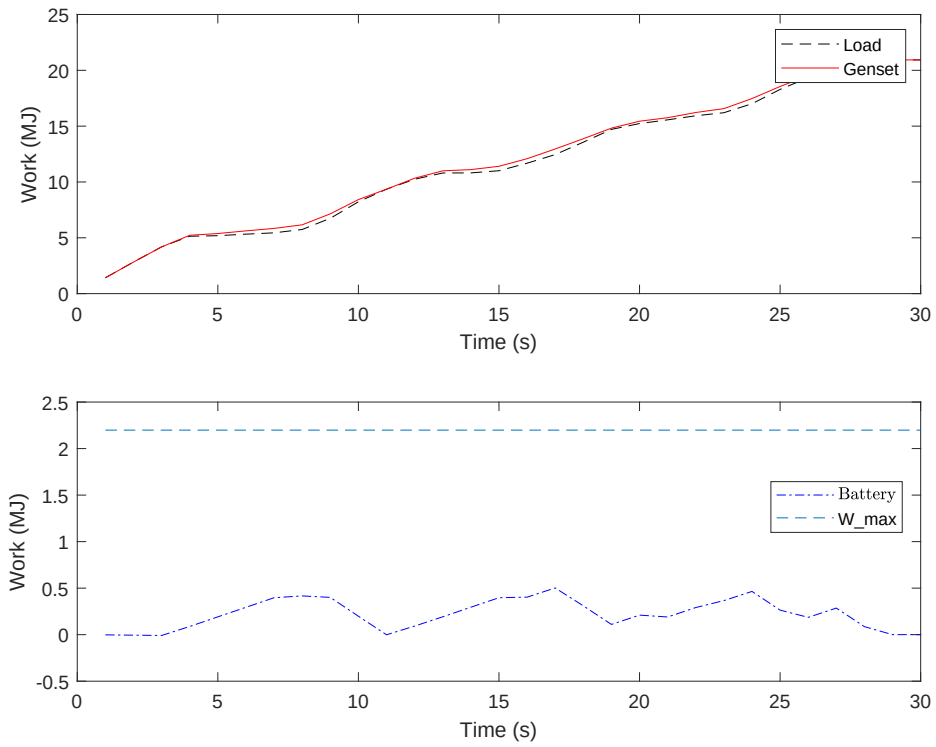

(a)

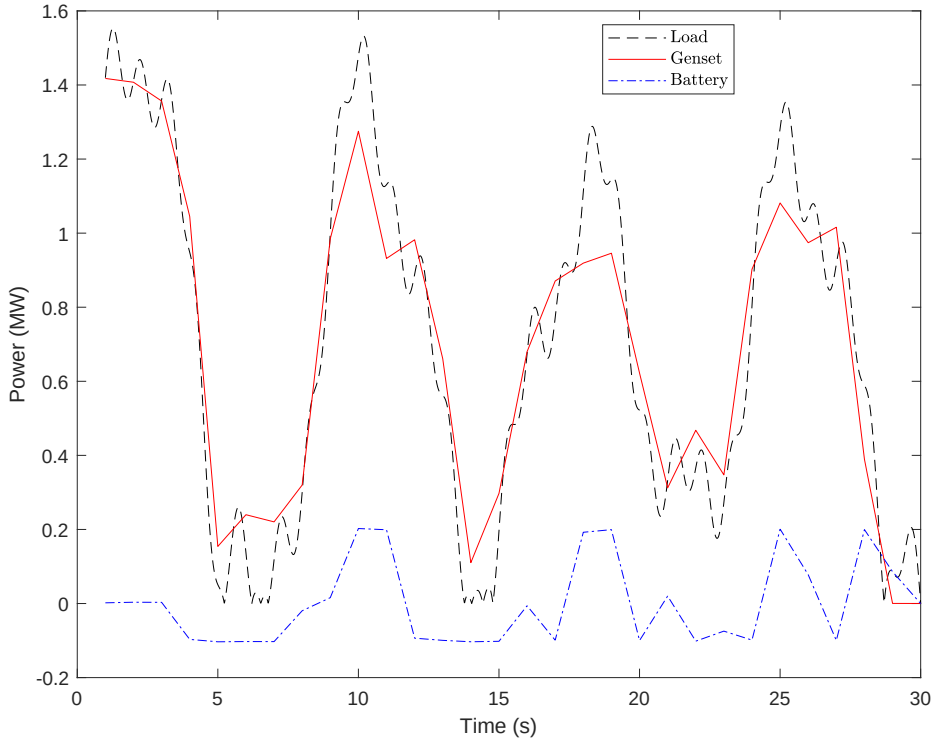

(b)

Figure 7.5: Optimal Peak shaving, Case 2: a) the energy band and battery work, and b) power generated by gensets.

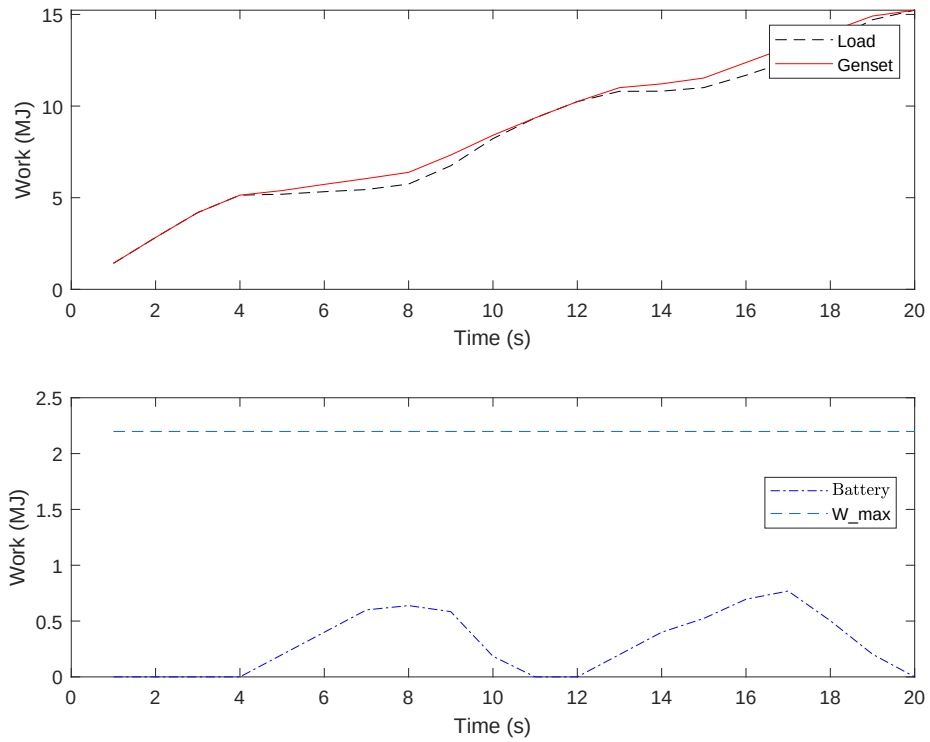

(a)

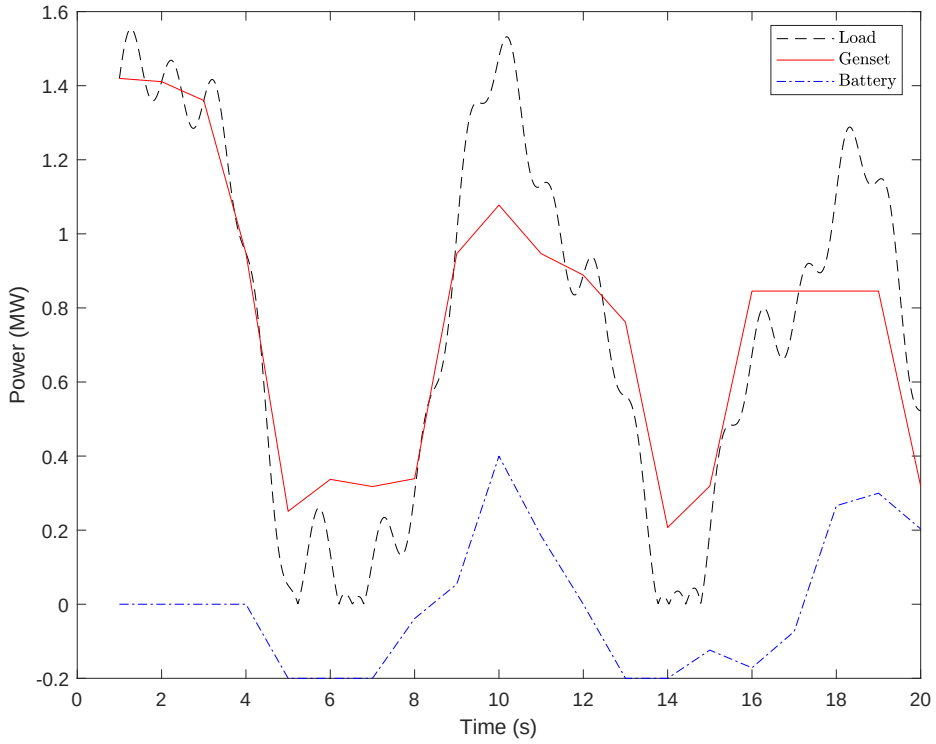

(b)

Figure 7.6: Optimal Peak shaving, Case 3: a) the energy band and battery work, and b) power generated by gensets.

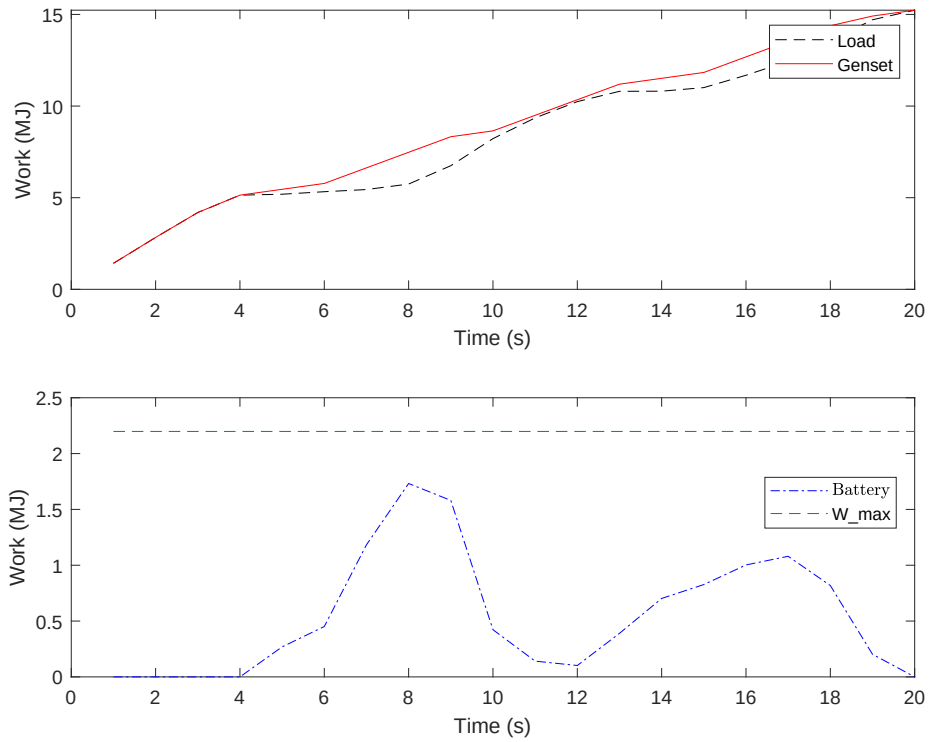

(a)

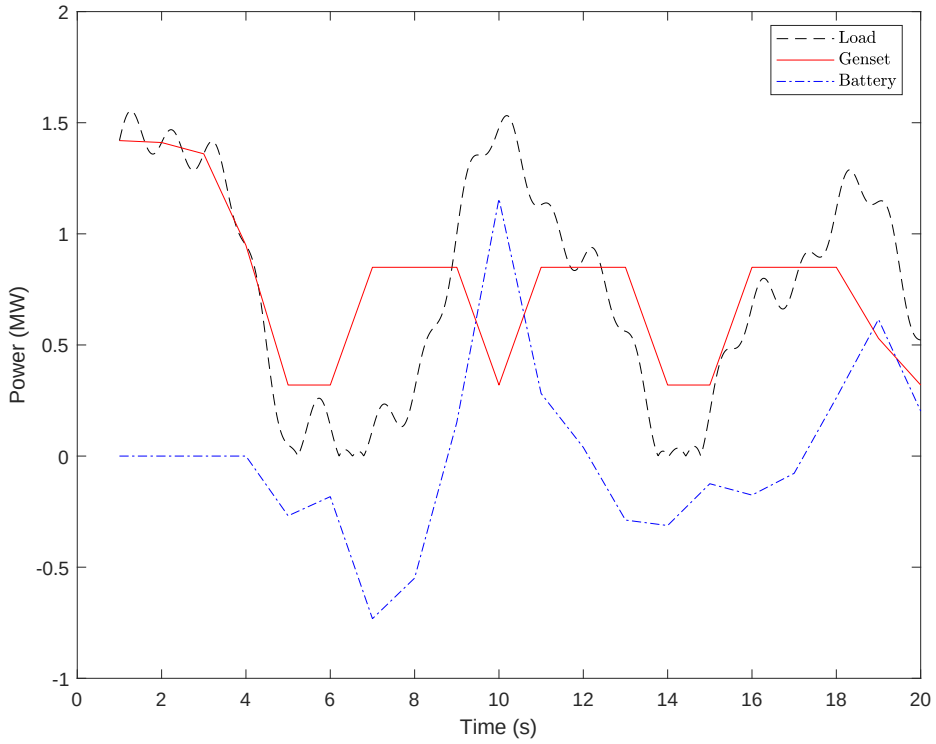

(b)

Figure 7.7: Optimal Peak shaving, Case 4: a) the energy band and battery work, and b) power generated by gensets.

7.2.2 Discussion

Figures 7.4 and 7.5 show the energy band, battery work, and the resulted power generation by the gensets, given different load profiles. Both results verify the reliability of the proposed optimal peak shaving strategy.

In the figure of energy band, it can be seen that the work of the genset (red line) follows tightly the load work (blue line) to draw the shortest path from the initial point to the final point, which is consistent with the energy band inequality Eq. (6.16). Thus, power generation by the gensets which is the first derivative of the work, is minimised. The figure of battery work shows the charging/discharging process of battery in response to the load peaks-charged when the lower peak occurs and discharge when the higher peak occurs. The third figure shows the power generated by the gensets after peak shaving with support of the BESS. When there is sufficient power stored in the battery, the gensets generate as less power as possible which is reflected on the power peaks tending to become flat. On the other hand, the gensets generate more power to meet the load demands and charge the BESS When the BESS power runs out.

The Figures 7.4 and 7.6 show the energy band, battery work, and resulted power generation by the gensets given different BESS capacity. The latter case has double BESS capacity. The results shows distinguished differences regarding the degree of peak shaving when it comes to a more powerful BESS. In the Figure 6.22, the battery work is relative small to the genset work, making the upper limit too close to the lower limit in the energy band. This leaves less space for the power peaks shaved by the BESS. On the contrary, the genset power peaks are shaved more obviously (the peak part tends to be more flat), while there is a more powerful BESS producing a broader energy band. Therefore, a more powerful BESS is beneficial to shave the power peak.

The Figures 7.4 and 7.6 show the energy band, battery work, and resulted power generation by the gensets, given different constraints for the objective function. The latter one is missing the constraint on the battery power, as presented in Eq. (6.24). Figure 7.6 shows an unsatisfying performance though a broader range of the peak is shaved and the BESS work $W_{battery}$ reaches its upper limit $W_{max}(t)$. In theory, the bright side without the constraint is that the BESS can be taken full advantage of all the time no matter how large the voltage and current is. However, the constraint is important to be considered for the sake of a longer service life

and safety concern, as over-discharge current and over-charge current cause wear and tear to the BESS.

Comparing to other existing methods, this optimisation algorithm ensures the gensets to run with its optimal frequency as much as possible. In addition, it can avoid considerable power loss due to a few disconnect/connect of gensets.

However, the optimal peak shaving strategy has a main disadvantage of expensive and time-consuming computations, since it has to derive all the possible solutions and choose the optimal one.

Chapter 8

Simulation results: hybrid marine power system with varying load

This chapter presents the performances of the load sharing function when the vessel is subjecting to complex environmental conditions. The DP system is switched on to stabilise and track the path.

8.1 Simulation overview

The parameters of the vessel is listed in Table 8.1 (Ren, Skjetne, and Hassani 2015).

Table 8.1: Setup of the vessel's main particulars

Principle Dimension	Values
Vessel Type	FPSO
Length between perpendiculars L_{pp} [m]	200
Breadth B [m]	44
Draught T [m]	12
Mass M [kg	1.004e+08
Centre of gravity C_G	[0,0,11]
Trans. metacentric height $\overline{GM_T}$ [m]	5500
Long. metacentric height $\overline{GM_L}$ [m]	7.95
Density of cable ρ_k [kg/m^3]	251.4
Radius of turret r_t [m]	20

Figure 8.1 shows the load profile history of the vessel conducting DP operation. The total load demand is comprised of the thruster loads (occupies 70-80%), the high priority loads

(static load which should not be reduced), and the low priority loads (static load which can be reduced if the load is too large). In the model, the high priority loads and low priority loads are assumed constant as 1 MW and 0.68 MW respectively. The oscillation of the load profile is the result of first-order wave loads. Wind and current velocities are assumed to be constant.

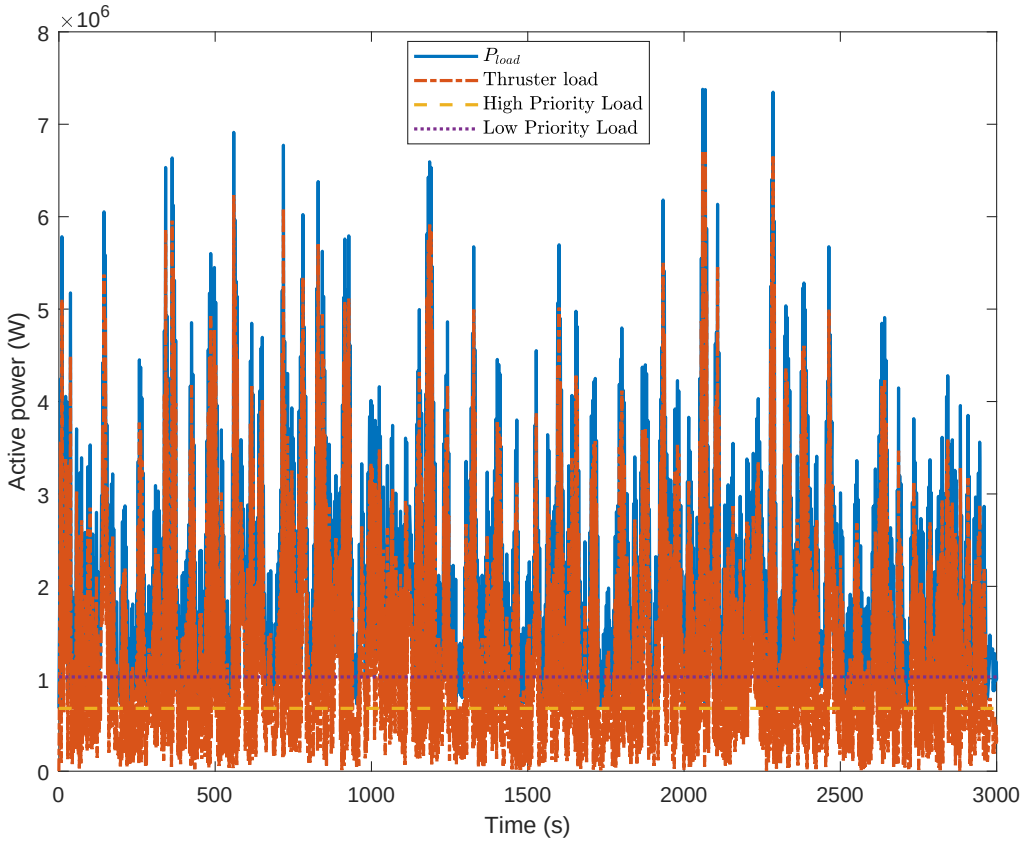

Figure 8.1: Load profile history of the vessel conducting DP operation

The time span for all the simulations is set as 3000 s, which is fair to evaluate the system performance. At the beginning 500 s, a ramp from 0 to 1 is multiplied to the load P_{load} to better test the performance of start-ups. From 500–2500 s, the load profiled adopted is consistent with the P_{load} from Figure 8.1. In the last 500 s, a droop from 1 to 0.25 is multiplied to the load profile to simulate the load deduction process.

To obtain a more precise illustration and comparison, the results from the simulations are divided into 6 sub-figures with a period of 500 s individually. Note that the sampling interval of the system for the gensets switching logic is selected as 10 s, and the length of the window is chosen as 20.

Based on the load profile, a hybrid marine power plant with a maximum power capacity of 7 MW is chosen, as listed in Table 8.2. The dimensioning of battery is based on Section 5.2 where the DoH is calculated as 0.15. The fuel consumption curves for two gensets come from Figure 2.3.

Table 8.2: Rated power for the gensets and battery

parameter	Values	unit
$P^r_{gen,1}$	2	MW
$P^r_{gen,2}$	4	MW
$P^D_{battery}$	1	MW
$P^C_{battery}$	0.5	MW

Case study 1 runs for 3000 s. The simulation results of a period of first 1000 s are presented due to space limits.
Case study 2 runs for 3000 s. The simulation results of a period of first 1000 s are presented due to space limits.

8.2 Case study 1: large varying load

This case study is used to verify the load sharing strategy when the vessel is subjecting to a large real-time varying-load. The magnitude of the load profile and the maximum power capability that HPS can offer are at the same level.

The simulation results are divided into two sections. The first section presents the first 500-second simulation results. A ramp from 0 to 1 is multiplied to the load P_{load} from Figure 8.1 to better test the performance of start-ups. The second section presents a period of 500–1000 s simulation results. The varying load is consistent with the corresponding time interval from Figure 8.1. The initial SoC input is given as 50.

8.2.1 Results

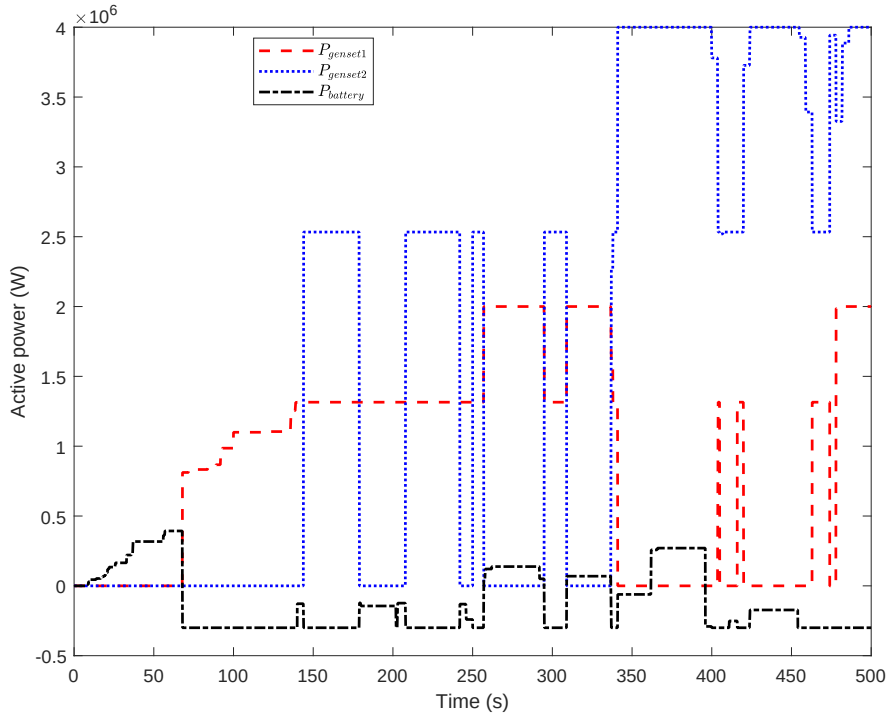

Figure 8.2: Case study 1, 0–500 s: individual power produced by the gensets and BESS.

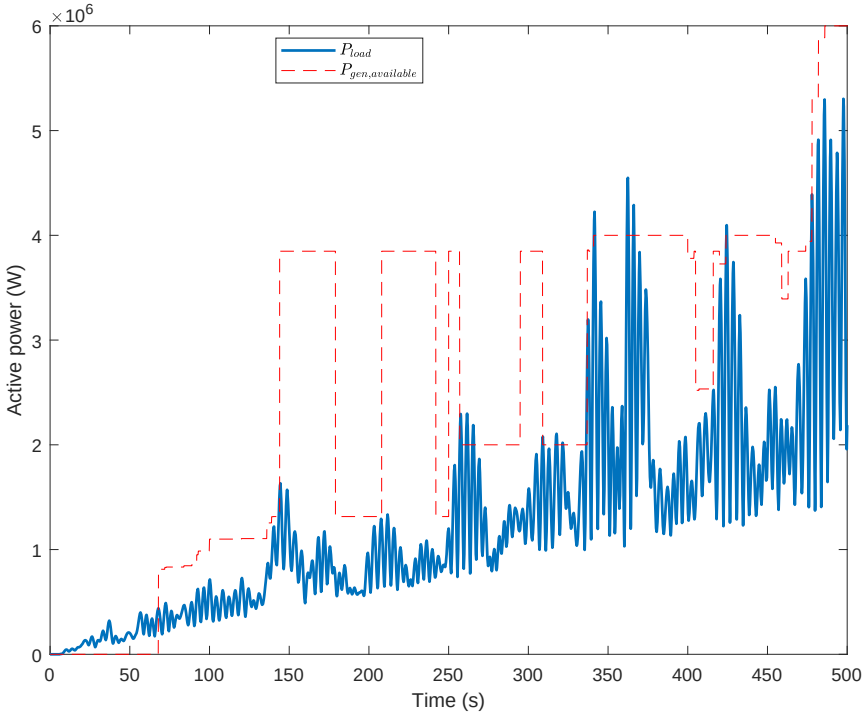

Figure 8.3: Case study 1, 0–500 s: the bus load and the available power provided by the gensets.

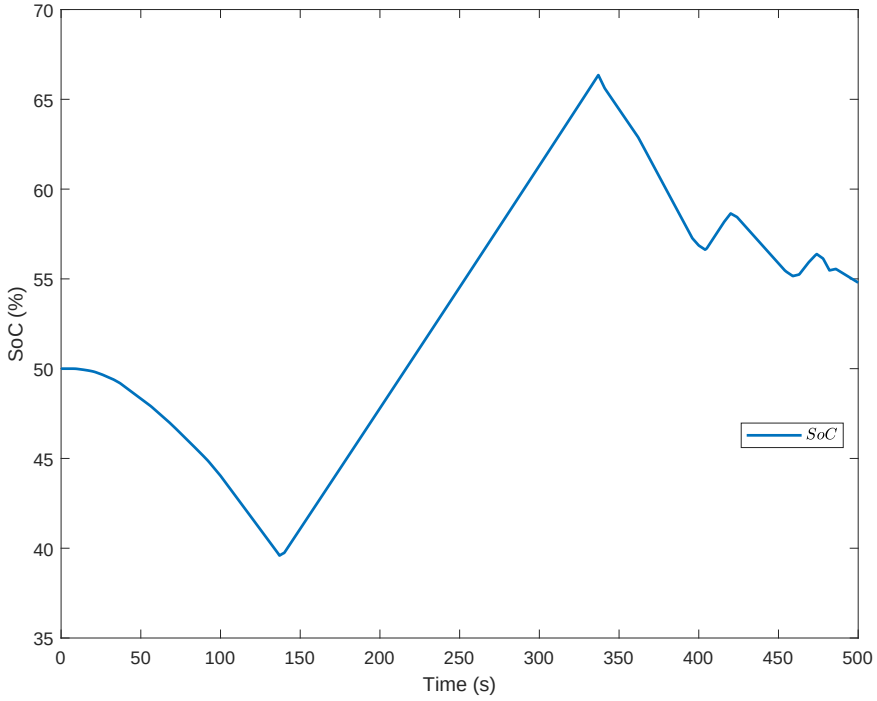

Figure 8.4: Case study 1, 0–500 s: the battery SoC.

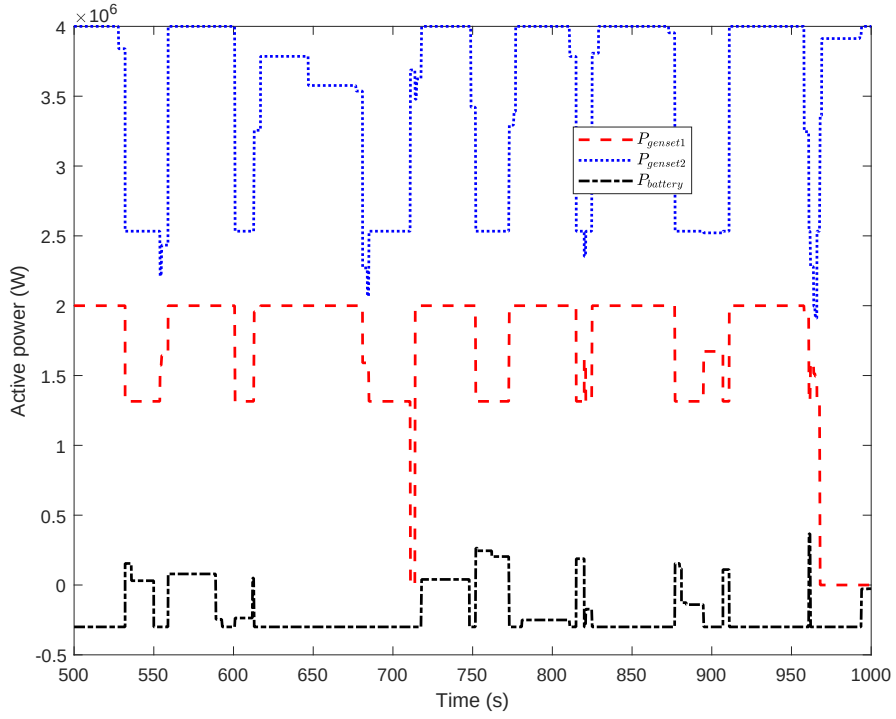

Figure 8.5: Case study 1, 500–1000 s: individual power produced by the gensets and BESS.

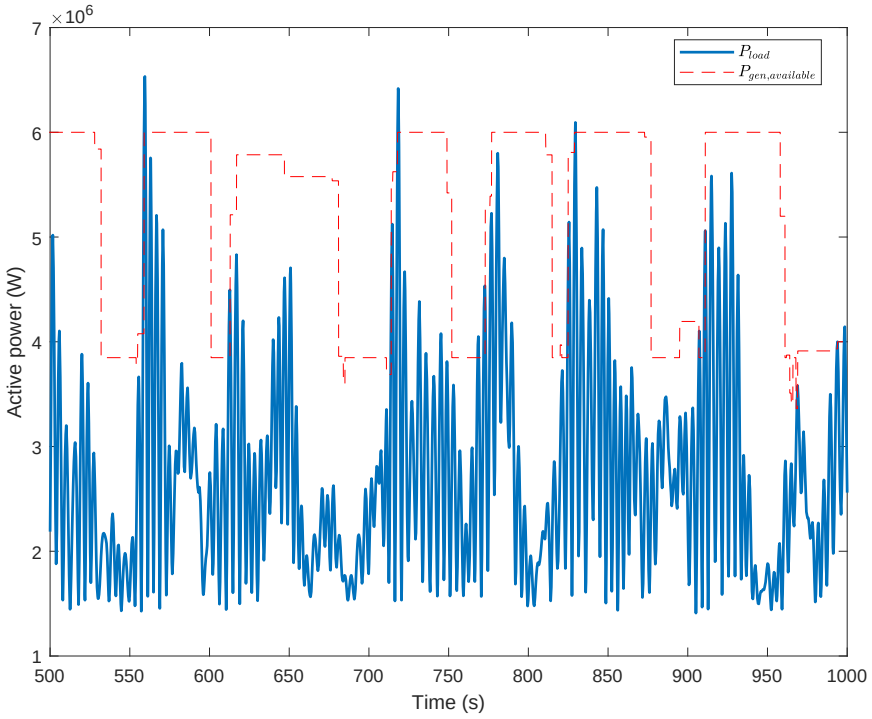

Figure 8.6: Case study 1, 500–1000 s: the bus load and available power provided by the gensets.

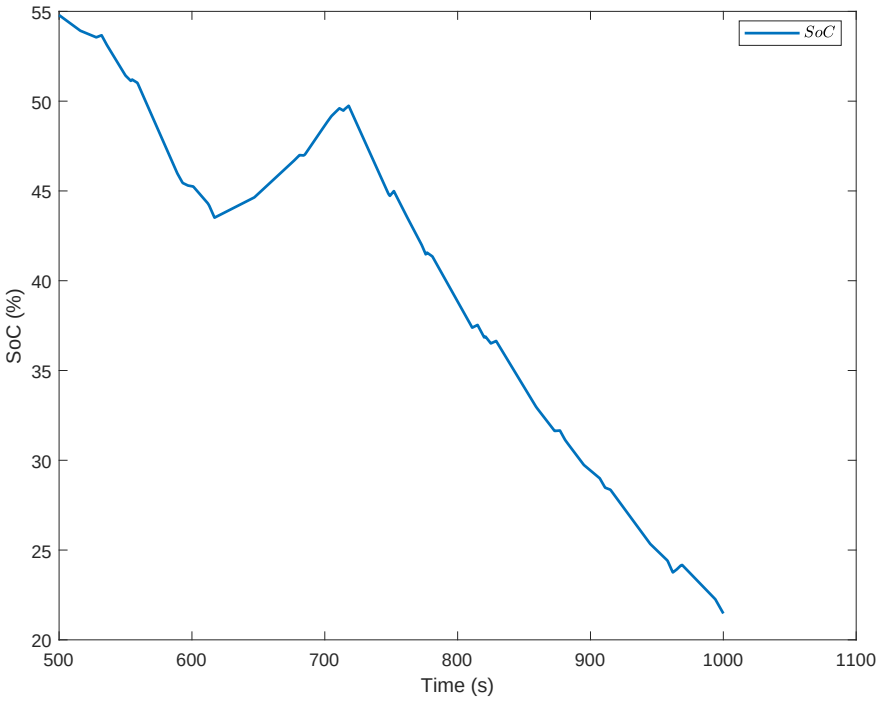

Figure 8.7: Case study 1, 500–1000 s: the battery SoC.

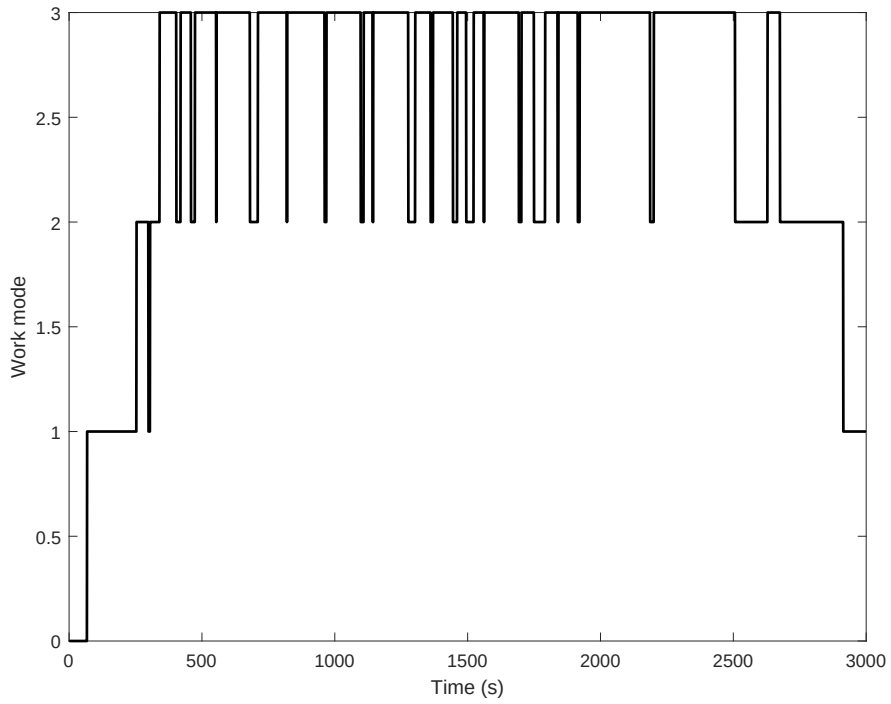

Figure 8.8: Case study 1, 0–3000 s: switching of the four working modes.

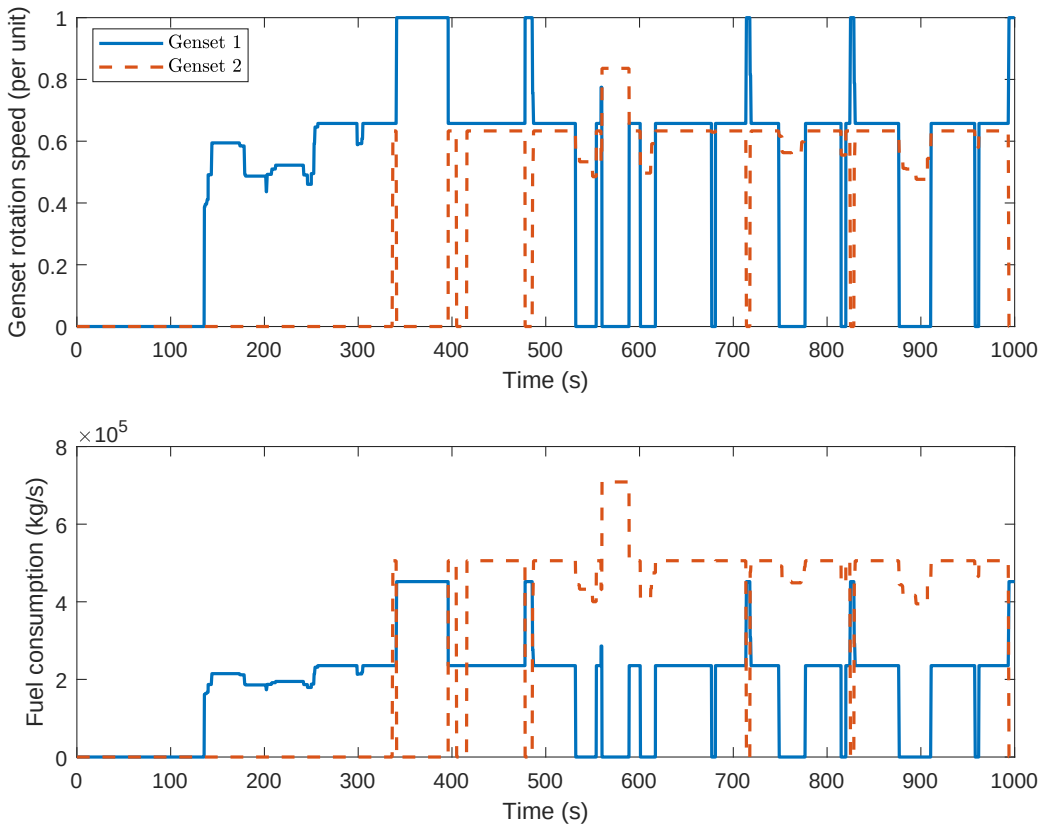

Figure 8.9: Simulation 2: genset rotation speed (upper) and fuel consumption (lower).

8.2.2 Discussion

0–500 s

In Figure 8.2, the energy stored in the battery is enough to balance the load demand in the first beginning 150 s, where the system is starting up with a low load. BESS is discharged as an independent power source while the gensets do not work. BESS is chosen for power supply as long as there is sufficient energy stored since the battery stays the top priority as the power source.

From 150 s to 350 s, the battery capacity dropped too much to meet the demand by working alone. Therefore, two gensets are activated at their optimal rates to supply the power, which leads to the minimum fuel consumption according to the selected SFOC curves in Figure 2.3. The gensets also charge the BESS at the same time, making the battery SoC increases by 20%.

From 350 s to 500 s, the genset rotation speeds enhance with the increased loads, resulting in the higher fuel consumption. PMS calculates the optimal load sharing between gensets and decides a proper working mode to minimise the fuel consumption. The switching logic decides the number of gensets connected to the bus as well as the BESS working mode.

Figure 8.3 shows the time-varying bus load and the available power supply by two gensets under the selected working mode. The peak of the available power appears at 6 MW where two gensets operate at their maximum speed. The working process only lasts for 20s. It can be seen that the switching frequency is relatively low and the gensets operates at their optimal rates in most time. Hence, the selected window effectively overcomes the rapid disconnections/connections of the gensets.

Figure 8.4 presents the history of battery SoC, aiming to show energy consumption and the charging/ discharging conditions. The SoC is limited within the pre-defined allowable range.

500–1000 s

Figure 8.5 shows how the load sharing among the two gensets and the batteries. To summarise, the system detects whether two gensets which both operate at their optimal speeds can meet the load demand. Otherwise, PMS decides the gensets speeds with the mission to minimise fuel consumption. Meantime, the BESS is used to supplement the power anytime.

It shows that when there is only one genset connected, it switches from the optimal rate to the maximum rate most time. This is because the load demand in the window is always larger than the unused situations in the algorithms.

Figure 8.6 shows the oscillations of the load profile, and the available power which can be supplied by the gensets. The load which is higher than the total genset rated power is compensated by the BESS.

Figure 8.7 shows the history of the SoC in the period. After reaching 90, the SoC does not grow anymore, which shows that the PMS manages to protect overcharging scenario.

Figure 8.8 shows the switching among the four working modes controlled by the PMS along 3000 seconds. The Y-axis refers to the different working mode: 0, 1, 2, and 3. Specific meanings are listed as follows:

- 0: BESS being the only power source $((C_1, C_2) = (0, 0))$
- 1: Genset No.1 and BESS cooperate $((C_1, C_2) = (1, 0))$
- 2: Genset No.2 and BESS cooperate $((C_1, C_2) = (0, 1))$
- 3: Two gensets and BESS cooperate $((C_1, C_2) = (1, 1))$

In the starting process and stopping process when the load is small, the working mode is mostly located at 1, i.e., the genset No.1 and BESS cooperate. From 500 s to 2500 s, PMS decides on the switching mode between mode 2 and mode 3. It shows that the BESS contributes all the time.

Figure 8.17 shows the genset speed and fuel consumption along 1000 s. From 400 s to 1000 s, the genset No.1 and No.2 run with close speeds at most time. This is because both the optimal speeds for the genset with minimum fuel consumption are in 70-80%. Since the genset No.2 has a larger rated power, it has more fuel consumption than the genset No.1.

8.3 Case study 2: small varying load

This case study is used to verify the load sharing strategy when the vessel is subjecting to small real-time varying load. The magnitude of the load profile is lower than the maximum power capability HPS can offer.

The simulation results are divided into two sections, with a period of 500 s respectively. The difference with case study 1 is that the adopted load profile is in half with the corresponding time interval in Figure 8.1. The initial SoC input is given as 50.

8.3.1 Result

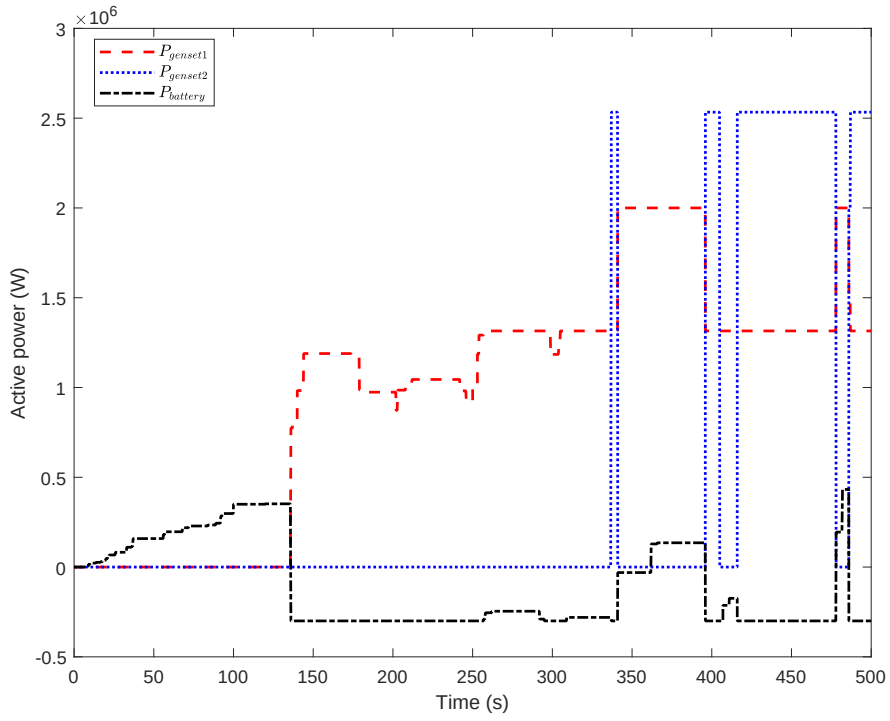

Figure 8.10: Case study 2, 0–500 s: individual power produced by the gensets and BESS.

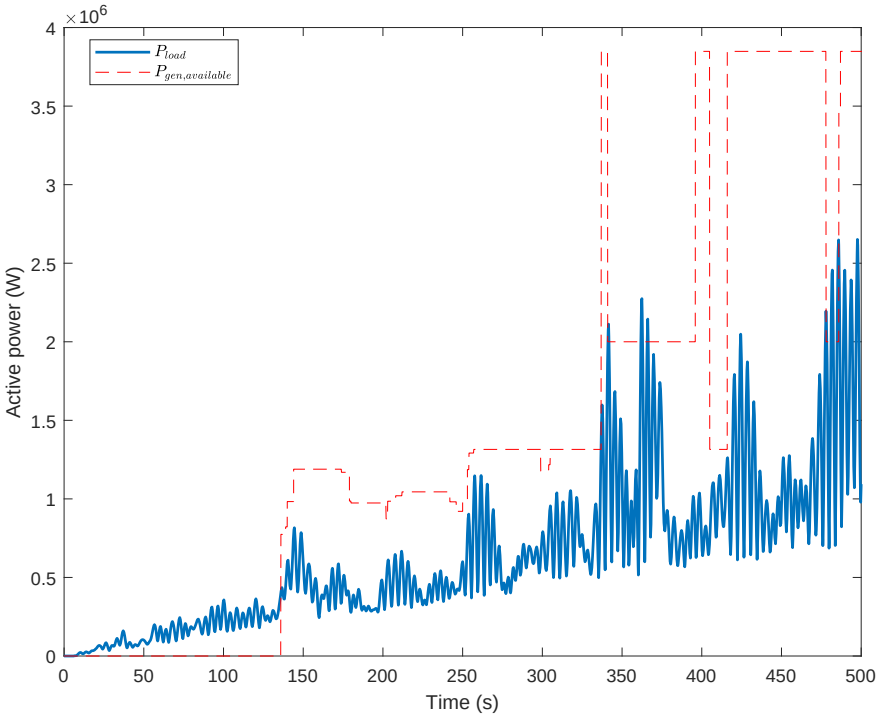

Figure 8.11: Case study 2, 0–500 s: the bus load and available power provided by gensets.

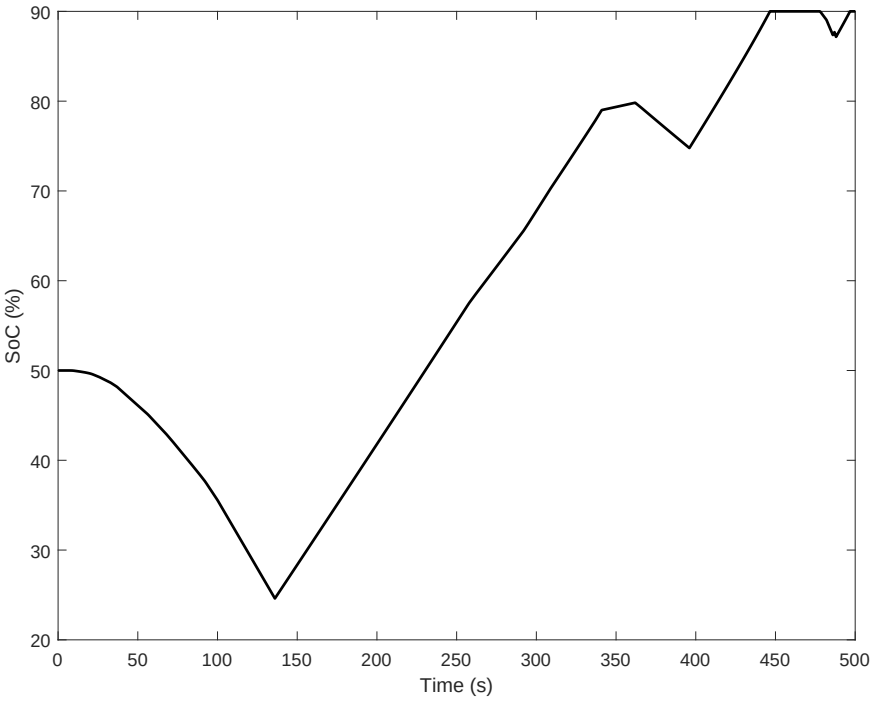

Figure 8.12: Simulation 2, 0-500s: the battery SoC.

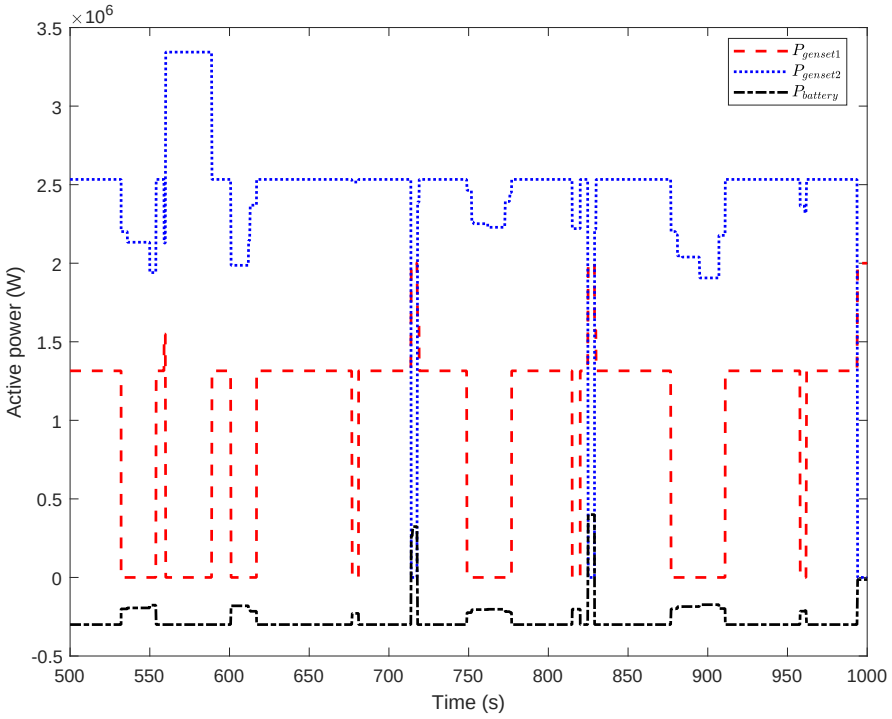

Figure 8.13: Case study 2, 500–1000 s: individual power produced by the gensets and BESS.

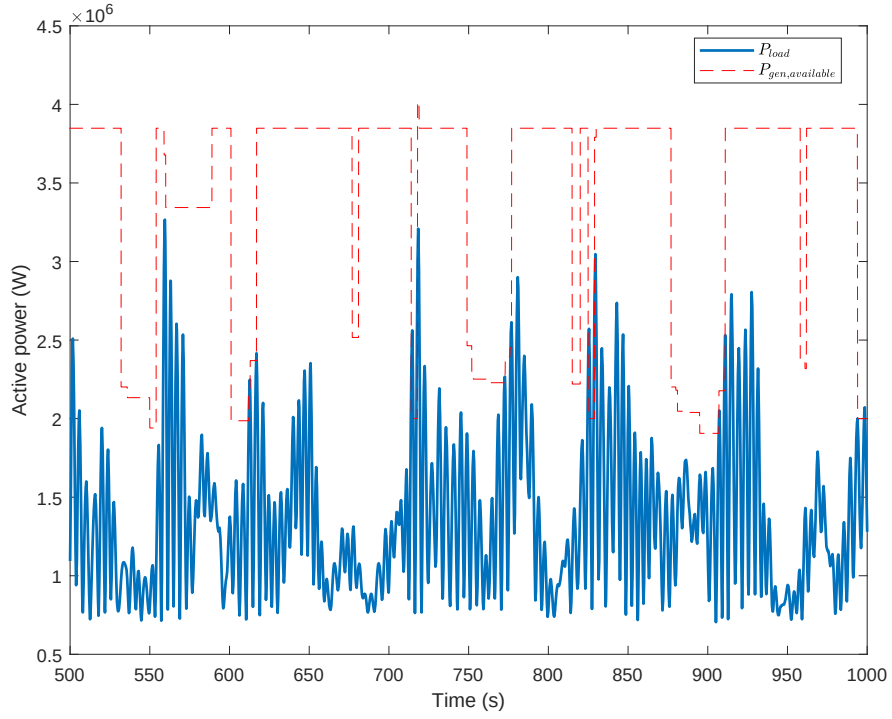

Figure 8.14: Case study 2, 500–1000 s: the bus load and available power provided by the gensets.

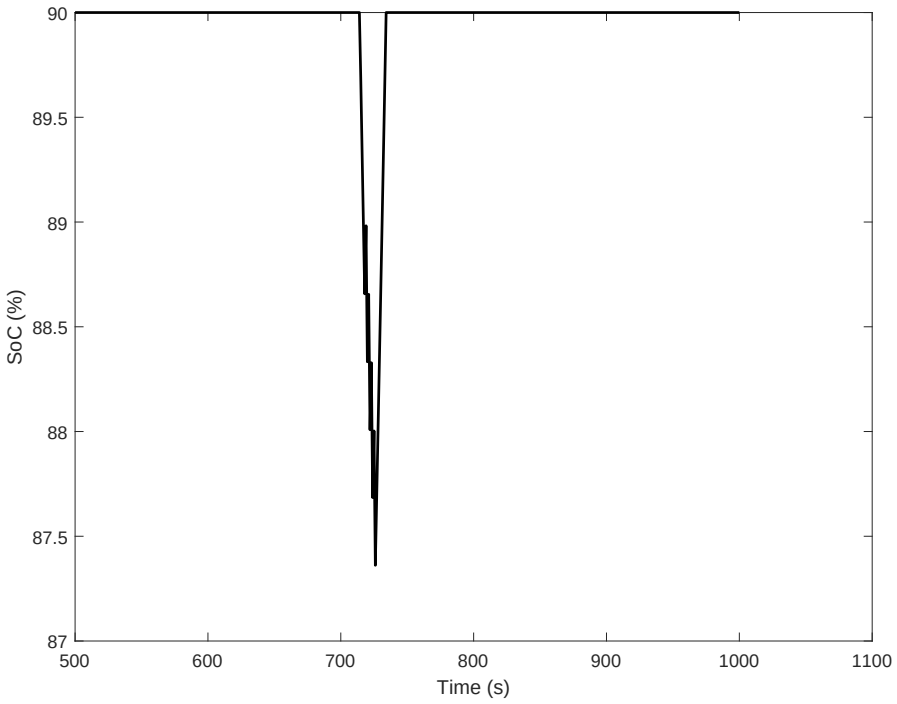

Figure 8.15: Case study 2, 500–1000 s: the battery SoC.

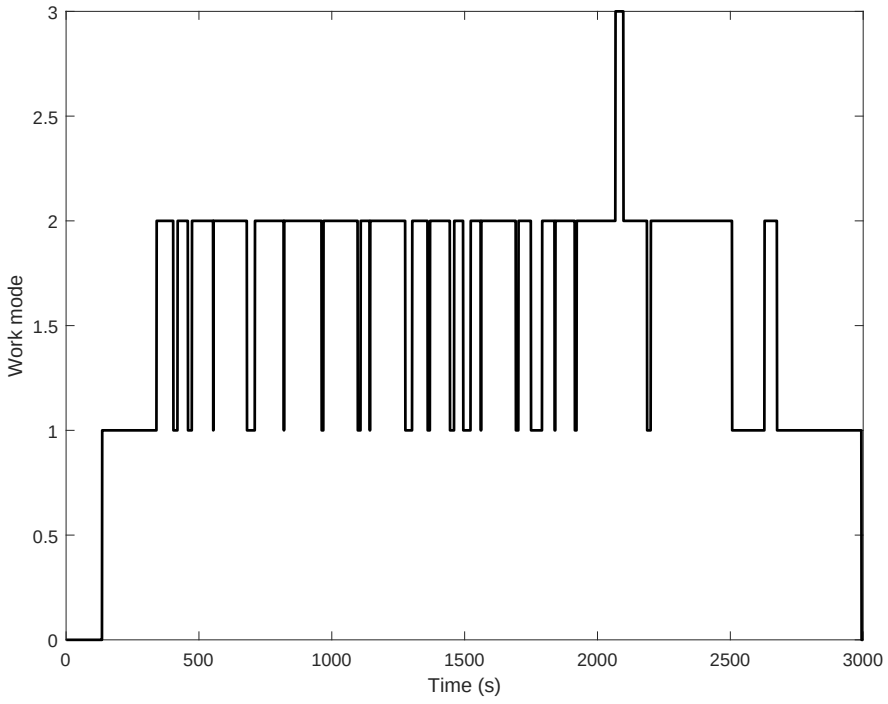

Figure 8.16: Case study 2, 0–3000 s: switch of the four working mode.

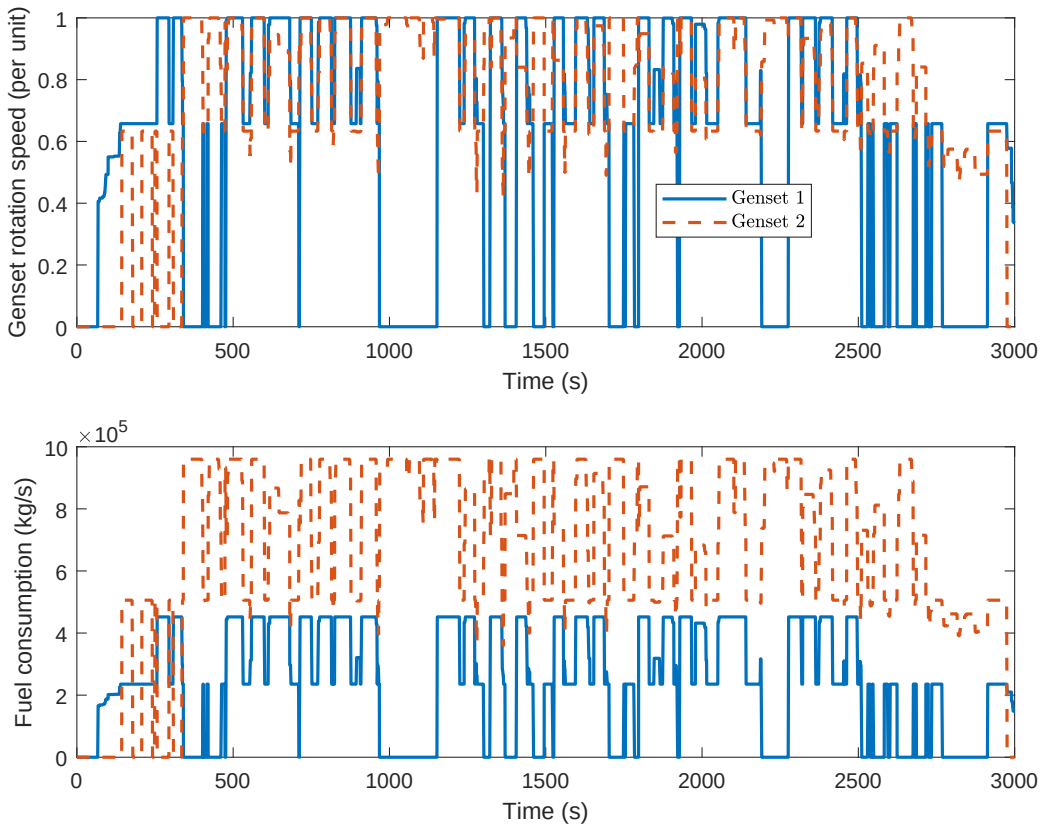

Figure 8.17: Case study 2, 0–3000 s: genset rotation speed (upper) and fuel consumption (lower).

8.3.2 Discussion

Case study 2 offers a more common situation in which the rated power of the system is much higher than the real-time varying loads.

In contrary to the working modes under large loads in Figure 8.8, Figure 8.16 shows that the PMS under small loads switches between mode 1 and mode 2 in most time. When one genset is capable to supply most of load demand, the uncovered peaks are compensated by the BESS. This greatly reduce the unnecessary fuel consumption because the other gensets should be switched on if the BESS is missed. It is concluded that the PMS is effective for the reduction of fuel consumption in a more general way.

There is no fast gensets switch on/off in the plots, meaning that the involvement of the BESS greatly reduce the disconnection/connection frequency of the gensets. This can reduce the wear and tear effects to the system and avoid unnecessary switch among gensets.

All the results verify the functionality of load sharing strategy. The power supplied by the PMS can meet the power demand with large fluctuation. The power generation follows the trend of the load profile.

Chapter 9

Conclusion and future work

9.1 Conclusion

The thesis aims to investigate the hybrid marine power system with the mission to reduce fuel consumption and gas emissions. By introducing the ESS in the work, the power plant has a better performance regarding the power generation and distribution. The peak shaving strategy and optimal load sharing algorithms are proposed.

Per unit genset model is developed. The battery module is developed by using the terminal voltage and SOC as outputs. According to the setup of the HPS, the algorithms are verified through simulations.

For the peak shaving strategy, ESS is used to smooth the power peaks by adopting the concept of energy band. The output power of the genset satisfies the power demand while the the power peaks are well shaved by the ESS. The simulation results well verifies the peak shaving strategy. For the load sharing strategy, there are four working modes among the gensets and ESS. The PMS decides on the working mode achieving enough power supply and, meanwhile, minimum fuel consumption.

The load sharing among gensets and ESS is the main target of the thesis. The fuel consumption is used as the optimising criteria for calculating the individual power output of each genset. Two case studies of implementing the strategy to the ships with time-varying load profiles are simulated. From the 3000s simulation results, the functionality of load sharing strategy is well verified. The power supplied by the PMS can meet the power demand with

large fluctuation. The involvement of the BSS greatly reduce the disconnection/connection frequency of the gensets. This can reduce the wear and tear effects to the system and avoid unnecessary switch among gensets.

It has reasons to believe that the optimal method is potential for the practical uses and contribute to the environmental-friendly maritime industry.

9.2 Limitations

Limitation are listed as follows to give constructive suggestions for future work:

1. The control scheme is limited to the power plant with a small number of gensets, i.e., in the thesis only 2 gensets are connected to the bus.
2. The rated power of battery is believed to set larger than the battery used in many ships so far.
3. The thesis considers the fuel consumption as the only optimising factor, while reduction of gas emissions such as CO_2 is not considered in the algorithms.

Bibliography

Ådnanes, Alf Kåre (2003). *Maritime electrical installations and diesel electric propulsion*. ABB.

Benhamed, S et al. (2016). "Dynamic modeling of diesel generator based on electrical and mechanical aspects". In: *2016 IEEE Electrical Power and Energy Conference (EPEC)*. IEEE, pp. 1–6.

Bø, Torstein I et al. (2015). "Real-time marine vessel and power plant simulation". In: *ASME 2015 34th International Conference on Ocean, Offshore and Arctic Engineering*. American Society of Mechanical Engineers, V001T01A007–V001T01A007.

Bo, Torstein Ingebrigtsen (2012). "Dynamic model predictive control for load sharing in electric power plants for ships". MA thesis. Institutt for marin teknikk.

Bø, Torstein Ingebrigtsen (2016). "Scenario-and optimization-based control of marine electric power systems". PhD thesis.

Borutzky, Wolfgang (2011). *Bond graph modelling of engineering systems*. Vol. 103. Springer.

Butler, Mark (2003). *HSC physics*. Macmillan Education AU.

Cai, Q et al. (2010). "A sizing-design methodology for hybrid fuel cell power systems and its application to an unmanned underwater vehicle". In: *Journal of Power Sources* 195.19, pp. 6559–6569.

Carrow, Robert S (2000). *Electrician's Technical Reference: Variable Frequency Drives*. Cengage Learning, p. 95.

Chen, Min and Gabriel A Rincon-Mora (2006). "Accurate electrical battery model capable of predicting runtime and IV performance". In: *IEEE transactions on energy conversion* 21.2, pp. 504–511.

Cosse, Roy E et al. (2011). "Turbine/generator governor droop/isochronous fundamentals-A graphical approach". In: *2011 Record of Conference Papers Industry Applications Society 58th Annual IEEE Petroleum and Chemical Industry Conference (PCIC)*. IEEE, pp. 1–8.

Dahl, Andreas Reason, Laxminarayan Thorat, and Roger Skjetne (2018). "Model Predictive Control of Marine Vessel Power System by Use of Structure Preserving Model". In: *IFAC-PapersOnLine* 51.29, pp. 335–340.

Dimitris Argyros, Tristan Smith (2014). *Global Marine Fuel Trends*. Lloyd's, pp. 4–5.

Dürr, Matthias et al. (2006). "Dynamic model of a lead acid battery for use in a domestic fuel cell system". In: *Journal of power Sources* 161.2, pp. 1400–1411.

Eidsvik (2015). *Viking queen*. https://www.eidesvik.no/news-archive/viking-queen-installation-of-energy-storage-system-article645-299.html. Web Page. [Accessed: 02-02-2019].

Emmanuel, Odunlade (2018). *Different Types of Batteries and their Applications*. `https://circuitdigest.com/article/different-types-of-batteries`, type=Web Page, note = [Accessed: 21-04-2019].

Explorer, The (2015). *The world's first electric car and passenger ferry*. `https://www.theexplorer.no/solutions/ampere--the-worlds-first-electric-car-and-passenger-ferry/`. Web Page. [Accessed: 02-02-2019].

Fossen, T. I. and T. Perez (2004). *Marine System Simulator*. http://www.marinecontrol.org. [Accessed: 01-05-2019].

Fukui, Wataru et al. (1992). *Vehicle speed governor*. US Patent 5,113,821.

Gao, David Wenzhong (2015). *Energy storage for sustainable microgrid*. Academic Press, pp. 79–121.

Global, Circuit (2017). *Automatic voltage regulator*. https://circuitglobe.com/automatic-voltage-regulator.html. Web Page. [Accessed: 15-04-2019].

Gudmundsson, Jon Steinar (2013). *Natural gas comparison*. `https://slideplayer.com/slide/13209765/`. [Accessed: 12-03-2019].

Gurvin, Erlend Kvam (2017). "Modeling and Simulation of a Super-redundant Marine Power Plant as a Hybrid Dynamical System". MA thesis. NTNU.

Han, Jingang, Jean-Frederic Charpentier, and Tianhao Tang (2014). "An energy management system of a fuel cell/battery hybrid boat". In: *Energies* 7.5, pp. 2799–2820.

Hou, Jun (2017). "Control and Optimization of Electric Ship Propulsion Systems with Hybrid Energy Storage". PhD thesis.

Karmiris, Georgios and Tomas Tengnér (2013). "Peak shaving control method for energy storage". In: *Corporate Research Center, Vasterås, Sweden*.

Kötz, R and MJEA Carlen (2000). "Principles and applications of electrochemical capacitors". In: *Electrochimica acta* 45.15-16, pp. 2483–2498.

Krause, Paul et al. (2013). *Analysis of electric machinery and drive systems*. Vol. 75. John Wiley & Sons.

Kuhn, Estelle et al. (2006). "Modelling Ni-mH battery using Cauer and Foster structures". In: *Journal of power sources* 158.2, pp. 1490–1497.

Layton, Bradley E (2008). "A comparison of energy densities of prevalent energy sources in units of joules per cubic meter". In: *International Journal of Green Energy* 5.6, pp. 438–455.

Levron, Yoash and Doron Shmilovitz (2012). "Power systems' optimal peak-shaving applying secondary storage". In: *Electric Power Systems Research* 89, pp. 80–84.

Miyazaki, Michel R, Asgeir J Sørensen, and Bjørn J Vartdal (2016). "Reduction of fuel consumption on hybrid marine power plants by strategic loading with energy storage devices". In: *IEEE Power and Energy Technology Systems Journal* 3.4, pp. 207–217.

Moore, Bill (2000). *Olympic Champion: Sydney's Solar Sailor*. `http://evworld.com/article.cfm?storyid=107`. [Accessed: 29-01-2019].

Oudalov, Alexdandre et al. (2006). "Value analysis of battery energy storage applications in power systems". In: *2006 IEEE PES Power Systems Conference and Exposition*. IEEE, pp. 2206–2211.

Patel, Mukund R (2011). *Shipboard electrical power systems*. Crc Press.

PBES (2017). *Datasheet:commercial marine lithium-ion energy storage*. `http://webcache.googleusercontent.com/search?q=cache:Uw673kdgctUJ:www.pbes.com/wp-content/uploads/2017/01/Marine-Brochure_A4_2017-01-12.pdf+&cd=1&hl=en&ct=clnk&gl=no`.

Plett, Gregory L (2004). "Extended Kalman filtering for battery management systems of LiPB-based HEV battery packs: Part 2. Modeling and identification". In: *Journal of power sources* 134.2, pp. 262–276.

Radan, Damir et al. (2016). "Integration, optimisation and benefits of energy storage for marine applications". In: *13th international naval engineering conference and exhibition*. Institute of Marine Engineering, Science and Technology Bristol, pp. 1–13.

Rakopoulos, Constantine D and Evangelos G Giakoumis (2009). *Diesel engine transient operation: principles of operation and simulation analysis*. Springer Science & Business Media.

Rao, P Sasidhara, G Sridhara Rao, and Krishna Vasudevan (2014). "Electrical Machines I". In:

Ren, Zhengru, Roger Skjetne, and Vahid Hassani (2015). "Supervisory control of line breakage for thruster-assisted position mooring system". In: *IFAC-PapersOnLine* 48.16, pp. 235–240.

Ren, Zhengru et al. (2018). "Development and application of a simulator for offshore wind turbine blades installation". In: *Ocean Engineering* 166, pp. 380–395.

Ren, Zhengru et al. (2019). "Integrated GNSS/IMU hub motion estimator for offshore wind turbine blade installation". In: *Mechanical Systems and Signal Processing* 123, pp. 222–243.

Sahib, Mouayad A (2015). "A novel optimal PID plus second order derivative controller for AVR system". In: *Engineering Science and Technology, an International Journal* 18.2, pp. 194–206.

Shahl, Dr.Suad Ibrahiim (2010). *Three-phase Induction Machines*.

Shepherd, Clarence M (1965). "Design of primary and secondary cells II. An equation describing battery discharge". In: *Journal of the Electrochemical Society* 112.7, pp. 657–664.

Skjetne, Roger (2017). *Notebook: genset optimization model, revision B*. NTNU.

Smith, TWP et al. (2015). "Third IMO GHG Study 2014–executive summary and final report". In: *Int. Maritime Organization (IMO)*.

Sørensen, Asgeir J and Øyvind N Smogeli (2009). "Torque and power control of electrically driven marine propellers". In: *Control Engineering Practice* 17.9, pp. 1053–1064.

Thorat, Laxminarayan and Roger Skjetne (2018). "Optimal Online Configuration and Load-Sharing in a Redundant Electric Power System for an Offshore Vessel Using Mixed Integer Linear Programming". In: *ASME 2018 37th International Conference on Ocean, Offshore and Arctic Engineering*. American Society of Mechanical Engineers, V001T01A047–V001T01A047.

Tremblay, Olivier, Louis-A Dessaint, and Abdel-Illah Dekkiche (2007). "A generic battery model for the dynamic simulation of hybrid electric vehicles". In: *2007 IEEE Vehicle Power and Propulsion Conference*. Ieee, pp. 284–289.

UNLV (2013). *Synchronous generator*. `http://www.egr.unlv.edu/~eebag/Synchronous%20Generator%20I.pdf`. Web Page. [Accessed: 03-04-2019].

Varesi, Kazem and Ahmad Radan (2011). "A novel PSO based technique for optimizing the DOH in hybrid electric vehicles to improve both the fuel economy and vehicle performance and reduce the emissions". In: *2011 2nd Power Electronics, Drive Systems and Technologies Conference*. IEEE, pp. 342–349.

Varesi, Kazem et al. (2015). “A Simple Technique for Optimal Selection of Degree of Hybridization (DOH) in Parallel Passenger Hybrid Cars”. In: *Automatika: časopis za automatiku, mjerenje, elektroniku, računarstvo i komunikacije* 56.1, pp. 33–41.

Woodward (2011). *Governing Fundamentals and Power Management*.

Zhou, Zhibin et al. (2013). “A review of energy storage technologies for marine current energy systems”. In: *Renewable and Sustainable Energy Reviews* 18, pp. 390–400.